
Project Report

Optimization of Biodiesel Production in a Microreactor System

Reutlingen, 10 January 2017

Submitted by:

Dorian Lukas Segadlo (PATM3)

Natalia Behring (PATM3)

Angelina Beiter (ACM3) (Project Manager)

Mahmood Mubarak Rajput (PATM3)



Hochschule Reutlingen
Reutlingen University

Aknowlegdement

This POL-Project was made at the Process Analysis and Technology Centre (PAT) and also the Reutlingen Research Institute (RRI) of the Reutlingen University from October 2016 until January 2017.

We would like to thank Prof. Dr. Karsten Rebner and Mona Stefanakis, MSc. for the great supervision of our work. Thank you so much for all the helpful meetings, phone calls and discussions.

Furthermore many thanks to all workers of the RRI, who helped us, when there were laboratory questions and needs.

In addition our gratitude goes to our cooperation company Festo AG & Co. KG, especially to Florian Ziecker and Andreas Häckh, who were our contact persons in this project. Thank you for your competent advice, support and the invitation to your company.

And of course we like to thank Prof. Waltraut Kessler and her husband Prof. Dr. Rudolph Kessler for their great help concerning questions about design of experiment and multivariate data analysis.

Table of Content

1	Indroduction.....	1
1.1	Background and Motivation	1
1.2	Objective.....	1
2	State of the Art	2
2.1	Production of Biodiesel.....	2
2.1.1	Transesterification of Oils	2
2.1.2	Effect of Type and Concentration of Catalyst.....	3
2.1.3	Effect of Molar Ratio of Alcohol to Oil.....	3
2.1.4	Effect of Reaction Temperature.....	3
2.1.5	Effect of Free Fatty Acid and Water in Feedstock.....	4
2.1.1	Methanol and KOH or Methoxid As educt?	4
2.1.2	Problems with H ₂ O in the reaction mechanism	4
2.2	Limitations of Conventional Methods of Biodiesel Production	4
2.3	Transesterification Process & Intensification Using Microreactor Technology.....	5
2.4	Comparative Study of % FAME obtained in batch reactors and Microreactor	6
2.5	Patents List for Industrial Biodiesel Production Processes	6
2.6	Influence of Factors affecting Percent FAME Yield in Microreactors	7
2.6.1	Spectroscopic Methods	8
2.6.2	Chromatography Methods	9
2.6.3	Thermo-gravimetric analysis methods.....	11
2.7	Market analysis.....	12
3	Material and Samples.....	14
3.1	Material	14
3.1.1	Chemicals	14
3.1.2	Laboratory Apparatus	14
3.1.3	Consumables.....	15

3.1.4	Equipment.....	15
3.2	Samples.....	16
4	Methods.....	17
4.1	Batch Reaction	17
4.1.1	Laboratory set-up and general how to.....	17
4.1.2	List of experiments.....	19
4.2	Pre-experiments with Microreactor:.....	21
4.2.1	Experimental Setup	21
4.2.2	Selection of Parameters for Pre-experiments	22
4.3	Mixing Experiments	22
4.3.1	Mixing experiment of Oil and Methanol with catalyst and without catalyst at room temperature	22
4.3.2	Collection of Spectral Data	24
4.3.3	DoE for Mixing Experiment.....	24
4.4	Experimental Set-Up	26
4.5	Spectrometer Parameters and References.....	27
4.5.1	Lambda 1050.....	27
4.5.2	TIDAS	27
4.5.3	Spectral Engine	28
4.6	Saponification Number	28
5	Results and Discussion	31
5.1	Evaluation of the Batch Experiment Data.....	31
5.1.1	Comparison of the batch production as in the master thesis of Matheo Baumann and the POL group.	31
5.1.2	Comparison of batch produced with and without dropping.	33
5.1.3	Comparison of step C of three different batch productions with and without mole sieve..	34
5.1.4	Comparison of batch produced with volumetric and molar ratio.	36
5.1.5	Comparison of batch produced with methanol and ethanol.	38
5.1.6	Evaluation of inline measurements.....	39

5.1.7	Conclusion	42
5.2	Evaluation of Microreactor Preexperiments Data	43
5.2.1	Comparison of Microreactor Biodiesel vs. Batch 09 Biodiesel	43
5.2.2	NIR Spectra of Biodiesel, Rapeseed Oil and Methanol with KOH	43
5.2.3	Temperature	45
5.2.4	Oil to Methanol Molar Ratio	47
5.2.5	Flow Rate	49
5.2.6	Conclusion	51
5.2.7	Recommendations	52
5.2.8	Mixing experiment of Oil and Methanol with catalyst and without catalyst at room temperature	52
6	PLS model for Mixing Experiments	55
6.1	Conclusion	58
7	Comparison of Working Packages	59
8	Prospect	1

List of Figure

Figure 1: Reaction mechanism of transesterification for vegetable oil. It is a three step process: in the first step triglycerides (Glyceride) convert to diglycerides, in step two diglycerides convert to monoglycerides and finally monoglycerides convert to glycerol resulting in FAME, where R1, R2, R3 represent long fatty acid chains.....	2
Figure 2: Side Reaction in Biodiesel Production including (a) Saponification of FFA and (b) Alkyl Ester Conversation to FFA by Hydrolysis [[5]]......	4
Figure 3: Laboratory setup for batch reaction 1) three neck flask 2) dropping funnel 3) reflux condenser 4) crystallization tray with water 5) hot plate 6) thermometer connected to hot plate 7) optical fibre 8) TIDAS spectrometer 9) laptop with software 10) NIR probe 11) Thermometer for the batch reaction.....	18
Figure 4: Laboratory test-setup for biodiesel production. 1) Pressurized glass bottles for Oil and Methanol with KOH solution, 2) HPLC pumps, 3) Spectrometer N 2.0, 4) Microreactor construction, 5) Flow cell, 6) Pressure sensor, 7) Thermostat Device, 8) PLC Panel with touch screen, 9) Light source, 10) Optical Fiber, 11) Laptop installed with software to collect spectral data.....	21
Figure 5: Mixtures of Methanol and rapeseed oil without KOH (left) and with KOH (right) during mixing at 540 rpm. Left: Still, two phases are formed with methanol as the upper phase. Right: Homogeneous mixing of the two components due to the started reaction.	23
Figure 6: Mixtures of Methanol and rapeseed oil without KOH (left) and with KOH (right) during mixing at 620 rpm. Left: A homogeneous mixture is formed. Right: Difference in color occurs due to the starting reaction.	23
Figure 7: Mixtures of Methanol and rapeseed oil without KOH (left) and with KOH (right) after mixing. Methanol and rapeseed oil separates (left). Glycerol and biodiesel are formed (right)	24
Figure 8: Column Graph for oil to methanol for biodiesel in wt% based on the D-optimal design.....	25
Figure 9: Laboratory setup for the mixing experiments: 1) hotplate with stirrer function 2) 250 mL flask 3) inline NIR probe 4) optical fiber 5) TIDAS spectrometer 6) PC with software	27
Figure 10: Score plot of the PCA after baseline correction. The old and new alcohol containing compounds can be clearly separated on PC1 from the old and new oil containing compounds. The old and new spectra of oil show great variance to old and new biodiesel spectra on PC2. ...	32
Figure 11: Loading of the PC1 (blue) and PC2 (red). PC1 and PC2 are influenced in the range of 2030 nm to 2400 nm. With PC1 the separation of the alcohol included samples from the other samples is carried out. With PC2 success the separation of oil samples and biodiesel samples	32
Figure 12: Spectra of four batches with Step A, Step B and Step C. Two of them was produced with dropping and two without. It can be detected no or minimal differences between spectra within each step.	33

- Figure 13: Spectra of batch step C. When comparing the samples of batch step C a difference in the absorption units of the spectra in the wavelength range ~1730- 1750 nm, ~ 1890-1930 nm and ~ 2280-2305 nm is visible..... 34
- Figure 14: Score plot of the PCA. The PC1 is explained by 57% against the PC2 explained by 18%. The samples are an irregular distribution on the scores plot. But the samples of batch step C with mole sieve can be distinguished from samples without mole sieve..... 35
- Figure 15: Loading plot of PC1 (blue) and PC2 (red). The maximum variance of PC1 is located at the wavelength range 2290- 2400 nm. The PC2 shows the variance at several regions. The first one is at the wavelength at ~1730nm, the second one in the wavelength range 1890- 1930 nm and the third one is located in the wavelength range 2250- 2400 nm. 35
- Figure 16: Score plot of the PCA of spectra. The samples of methanol with KOH and biodiesel step A volumetric ratio can be clearly separated on PC1 from the samples of Bunge biodiesel, step B, step C and step A molar ratio. The methanol with KOH and biodiesel step volumetric ratio groups shows the difference on the PC2, where the methanol with KOH is above-average on PC2 and the biodiesel step A volumetric ratio is below average on PC2. 37
- Figure 17: Loading plot from PC1 (blue) and PC2 (red). The variance on PC1 is largely determined by the CH₃ and CH₂ combination bands. On PC1 two sample groups (step A volumetric ratio and methanol with KOH), which lie above average, can be clearly distinguished from the other groups (step A molar ratio, steps B, steps C and Bunge biodiesel), which lie below average. On PC2, the step A volumetric ratio has negative absorption and the samples of methanol with KOH have positive absorption. 37
- Figure 18: Line plots of baseline corrected spectra. In the Figure 18 a) the spectra of ethanol with KOH and the spectra of methanol KOH are shown. The Figure 18 b) and 18 c) demonstrate spectra of step A as well as step C produced with methanol and ethanol. 39
- Figure 19: Scores plots of inline measured Batch 5, Batch 6, Batch 7 and Batch 8. The Figure 19 a) shows the distribution of scores from batch 5(filled symbols) and 6 (not filled symbols) after baseline correction, smoothing and recalculation of outliers. The Figure 19 b) demonstrates the scores of batch 7 (filled symbols) and batch 8 (not filled symbols) after baseline correction and smoothing according to Savitzky-Golay polynomial fit. In addition, in both scores plots the samples of Bunge biodiesel, rapeseed oil and methanol can be seen..... 40
- Figure 20: Loading plots of PC1 (blue) and PC2 (red). The variance on PC1 is more determined by the overtones CH₃ & CH groups and ROH group at 2000 nm to 2100 nm. The absorption maxima on PC2 are at roughly ~ 1420 nm and at ~ 2060 nm. The absorption minimum lies at ~ 1610 nm. ... 41
- Figure 21: All spectra are baseline corrected. The biodiesel samples from microreactor before demethanolization MR step A(red) and after demethanolization MR step B(light purple) were compared with step A & step B biodiesel samples of batch 09 and Bunge Biodiesel sample. Microreactor biodiesel samples show all the characteristic CH₃, CH₂ and CH band peaks similar to Batch 09 and Bunge Biodiesel. Microreactor sample carries slightly higher absorption from

- 2000 to 2050 nm and also at 2258 nm which may be due to some glycerol dissolved in the sample. 43
- Figure 22: Baseline corrected and smoothed with Savitzky-Golay polynomial fit (2nd order, points 25) spectra of Bunge Biodiesel, Rapeseed Oil and Methanol with KOH measured with Spectral Engine N2.0. The 1st overtone bands of CH₃, CH₂ and CH are visible from 1650 nm to 1780 nm. Also the 1st overtone bands ROH & H₂O are prominent from 1900 nm to 1950 nm. Oil and Biodiesel show same characteristic peaks at 1720 and 1764 nm, but biodiesel exhibits higher absorption at 1664 nm. While methanol shows maximum absorption from 1900 nm to 1960 nm due to hydroxyl bond stretching. 43
- Figure 23: Shows Score plot of pure components, PC1 explains the 100% variance between samples that differentiates methanol samples from the biodiesel and rapeseed oil samples. Methanol is below average on PC1 and other two sample groups are above average on PC1. PC2 explains 0% variance in samples, here methanol is slightly below average, while biodiesel and rapeseed oil separate out into two different groups, but this separation is meaningless. 44
- Figure 24: In Loading plot, PC1 shows positive loadings for characteristic peaks of CH₃, CH₂ and CH absorption bands at 1664 nm, 1720 nm & 1774 nm respectively, which represents that biodiesel and oil. The negative loading peaks on PC2 represents methanol with characteristic 1st overtone CH₃ absorption bands at 1680 nm and 1st overtone ROH and H₂O absorption bands from 1900 nm to 1980 nm. 45
- Figure 25: Spectra are baseline corrected and smoothed with Savitzky-Golay Polynomial fit (2nd order, points 25). The 1st overtone of CH₃, CH₂ and CH absorption bands are visible in the wavelength range of 1650 nm to 1780 nm for all temperatures. From 1900 to 1950 nm, hydroxyl groups show stretching at 60 °C and 65 °C. 46
- Figure 26: For PCA model wavelength from 1600 nm to 1950 nm was selected. PC1 explains 98% variance in the samples. The samples at 40 °C and 50 °C group closer to oil as discussed above. The samples of 60 °C and 65 °C group in between the biodiesel and methanol 46
- Figure 27: On PC1 the variance is mainly due to CH₃, CH₂ and CH vibrations, which represents the biodiesel and oil groups. On PC2 the two separate groups can be visualized, negative loading from 1650 to 1750 nm which are due to 1st overtone CH₃ vibrations, represents methanol group and the positive loading from 1800 to 1900 nm are due to CH₂, CH and ROH vibrations, which are most probably due to the Glycerol phase in solution. 47
- Figure 28: All spectra are baseline corrected and smoothed with Savitzky-Golay Polynomial fit (2nd order, points 15). At molar ratios below 1:6, spectra are identical and closer to oil spectra. While samples with a molar ratio of 1:6 and above show 1st overtone 48
- Figure 29: PC1 explains 98 % variance in samples, separates sample into two groups on behalf of 1st overtone CH₃, CH₂ and CH absorption bands in the wavelength range from 1650 nm to 1800 nm. The samples with oil to methanol molar ratio below 1:6 group closer to oil, indicating that there was not much reaction took place. While on PC1 samples with oil to methanol molar ratio at 1:6

and above, group in between biodiesel and methanol samples. This is possibly because of glycerol formation and intermediate products as mono-, and di- glycerides. PC2 covers only 1% of variance which is mainly due to negative score of Methanol 48

Figure 30: On PC1 the variance is mainly due to CH₃, CH₂ and CH vibrations, which represents the biodiesel and oil groups. On PC2 the two separate groups can be visualized, negative loading from 1650 to 1750 nm which are due to 1st overtone CH₃ vibrations, represents methanol group and the positive loading from 1800 to 1900 nm are due to CH₂, CH and ROH vibrations, which are most probably due to the Glycerol phase in solution. 49

Figure 31 All spectra are baseline corrected and smoothed with Savitzky-Golay Polynomial fit (2nd order, points 25). At a flow rate of 10 ml/min, spectra are identical and closer to Biodiesel spectra. While samples at 15 ml/min, 20 ml/min and 25 ml/min show 1st overtone CH₃, CH₂ and CH bands between 1600 nm and 1800 nm, and ROH absorption bands from 1900nm to 1950 nm. . 50

Figure 32: PC1 explains 99% variance in the samples. The samples at 10 ml/min are above average on PC 1 while the samples at other flow rates are below average on PC1. PC2 explains only 1 % variance, which is mainly due to negative scores of Methanol. 50

Figure 33: On PC1 the variance is mainly due to CH₃, CH₂ and CH vibrations, which represents the biodiesel and oil groups. On PC2 the two separate groups can be visualized, negative loading from 1650 to 1750 nm which are due to 1st overtone CH₃ vibrations, represents methanol group and the positive loading from 1800 to 1900 nm are due to CH₂, CH and ROH vibrations, which are most probably due to the Glycerol phase in solution. 51

Figure 34: Baseline corrected spectra of selected wavelength region from 2200 nm to 2300nm. In this wavelength region, characteristic CH₃ combination band peak of biodiesel samples at 2258nm distinguish it from methanol and rapeseed oil samples. 53

Figure 35: PC1 explains 95 % variance in the data set, the samples having Biodiesel and oil are above average on PC1 with similar scores approx. 0.5. The maximum variance on PC 1 is mainly due to methanol, having relatively high negative scores about -3 53

Figure 36: Baseline corrected and smoothed with Savitzky-Golay polynomalfit(2nd order, points 5) PC 1 the variance is mainly due to CH₃- and H₂O- vibrations with high negative loadings, show that the methanol is negatively correlated with it. On PC2, the two sample groups can be distinguished clearly the biodiesel phase is below average and the Oil phase above average. 54

Figure 37: Baseline corrected spectra of all mixing experiments. The samples are grouped according to Biodiesel wt% in samples. The samples with 60-100 wt % of biodiesel shows characteristic CH₃ & CH₂ absorption peaks at 1664 nm. While this peaks become less prominent with lower concentration of biodiesel. Whereas in samples with biodiesel wt% from 20 – 60 %, characteristic CH₃, CH₂ and CH absorption peaks of biodiesel and Oil are visible at 1724nm and 1775 nm.... 55

Figure 38: Shows the Score plot for wavelength ranging from 1100nm to 2100 nm. The samples are grouped according to biodiesel wt%. The factor 1 explains the 74% variance in spectra and factor 2 explains the 14 % variance in spectra..... 56

- Figure 39: Shows the difference of the explained variance for the predicted (blue) and the reference (red) values. To best predict the values of components we will use 7 factors as they explain the 98% variance samples. **Fehler! Textmarke nicht definiert.**
- Figure 40: The model for Rapeseed Oil shows R-square value 0.95 in validation for 7 factors, and the error in cross validation is about 5.897 on scale of -20 to 120 which is about 4.21%. **Fehler! Textmarke nicht definiert.**
- Figure 41: The model for Methanol shows R-square value 0.91 in validation for 7 factors, and the error in cross validation is about 7.42 on scale of -10 to 100 which is about 6.58%. 57
- Figure 42: The model for Bunge Biodiesel shows R-square value 0.97 in validation for 7 factors, and the error in cross validation is about 4.63 on scale of -10 to 100 which is about 4.2%. 58
- Figure 43: The model for Glycerine shows R-square value 0.85 in validation for 7 factors, and the error in cross validation is about 1.347 on scale of -2 to 10 which is about 11.2%. 58

List of Figures in Appendix

- Figure A 1: The line spectra collected at different temperatures along with pure components. No pre-treatment was applied to spectral data. At temperature of 40 and 50 the spectra was noisy due to emulsion formation. II
- Figure A 2: Left: Step B of batch 11 without water Right: 20 mL step B of batch 11 with 20 mL demineralised water. Before mixing two phases were formed..... IV
- Figure A 3: Left: Step B of batch 11 without water Right: 20 mL step B of batch 11 with 20 mL demineralised water. One phase is formed..... IV

List of Tables

Table 1: Comparison between Different Processing Factors of Biodiesel Production in Batch Reactor and Microreactors [50].....	6
Table 2: Online available Patents for Biodiesel Production Process	6
Table 3: Online available Patents for Biodiesel Production ProcessAnalytical Methods for Monitoring of Transesterification in Microreactors	7
Table 4: Biodiesel producing comapanies in Germany	12
Table 5: Chemicals for all experiments	14
Table 6:Laboratory apparatus	14
Table 7: Consumables.....	15
Table 8:Equipment	15
Table 9:Laboratory samples	16
Table 10: The components and the amounts for one experiment of the different batch reactions.....	19
Table 11: Molar ratio, temperature, rpm, mixing time, wt% of KOH and volume of methanol and oil for the two experiments to show the effect of KOH at room temperature	22
Table 12:Minimum and maximum values in wt% for the DoE.....	24
Table 13: Final DoE with the wt% for all components for each run.....	26
Table 14: Characteristic Features of Spectral Engine Mobile Spectrometers	28
Table 15: Amounts and Volumes of the determination of the saponification number, respectively the average molar weight of oil	29
Table 16: Determined volumes of the blindtest for the determination of the saponification number, respectively the average molar weight of oil	29
Table 17: Limits of factors to perform the DoE for the microreactor preexperiments	52

List of Tables in Appendix

Figure A 1: The line spectra collected at different temperatures along with pure components. No pre-treatment was applied to spectral data. At temperature of 40 and 50 the spectra was noisy due to emulsion formation.	II
Figure A 2: Left: Step B of batch 11 without water Right: 20 mL step B of batch 11 with 20 mL demineralised water. Before mixing two phases were formed.....	IV
Figure A 3: Left: Step B of batch 11 without water Right: 20 mL step B of batch 11 with 20 mL demineralised water. One phase is formed.....	IV

Abbreviations

C	Carbon
CaO	Calcium oxide
CFDA	Continuous fuel dilution analyzer
CLS	Classical least square
DoE	Design of experiments
FAAE	Fatty acid alkyl esters
FFA	Fatty acid alkyl
FMEA	Failure mode and effects analysis
FTIR	Fourier transform infrared spectroscopy
GC	Gas chromatography
H	Hydrogen
HPLC	High-performance liquid chromatography
KOH	Potassium hydroxide
MCR	Multivariate Curve Resolution
MgO	Magnesium oxide
MIR	Middle infrared
MVA	Multivariate data analysis
N	Nitrogen
NaOH	Sodium hydroxide
NIR	Near infrared
O	Oxygen
PCA	Principle component analysis
PLS	Partial least square
rpm	Revolutions per minute
RRI	Reutlingen Research Institute
RSM	Response Surface Methodology
UV	Ultra violet
Vis	Visible

Unit Directory

Unit of	Symbol	Description
Amount of substance	mol	
Degree Celcium	°C	Celsius is a scale and unit of measurements for temperature
Length	nm	
Mass	g	
Mass fraction	wt. %	Mass fraction can be expressed with a denominator of 100 as percentage by mass
Molar fraction	mol %	Molar fraction can be expressed with a denominator of 100 as molar percentage
Reciprocal length	cm ⁻¹	
Time	sec./min	
Volume	cm ³ / L	

1 Indroduction

1.1 Background and Motivation

Biodiesel is a renewable and environmentally friendly fuel which is traditionally being produced in batch reactors on industrial scale. The batch processing of biodiesel is not cost effective due to low heat and mass transfer in batch reactors, excess alcohol consumption and large reaction time. Microreactors provide innovative process intensification solution to these problems with feature of continues production of biodiesel, less reaction time and low overall cost of production. Various successful attempts have been conducted to produce biodiesel in microreactors [1]. Jovanovic, et al, filed the first patent application for biodiesel production in microreactor, US 2009/0165366 A1 [5].

The biodiesel production in microreactor is commonly monitored by offline analytical techniques e.g. Gas Chromatography or High-Pressure Liquid Chromatography. These methods are time-consuming and provide less information about the reaction. Infrared spectroscopy is a fast and reliable analytical tool for organic compounds. Biodiesel shows characteristic spectrum in near infrared range, which could be used for the inline/offline quality control of biodiesel in microreactor.

1.2 Objective

The aim of the project is to use spectroscopy as a tool for qualitative and quantitative analysis to optimize both productions of biodiesel and process control in batch and microreactors. Furthermore, new insights in the synthesis of biodiesel, process analysis and quality control in batch and in microreactors should be obtained with regard to industrial processes. Multivariate Data Analysis (MVA) and Design of Experiments (DoE) are useful tools to process spectroscopic data into a meaningful model and to predict the outcome of experiments.

The experiments to be performed are separated into batch and microreactor experiments. By using inline NIR flow cells and UV/Vis/NIR spectrophotometer the samples in the batch are measured during the production, mixing and purification steps. In batch, a mixing experiment with the components methanol, biodiesel, oil, and glycerol by creating a simplex DoE has to be performed to determine optimal ingredient mixtures for desired product. In addition, the proof limit and determination limit of the measuring devices will be determined by mixing methanol and biodiesel in different ratios in batch. The microreactor model system includes pump systems, a heating system for the microreactor, mixing and heating structure plates of the microreactor, tubing, an inline NIR flow cell as well as pressure and feedback control system. This system realizes automation and process control of the production of biodiesel in microreactors. The samples after production, circulation and purification steps in the microreactor are measured by an inline NIR flow cell and also by UV/Vis/NIR spectrophotometer. The spectra of batch and microreactor measurements and reference biodiesel samples are evaluated and compared by a Principal Component Analysis (PCA). Furthermore, a DoE is created to find significant impacts on the process outcome and the optimum reaction conditions for the biodiesel synthesis in microreactors.

2 State of the Art

2.1 Production of Biodiesel

The global warming issues and reducing fossil fuel deposits have increased the demand for alternative fuels and renewable energy resources to fill the energy gap. Beside other renewable energy resources, i.e. wind energy, solar energy and geothermal energy, biodiesel is found to be a promising alternative fuel for diesel engines among other biofuels [1]. It is usually produced by transesterification of vegetable oils, animal fats, and waste oils etc. with an alcohol such as methanol or ethanol in the presence of a catalyst, such as sodium or potassium hydroxide. The newly formed chemical compounds are methyl esters (Biodiesel) as shown below[2]:

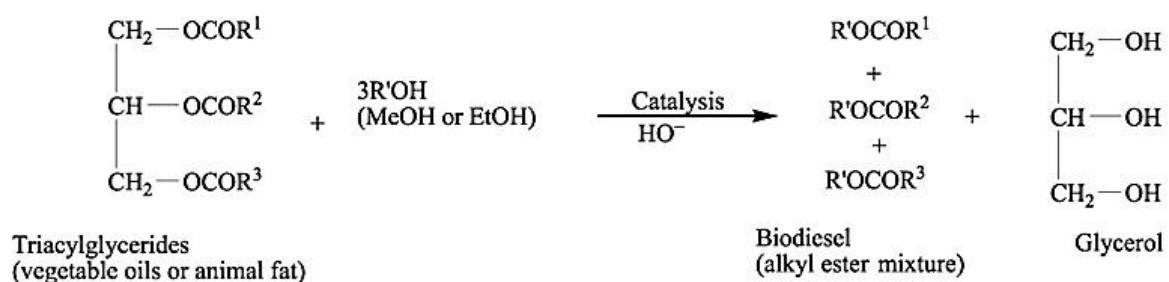


Figure 1: Reaction mechanism of transesterification for vegetable oil. It is a three step process: in the first step triglycerides (Glyceride) convert to diglycerides, in step two diglycerides convert to monoglycerides and finally monoglycerides convert to glycerol resulting in FAME, where R1, R2, R3 represent long fatty acid chains.

Currently, there are several well established and accepted technologies available to produce biodiesel. Vegetable oils/animal fats can easily be modified by reducing their viscosity and can then be used as diesel engine fuel. These modification processes involve micro-emulsions, pyrolysis of vegetable oil and transesterification [3]. Transesterification is the most commonly used method for biodiesel production on industrial and laboratory scale and will be discussed in more detail in the following sections.

2.1.1 Transesterification of Oils

The transesterification involves the reaction between oils (triglycerides) and alcohol which form biodiesel (fatty acid alkyl esters, FAAE) as the main product and glycerin as a by-product, as shown in Figure 1. It is a three step process: in the first step triglycerides convert to diglycerides, in step two diglycerides convert to mono-glycerides and finally, monoglycerides convert to glycerol resulting in one FAAE molecule in each step from each glyceride [3]. There are several factors which influence the yield of biodiesel during the transesterification process, as listed below [1],[3]-[4]:

- Free fatty acid content and water content of the feedstock
- Reaction temperature
- The molar ratio of alcohol to oil
- Type and concentration of catalyst
- Type/chemical structure of alcohol

- Reaction time
- The intensity of mixing (rpm)
- Use of co-solvents

2.1.2 Effect of Type and Concentration of Catalyst

The triglycerides and alcohols are not soluble in each other. Without a catalyst, transesterification proceeds therefore slowly, due to the poor surface contact of the reactants. The use of a catalyst improves the surface contact and the reaction proceeds faster and hence increase the biodiesel yield. Commercially, biodiesel is produced in a homogenous base catalytic transesterification process, where the catalyst remains in the same liquid phase as the reactants. The homogeneous catalysts include NaOH, KOH, and sulfuric acid; the heterogeneous ones involve lipases, CaO and MgO[1]. The amount of free fatty acids (FFA) in the feedstock highly affects the selection of a catalyst as acidic or basic. For feedstocks low in FFAs content < 5%, the base catalyzed reaction will give better yield with less reaction time while for feedstocks higher in FFAs content > 5%, the FFAs are first converted into FFAE by acid catalytic esterification followed by alkali transesterification to achieve the maximum yield[5]. Various studies show that a 98% biodiesel yield can be achieved by base catalytic (NaOH and KOH) transesterification processes performed under low temperature (333–338 K) and pressure (1.4–4.2 bar) conditions with low catalyst concentrations (0.5–2 wt.%) [6].

2.1.3 Effect of Molar Ratio of Alcohol to Oil

The basic transesterification reaction requires three moles of alcohol and one mole of triglyceride to yield three moles of FFAE and one mole of glycerol. The alcohol to oil molar ratio depends on the type of catalyst used. Various studies have been conducted to find out the optimum molar ratio values with other process factors i.e. temperature, wt. % of catalyst etc. for maximum yield of FFAE [7],[8],[4]. Rapeseed oil was metabolized using 1% NaOH or KOH, the best conversion was achieved at a molar ratio of 6:1 of methanol to oil [9]. Increasing the methanol content above this limit neither increases the product yield nor the ester content, but rather promotes the emulsion formation due to the polar hydroxyl group attached to it[10].

2.1.4 Effect of Reaction Temperature

Transesterification can occur at different temperatures ranging from 44.85 °C to 64.85 °C, depending on the oil used. It is recommended that the reaction temperature should not exceed the boiling point of the alcohol used; otherwise, the alcohol will boil, which will result in a much lower yield of FFAE. The boiling point of methanol is 60.5 °C. A study shows that a temperature above 49.85 °C negatively effects the product yield from neat oils, but had a positive impact on waste oils due to their higher viscosity.

2.1.5 Effect of Free Fatty Acid and Water in Feedstock

The purity of the feedstock significantly influences the efficiency of the alkali-catalysed transesterification process [10]. The FFA content and the water concentration of the reactants promote saponification and hydrolysis reactions as shown in Figure 2, reducing the biodiesel yield. The soap formation inhibits the biodiesel and glycerin phase separation process and also more wastewater will be produced in later stages of purification[11].

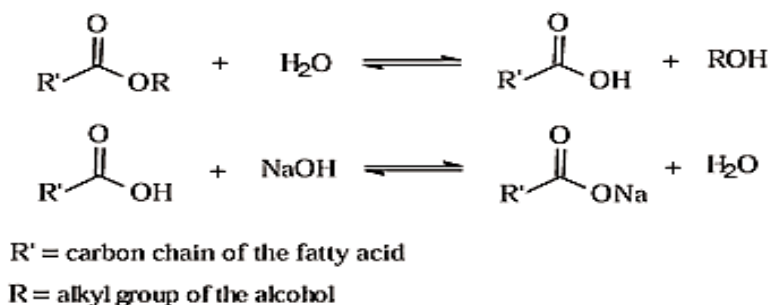


Figure 2: Side Reaction in Biodiesel Production including (a) Saponification of FFA and (b) Alkyl Ester Conversion to FFA by Hydrolysis [[5]].

2.1.1 Methanol and KOH or Methoxid As educt?

The alkaline catalysts use for transesterification of Oil includes hydroxides of Potassium and sodium and also Methoxides of K and Na. Studies show that when alkali hydroxides are mixed with Methanol small amount of water also produces that decrease catalyst efficiency. On the other hand, the use of methoxides speeds up the transesterification reaction and no water is produce. [12]

2.1.2 Problems with H₂O in the reaction mechanism

The presence of water in the reaction mixture promotes the soap formation, which consumed the catalyst and reduced catalyst efficiency. The soaps cause an increased viscosity, formation of gels and made the separation of glycerol difficult. [13]

2.2 Limitations of Conventional Methods of Biodiesel Production

The reaction kinetic studies show that transesterification of vegetable oil is a reversible reaction; hence backward reactions will affect the product yield [14]. According to Le Chatelier's principle, large quantities of alcohol are required to shift the equilibrium of the reaction to the product side thus increasing the yield of biodiesel [15] but that raises the production cost. The alcohol consumption can be reduced by using acid or alkaline catalysts, which could improve the reaction rate and biodiesel yield. The application of acid catalyst is limited due to the slow process, high-temperature requirements and corrosion issues. The use of homogeneous alkaline catalysts overcomes these issues, but the presence of water and FFA in feedstock promotes the saponification reactions as shown in Figure 2 and reduces the catalyst efficiency. The dissolved soap in the glycerol phase would increase the solubility of methyl ester in the glycerol and complicate the subsequent separation process [16] and subsequently result in more waste water in purification stages. These side reactions

can be avoided by replacing alkaline catalyst with enzyme catalysts, which, however, reduces the speed of the transesterification to 2-24 hours.

The application of a heterogeneous catalyst provides an alternative solution to replace the homogeneous catalyst because of its non-corrosive and environment-friendly nature. However, the mass transfer problems associated with the three phase system (triglycerides, alcohol, and solid catalyst) in the reaction mixture affect the pore diffusion process and reduce the available active sites for reaction and thus decrease the rate of the reaction[17].

On a laboratory scale, biodiesel has been successfully produced using supercritical alcohols without a catalyst. This strategy overcomes the mass transfer limitation by enabling the mixture of triglyceride and alcohol to become a homogeneous phase [18]. The supercritical alcohols transesterification reaction requires high temperature(>300 °C) and pressure(>40 MPa) conditions that not only increase the production cost but also raise safety issues associated with the large-scale industrial production of biodiesel.

The downstream process for both the catalytic and non-catalytic transesterification process receives a mixture of biodiesel, glycerol and unreacted reactants and catalysts. To obtain high purity biodiesel, further processing stages such as glycerol phase separation, catalyst neutralization, and water wash are complementary. These processing steps are time-consuming and require additional cost. A recent report revealed that the current downstream processing alone constituted over 60-80% of the total cost of a transesterification process plant [19].

2.3 Transesterification Process & Intensification Using Microreactor Technology

As discussed above, traditional biodiesel production methods are facing issues like long residence time, high operation costs and energy consumption and low efficiency. The new innovative technologies for process intensification provide reliable solutions to these problems. The main features of these processes are enhanced reaction rate, reduced molar ratio of alcohol to oil, and low energy input realized by intensification of mass and heat transfer.

These technologies, which include innovative reactor designs, such as static mixers, micro-channel reactors, oscillatory flow reactors, cavitation reactors, rotating/spinning tube reactors, microwave reactors, and reaction/separation coupled technologies, such as membrane reactors, reactive distillation, and centrifugal contactors, have significant potential for the enhancement of biodiesel production[20].

Microreactors, which can achieve rapid reaction rates by utilizing high surface area/volume ratio, improving the efficiency of heat mass transfer and shortening the diffusion distance, have shown quite a high yield of biodiesel at short residence times in biodiesel production[21]. Researchers believe that implementation of this technology into biodiesel production could be a next big breakthrough not only in process intensification but also in process economics.

2.4 Comparative Study of % FAME obtained in batch reactors and Microreactor

Table 1: Comparison between Different Processing Factors of Biodiesel Production in Batch Reactor and Microreactors [50]

Reactor Type	FAME [%]	Residence time [min]	Temperature [°C]	Oil	Catalyst
Stirred-tank reactor	58.8–97.3	40–70	60	Palm oil	KOH
Microwave heating reactor	94.4–95.25	0.56	50	Soybean oil	KOH
Ultrasonic Reactor	72–96	10–30	38	Palm oil	KOH
Reactive distillation reactor	41.5–97	2.67–6.67	55	Canola oil	KOH
Microreactor	82–89	0.43	60	Soybean oil	KOH

2.5 Patents List for Industrial Biodiesel Production Processes

Table 2: Online available Patents for Biodiesel Production Process

Patent Number	Publication Info	Priority Date	Reference
US8580119 B1	Nov 12, 2013	Nov 27, 2012	[22]
US8603198 B2	Dec 10, 2013	Jun 23, 2008	[23]
US 8624073 B1	Jan 7, 2014	Feb 5, 2013	[24]
US 20090126262 A1	May 21, 2009	Nov 20, 2007	[25]

Reaction Conditions for Synthesis of Biodiesel from different Vegetable Oils in Microreactors

2.6 Influence of Factors affecting Percent FAME Yield in Microreactors

Table 3: Online available Patents for Biodiesel Production Process Analytical Methods for Monitoring of Transesterification in Microreactors

Oil	Microreactor	Catalyst amount	Temperature [°C]	Molar ratio (MetOH:Oil)	Residence Time	FAME Yield [%]	References
Rapeseed oil	Quartz capillary (i.e.: 0.25 mm)	1 wt% KOH	60	6:1	5,89 min	99,4	[26]
Sunflower oil	Microtube Reactor with T-shaped mixer. (i.e.: 0.8 mm)	4,5 wt% Or 1 % KOH	60	23.9:1	100 s	100	[27]
Soybean oil	Stainless Steel Tube filled with spherical steel balls	KOH	60	16:1	1 min	-	[28]
-	Parallel microchannels on a plastic plate	NaOH	40-45	-	4-10 min	90-96	[29]]
Soybean oil	Zigzag microchannel reactor	1,2 wt% NaOH	56	9:1	28 s	99,5	[30]
Soybean oil	Microreactor (microchannel width: 100 µm)	1 wt% NaOH	25	7.2:1	10 min	91	[31]
Cottonseed oil	RIMM and SIMM-V2	1wt% KOH	70	8:1	17 s	99.5	[26]
-	Microreactor (channel width: 300 µm)	0,1 M CH ₃ ONa	r.T	-	2.6 min	100	[32]
Sunflower oil	Microtube (I.D: 1.27 mm)	3 wt% NaOH	60	9:1	80 s	97	[33]
Soybean oil	Micromixer connected to an empty tube; I.D: 1-cm L: 10-cm	2 wt % KOH	60	6:1	38 s	99.2	[28]
Soybean	Microreactor I.D: 0.8 mm	1.2 wt% KOH	60	9:1	180 s	98%	[22]

The final product, which is biodiesel, always includes undesirable rests like unreacted chemical precursors triacylglycerol, residual alcohol, and residual catalyst. In addition, the small amount of mono- and diacylglycerols, which are formed during the reaction, can be found in the biodiesel. Such contaminants can negatively influence the desired biodiesel quality and lead to operational problems including engine deposits and clogging of the filter [34] [35] [10, 36].

The determination of biodiesel quality and monitoring of the transesterification are therefore a very important issue in the future biodiesel production [36]. Various analytical methods have been developed for analyzing chemical compounds and physical properties of biodiesel. Two of the generally used analytical methods are chromatography and spectroscopy [37].

2.6.1 Spectroscopic Methods

Mid-infrared spectroscopy (MIR) includes the spectral range from 2500 to 25000 nm, where all molecular bonds such as O-H, C-H, N-H and C=O would be absorbed [38]. Because of higher intensity and specificity of the signal in this region, the MIR can be used for qualitative as well as quantitative analyses of chemical components. The MIR plays an important role for analyses of educts of biodiesel, especially for free fatty acid (FFA). The research results of Sherazi et al. demonstrates that FTIR spectroscopy is a simple, convenient, and accurate alternative to the standard titrimetric method for the determination of FFA. This approach allows no sample preparation, low amount of needed lipid extract and rapid determination of the FFA [39].

Other research work reported the online monitoring of variables of transesterification reaction such as ratio of alcohol to oil and amount of catalyst by using of the Continuous Fuel Dilution Analyzer (CFDA) FTIR. The resulting curves measured at 1436 cm^{-1} demonstrate that more methanol leads to the changes in spectra. With a help of partial least square (PLS) calibration, the course of the biodiesel process can also be investigated[40].

In his review, Zhang describes that MIR can be used to determine the biodiesel blend level, biodiesel properties and different contaminations inside the biodiesel [35]. Near infrared spectroscopy (NIR) represents the spectrum of a combination of tones and overtones, especially of functional groups such as CH, OH and NH bonds [38]. NIR can be used for quantitative analyses of chemical mixtures. This method is more cost-effective and less time-intensive and needs little or no sample preparations compared to conventional analytical methods (HPLC and GC). These are the reasons why the NIR has received increased interest in the process control [41].

NIR spectroscopy was used for the analysis of the turnover from triacylglycerol feedstock to methyl ester process. The spectra change of these classes of compounds is the basis for the quantitation of the final product. In the NIR range at 6005 and at 4425– 4430 cm^{-1} , methyl esters display peaks, but triacylglycerols are the only shoulder that could be found. Better quantitation has resulted by the absorption at 6005 cm^{-1} . Hence ethyl esters and perhaps even higher esters may be characterized also by near-infrared spectroscopy from triacylglycerols [42].

Naresh et al. developed an analytical method for the monitoring of the transesterification reaction. The Fourier-Transformations-Infrared spectroscopy (FTIR) was appropriate to investigate the biodiesel part in the reaction mixture. The nonlinear classical least-square (CLS) method for calibration was developed to predict the concentration of biodiesel and oil. The results show that this method allows the identification of the oil and biodiesel content in the biodiesel– petrodiesel– oil with an accuracy of about 95.32% [43].

The content of water and methanol in industrial and laboratory-scale biodiesel samples was analyzed by Felizardo et al. A qualitative analysis of the spectra by principle components analysis was performed and partial least squares regression was used to develop calibration models. The results show that NIR spectroscopy in combination with multivariate calibration is a capable system to evaluate the quality of biodiesel in both laboratory- scale and industrial scale samples [44].

Coronado et al. reported that regressions based on near-infrared spectroscopy were developed for relatively inexpensive and rapid on-line of the determination of the concentration and significance of biodiesel-diesel blends. Methyl esters of five different oils and two different brands of commercial-grade were used in the calibration and validation processes. The NIR range of 2080 to 2200 nm was found suitable [45].

Baptista et al. worked on the application of NIR spectroscopy to find out the ester amount in biodiesel as well as the part in linolenic acid methyl esters (C18:3) in industrial and laboratory-scale biodiesel samples. Principal component analysis (PCA) was used for the qualitative analysis of the spectra and partial least squares regression (PLS) was chosen to establish the calibration models between analytical and spectral data. The main results presented that NIR spectroscopy, in combination with multivariate calibration, seems to be a promising technique for the biodiesel quality control in laboratory-scale and industrial scale samples [46].

The two IR techniques MIR and NIR spectroscopy are promised methods for quantification and qualification of biodiesel quality. The advantages of these methods are faster, more sensitive and less costly for process monitoring and analysis.

2.6.2 Chromatography Methods

As mentioned above, after biodiesel production there can be leftovers in the biodiesel which can be unreacted starting material (TAG), residual alcohol, and residual catalyst. Furthermore, there can be monoacetyl glycerol (MAG) and diacetyl glycerol (DAG) in the final biodiesel caused by the stepwise transesterification. To detect this intermediate, chromatography methods such as GC (gas chromatography), HPLC (high-performance liquid chromatography) and GPC (gel permeation chromatography) can also be used.

2.6.2.1 Thin Layer Chromatography

The thin layer chromatography (TLC) for detection of biodiesel components mostly is used with flame ionization detection (FID) (TLC/FID). The first paper about this method was published by Freedman et

al in 1984 [47]. This paper also tells about the advantage of this method: The technique is easy to learn and use but because of the outweighing disadvantages, which are lower accuracy and material inconsistencies, as well as sensitivity to humidity and the relatively high cost of the instrument, it has been largely abandoned [48] [47].

In addition, the effect of reaction time on transesterification was carried out by Leung and Gao in 2006 [10] [8].

2.6.2.2 Gas Chromatography

Gas chromatography is the most widely used method for the analysis of biodiesel as well as glycerol, mono- di, and triglycerides in vegetable oil as well as methyl and ethyl esters because of the higher accuracy in quantifying even minor components [36] [49] [8]. Although the GC analysis can be influenced by factors like baseline drifts, overlapping signals, and aging of standard or samples, this is not always clearly addressed in standards and reports.

Freedman et. al were the first who discussed the quantification of esters, mono-, di- and triacylglycerols with the use of capillary gas chromatography. Therefore it was used a 100% dimethylpolysiloxane column (1,8 m x 0.32 mm i.d.). [50]. Moreover, there are similar reports such as Mariani et al. or Plank and Lorbeer [51] [52]. However, they used other specifications of the column as Freedman ((5%-phenyl)-methylpolysiloxane, column length, etc.). The determination of a specific contaminant in the methyl esters was also discussed in all of the mentioned reports.

Also the determining of methyl and ethyl esters from used frying oil by GC is a well-known method [53] [54] [55] [56].

In 1997 Cvengrošová et al investigated the analysis for rapeseed ethyl esters on GC using a flame-ionization detector (FID) with a 1.8 m x 4 mm i.d. packed column [57]. The usage of FID for GC analysis is very common and has been mentioned in several reports [58] [59] [36]. Variations of the types of column packing as well as different carrier gasses, such as nitrogen [60] [61] [62] [63] [64], helium [65] [66] and hexane, are also discussed. In addition, mass spectrometric detectors are also a often used method of choice [60] [61] [62] [63] [64].

2.6.2.3 High-Performance Liquid Chromatography

There are fewer reports about High-Performance Liquid Chromatography (HPLC) for analysis of biodiesel available despite the advantage of saving analysis time by loss of time- and reagent consuming derivatization compared to GC [36] [49].

The first system for the detection of mono-, di- and triacylglycerols as well as methyl esters as classes of compounds by HPLC was the use of an isocratic solvent system, which was chloroform with an ethanol content of 0,6% on cyano-modified silica columns coupled to two permeation chromatography (GPC) columns with density detection [67]. Other reports tell the quantification of the percentage yield of ethyl esters by means of HPLC on a silica column using hexane: diethyl ether: acetic acid (90:10:0,5 v/v) as mobile phase [68], [69]. There are also studies of using the HPLC with pulsed

amperometric detection [70] or an evaporative light scattering detector (ELDS) for quantitating product esters, free fatty acids, and acylglycerols [71]. For the usage of reversed-phase HPLC with two gradient solvent systems, different detection methods have been worked out, such as UV detection at 205 nm, ELDS, and atmospheric pressure chemical ionization mass spectrometry (APCI-MS) in positive-ion mode. [72] Eventually, the sensitivity and linearity of each detection method varied with the individual triacylglycerols. In this case, the most suitable detection method for the analysis of rapeseed oil and biodiesel is APCI-MS. [72] [36]

2.6.2.4 Gel Permeation Chromatography

There is literature about using gel permeation chromatography (GPC) such as those of Jacobsen et al. who used an RI detector and THF as a mobile phase [73] or Darnoko et al, who use a very similar concept as with the analysis with HPLC [74].

2.6.3 Thermo-gravimetric analysis methods

To determine the yields of alkyl ester, it is also possible to use thermo-gravimetric analysis (TGA). This was carried out by Çaylı et al, Goodrum et al and Chand et al [75-77].

2.7 Market analysis

The market analysis was made to show the distribution of biodiesel producers in Germany and also in Europa. Unfortunately there were some difficulties getting the information of interest. There were also phone calls with some producers in Germany made. One company told that biodiesel is not going through a good time in public and that's the reason why on the one hand it's hard to find the producing companies and on the other hand why these companies don't want to give further information about their production amount. The only information they give is the production capacity per year. Furthermore, the spoken company told that every company would say, that their machines work 365 days per year, 24 hours per day if ask for the percentage of capacity. There are some market surveys about biodiesel available but all of them are very cost expensive.

The table below shows the biodiesel producing companies that were found for Germany.

Table 4: Biodiesel producing companies in Germany

producer	location	production capacity [t per year]
ADM Hamburg AG- Werk Hamburg	Hamburg	n.a.
ADM Hamburg AG- Werk Leer	Leer	n.a.
ADM Mainz GmbH	Mainz	n.a.
BIO-Diesel Wittenberge GmbH	Wittenberge	120.000
Bioeton Kyritz GmbH	Kyritz	80.000
BIOPETROL ROSTOCK GmbH	Rostock	200.000
Biowerk Sohland GmbH	Sohland	50.000
BKK Biodiesel GmbH	Rudolstadt	4.000
C. Thywissen GmbH	Marl	n.a.
Cargill GmbH	Frankfurt/Main	300.000
EAI Thüringer Methylsterwerke GmbH (TME)	Harth-Pöllnitz	45.000
ecoMotion GmbH	Lünen, Sternberg, Malchin	212.000
gbf GmbH German Biofuels	Pritzwalk	130.000
german biofuels GmbH	Falkenhagen	130.000
Glencore Madebur GmbH	Magdeburg	180.000
Glencore Magdeburg GmbH	Magdeburg	70.000
Gulf Biodiesl Hall GmbH	Halle	56.000
KFS-Biodiesel GmbH	Cloppenburg	30.000
KL Biodiesel GmbH & Co. KG	Lülsdorf	120.000
Louis Dreyfus commodities Wittenberg GmbH	Lutherstadt Wittenverg	200.000
MBF Mannheim Biofuel GmbH	Mannheim	100.000
Mercuria Biofuels Brunsbüttel GmbH	Brunsbüttel	250.000

NEW Natural Energie West GmbH	Neuss	260.000
Petrotec AG	Emden	100.000
Petrotec AG	Südlohn	85.000
Rapsol GmbH	Lübz	6.000
TECOSOL GmbH (ehem. Campa)	Ochsenfurt	75.000
Ullrich Biodiesel GmbH/IFBI	Kaufungen	35.000
Verbio Diesel Bitterfeld GmbH & Co. KG (MUW)	Greppin	190.000
Verbio Diesel Schwedt GmbH & Co. KG (NUW)	Schwedt	250.000
Vesta Biofuels Brunsbüttel GmbH & Co. KG	Brunsbüttel	150.000
Vogtland Bio-Diesel GmbH	Großfriesen	2.000

3 Material and Samples

3.1 Material

In the following sub-chapters, there are listed, the used chemicals, the consumables, the equipment for the measurement and preparation of the samples and the samples itself that were tested.

3.1.1 Chemicals

The chemicals that were used for all experiments are listed below.

Table 5: Chemicals for all experiments

Substance	Description	Producer
Methanol	Methyl-Alkohol; chemisch rein in 2 L Salzkonten	Brenntag GmbH
Ethanol	Ethanol 99 vg. 1 % MEK	Brenntag GmbH
Isopropanol		
Potassium-Hydroxide	Purum p.a.; Pastillenform; $\geq 85\%$ (T)	Fluka Chemie GmbH
Molecular sieve	Molekularsieb 0,3 nm in Perform; absorbiert NH_3 , H_2O ; geeignet zur Trocknung polarer Lösungsmittel	Merck KGaA
Magnesium-Dioxide		
Rapeseed Oil		Gut & Günstig

3.1.2 Laboratory Apparatus

Table 6: Laboratory apparatus

Substance	Description	Producer
Round-bottom flask	mit Rundschliff und Implosionsschutz; 500 mL	Schott Duran®; Sovirel France
Three-neck-flask	500 mL	Schott Duran®
Erlenmeyer-flask	250 mL	Schott Duran®
Separating funnel	k.A.	Schott Duran®
Dropping funnel	200 mL	Schott Duran®
Crystallisation bowl	k.A.	Fisherbrand®
Beaker glass	250 mL; 500 mL; 600 mL; 1000 mL; 3000 mL	Schott Duran®

Volumetric flask	250 mL	Fisherbrand
Measuring Zylinder	500 mL, 100 mL	
disposable pipette	-k.A.	k.A.
Eppendorf pipette	0-1000 µL	Eppendorf AG
Volumetric pipette	50 mL, 100 mL,	Brand
Burette	50 mL	Scherf
Glas stirrer	k.A.	k.A.
Magnetic stirrer	k.A.	k.A.
Glass stopper	k.A.	k.A.
Plastic stopper	k.A.	k.A.
suction flask	k.A.	k.A.
Crucible with adapter	k.A.	Haldenwanger Berlin
Water jet pump	k.A.	Brand
Küvette 0,5 mm	Schichtdicke: 0,5 mm; 106-QS (Quarzglas Suprasil® 200-2500 nm);	Hellma GmbH & Co. KG Mülheim

3.1.3 Consumables

Table 7: Consumables

Substance	Description	Producer
Bottles with snap-on caps	25 mL; dimensions 65 mm x 26 mm	k.A.
sealing film	Parafilm PM-996; Rolle mit	Bemis AG
Lint-free tissues	Kimtech Science (KC7552)	Kimberly Clark
Fibre paper	Art.-Nr.: 9.413220	Lab Logistics
Mucasol		Group GmbH
Rundfilter 595	595 Rundfilter, Durchmesser 125 mm; Ref.No.	k.A.
		Schleicher & Schuell

3.1.4 Equipment

Table 8: Equipment

Substance	Description	Producer
Solid stand		
Solid stand equipment		
Magnetic stirrer with electric heating plate	IKA RCT basic mit elektr.	Ika Rct Basic (Janke & Kunkel)
contact thermometer	Kontaktthermometer Ika ETS-D5: Pt1000-Meßfühler; -10°C bis 450°C	

Magnetic stirrer with electric heating plate contact thermometer	Typ Arex digital pro mit Vertex Digital Thermoregulator	VELP Scientifica
Flow cell	Hellma Axiom FFV-320R-X : Temperierbare Transmissions-Messzelle mit einstellbarem Lichtpfad von 0,5 mm bis 12 mm; max. Temperatur: 180°C; max. Druck: Durchflussmesszelle Hellma 170.700	Hellma Axiom GmbH
Flow cell		Hellma Axiom GmbH
Transmissions-Immersionssonde	TIDAS 1121, Type: ASPEN, 1mm	J & M analytics
Weighing machine	Mettler PM460 DeltaRange Balance: Feinbereich: 60 g; Grobbereich: 400 g;	Mettler-Toledo GmbH
Digital thermometer	Stabthermometer Modell E514; Messbereich: -45°C bis 200°C	Sunsartis ®
Rotationsverdampfer	Typ Rotavapor RE-111 mit Wasserbad Büchi	Büchi
Druckmessgerät	DVR 1: 1-1300 mbar	Vacuubrand
Vakuumpumpe		KNF Neuburger Laborbedarf
Tungsten Lichtquelle	Tungsten-Vakuum-Lampe; #61005	Spectral Engines AG
Lichtwellenleiter	P1000-2-VIS/NIR; 727-733-2447	OceanOptics

3.2 Samples

Table 9: Laboratory samples

Batch Samples ID	Description	Ratio	Measurement Type
Batch_01_A,B,C(1-5)	Like Matheo	Volumatric	Offline
Batch_02_A,B,C(1-5)	Like Matheo	Volumatric	Offline
Batch_03_A,B,C(1-5)	Like Matheo	Volumatric	Offline
Batch_04_A,B,C(1-5)	Like Matheo	Volumatric	Offline
Batch_Alltogether_1st_A,B,C(1-5)	Alltogether(Oil+M+KOH)	Volumatric	Offline
Batch_Alltogether_2nd_A,B,C(1-5)	Alltogether(Oil+M+KOH)	Volumatric	Offline
Batch_07_A,B,C(1-5)	Like Matheo	Volumatric	Inline-TDIAS/Offline
Batch_08_A,B,C(1-5)	Like Matheo	Volumatric	Inline-TDIAS/Offline
Batch_09_A,B,C(1-5)	Alltogether(Oil+M+KOH)	Molar	Inline-TDIAS/Offline
Batch_10_A,B,C(1-5)	Alltogether(Oil+M+KOH)	Molar	Inline-TDIAS/Offline
Batch_11_A,B,C(1-5)	Alltogether(Oil+E+KOH)	Molar	Inline-TDIAS/Offline

4 Methods

4.1 Batch Reaction

4.1.1 Laboratory set-up and general how to

The first experiments that were done were the so-called batch experiments. There, Biodiesel was produced in a discontinuous process in vessels.

The first batches were performed according to the instructions of Matheo Baumann and his master thesis, to proof if the same result could be achieved. Baumann performed all his experiment with a volumetric ratio.

Thus, a solution of 360 mL methanol and 1.08 g KOH were heated up to 58 °C in a three neck flask, using a reflux condenser and a water bath. If the temperature was reached, 60 mL of rapeseed oil were added via a dropping funnel within 6- 10 minutes. After the dropwise addition, the reaction was continued for a further 30 minutes. Finally, samples of this first step were taken for the spectra and the further purification steps are carried out (Step A).

The first purification step is the deposition of glycerol. Therefore the methanol of reaction mixture was separated with a rotary evaporator. Afterward the two phases (glycerine lower and the biodiesel upper phase) were separated with a separating funnel. This step lasted several hours until two sharp phases were visible. Glycerol was drained and a sample was taken (Step B).

However, the biodiesel phase still contained impurities (e.g. soap formation and salts). This was neutralized by the addition of a dilute hydrochloric acid and washed with distilled water in two to three washing operations.

The last step was the drying of the biodiesel of any existing water. Therefore a molar sieve was used. Another sample was taken (Step C).

There were also made some experiments by using magnesium sulfate for drying, which is a common method in the organic chemistry. But there were no differences apparent between both methods. So the molar sieve was used because of its recycling abilities.

Then, some experiments were made with a volumetric and molar ratio but without the dripping step of the oil. Therefore all the educts were mixing together in the three neck flask from the beginning. These experiments are called "altogether".

For the batch reactions the TIDAS spectrometer and the inline NIR probe connected by optical fibers was used to measure the different mixtures. In 500 mL three neck flask the components were weighed and a magnet stirrer was added. To fix both the inline NIR probe and the flask laboratory clamp was used. Due to the high intensity of the light source, an additional optical fiber was interconnected to reduce the intensity. Otherwise, the spectra will not be plotted completely.

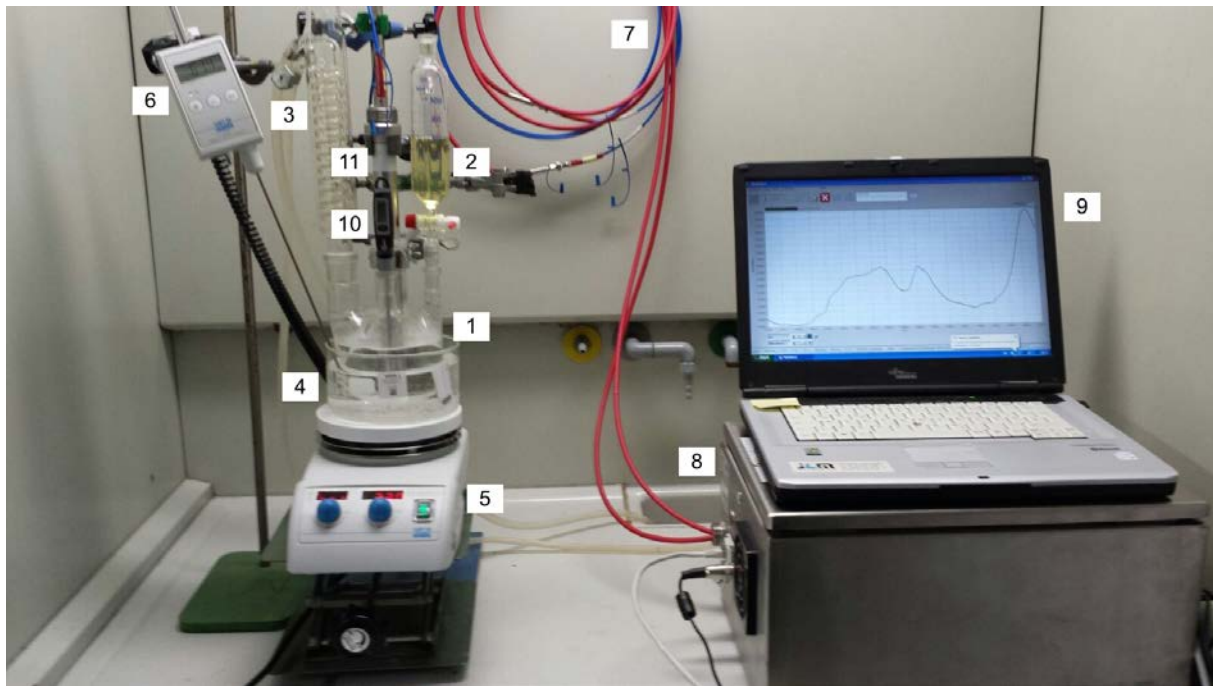


Figure 3: Laboratory setup for batch reaction 1) three neck flask 2) dropping funnel 3) reflux condenser 4) crystallization tray with water 5) hot plate 6) thermometer connected to hot plate 7) optical fibre 8) TIDAS spectrometer 9) laptop with software 10) NIR probe 11) Thermometer for the batch reaction

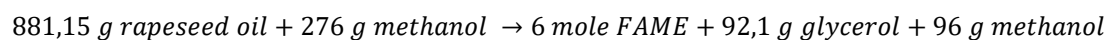
4.1.1.1 Molar Ratio

The following shows the reaction of biodiesel synthesis:



According to the law of le Chatelier, the amount of methanol is doubled to force the equilibrium on the product side. This method is also used in industry. In the second line, the molar weights of the single substances are added. Please note that the used number for the molar weight of the rapeseed oil was determined experimentally by the saponification number. The molar weighs for FAME is unknown because of the changing structure. $1 \text{ mol rapeseed oil} + 6 \text{ mol methanol} \rightarrow 6 \text{ mole FAME} + 1 \text{ mol glycerol} + 3 \text{ mol methanol}$

$$1 \text{ mol} \cdot 881,15 \frac{\text{g}}{\text{mol}} + 6 \text{ mol} \cdot 46 \frac{\text{g}}{\text{mol}} \rightarrow 6 \text{ mol FAME} + 1 \text{ mol} \cdot 92,1 \frac{\text{g}}{\text{mol}} + 3 \text{ mol} \cdot 32 \frac{\text{g}}{\text{mol}}$$



These results were adjusted for the sizes of the used lab equipment. So, the following weights were used for the experiments with a molar ratio:

$$m(\text{KOH}) = 5,69 \text{ g}$$

$$m(\text{methanol}) = 64,1 \text{ g}$$

$$m(\text{rapeseed oil}) = 294,4 \text{ g}$$

$$v(\text{methanol}) = 81\text{mL}$$

$$v(\text{rapeseed oil}) = 320\text{mL}$$

The amount of KOH which was used as a catalyst was calculated with the rule of three comparing the values of the used amount of the volumetric ratio.

molar weights:.

Densities:

molar weights:

$$\delta = \frac{m}{V}$$

$$M(\text{rapeseed oil}) = 881,15 \frac{\text{g}}{\text{mol}}$$

$$\delta(\text{rapeseed oil}) = 0,920 \frac{\text{g}}{\text{mL}}$$

$$M(\text{glycerol}) = 92,1 \frac{\text{g}}{\text{mol}}$$

$$\delta(\text{methanol}) = 0,791 \frac{\text{g}}{\text{mL}}$$

$$M(\text{methanol}) = 46 \frac{\text{g}}{\text{mol}}$$

$$M(\text{KOH}) = 32 \frac{\text{g}}{\text{mol}}$$

The experiments were performed after the same instruction like mentioned above. The only changes were the weights respectively the volumes of the used substances.

4.1.2 List of experiments

In table 10 the components and the amounts for one experiment of the different batch reactions are mentioned.

Table 10: The components and the amounts for one experiment of the different batch reactions

Number of batches	Name	Component	Amount experiment	for one	Total amount
6	Batches like Matheo	KOH	1,08	g	6,48 g
		Methanol	0,36	L	2,16 L
		Oil	0,06	L	0,36 L
2	altogether Volumetric Ratio	KOH	1,08	g	2,16 g
		Methanol	0,36	L	0,72 L

		Oil	0,06	L	0,12	L
2	altogether Molar Ratio	KOH	5,69	g	11,38	g
		Methanol	0,081	L	0,162	L
		Oil	0,32	L	0,64	L
2	altogether Molar Ratio	KOH	1,8	g	3,6	g
		Ethanol	0,035	L	0,07	L
		Oil	0,1	L	0,2	L

4.2 Pre-experiments with Microreactor:

4.2.1 Experimental Setup

The laboratory test setup for biodiesel production is presented in Figure A, the details of the individual component are described in the section 3.1.4. The values of the flow rate of Oil and Methanol with KOH solution and temperature in microreactor are selected at PLC panel(8), which then regulates the HPLC pumps(2) and thermostats (7) at set values respectively.

In the current setup, the maximum total flow rate achievable with pumps was 50 ml/min, a temperature of 40 °C. The reactants were pumped into microreactor through two inlets in bottom mixing plate. Then the mixture flows to upward direction and leaves the microreactor construction from the top plate and flows through the flow cell. It is important to notice that no air is pumped into the system otherwise it will influence the spectroscopic measurements in the flow cell. The temperature in microreactor is maintained by circulating the water through heating plates at a set temperature value. The temperature sensor was inserted into the bottom plate that monitors the temperature in the microreactor.

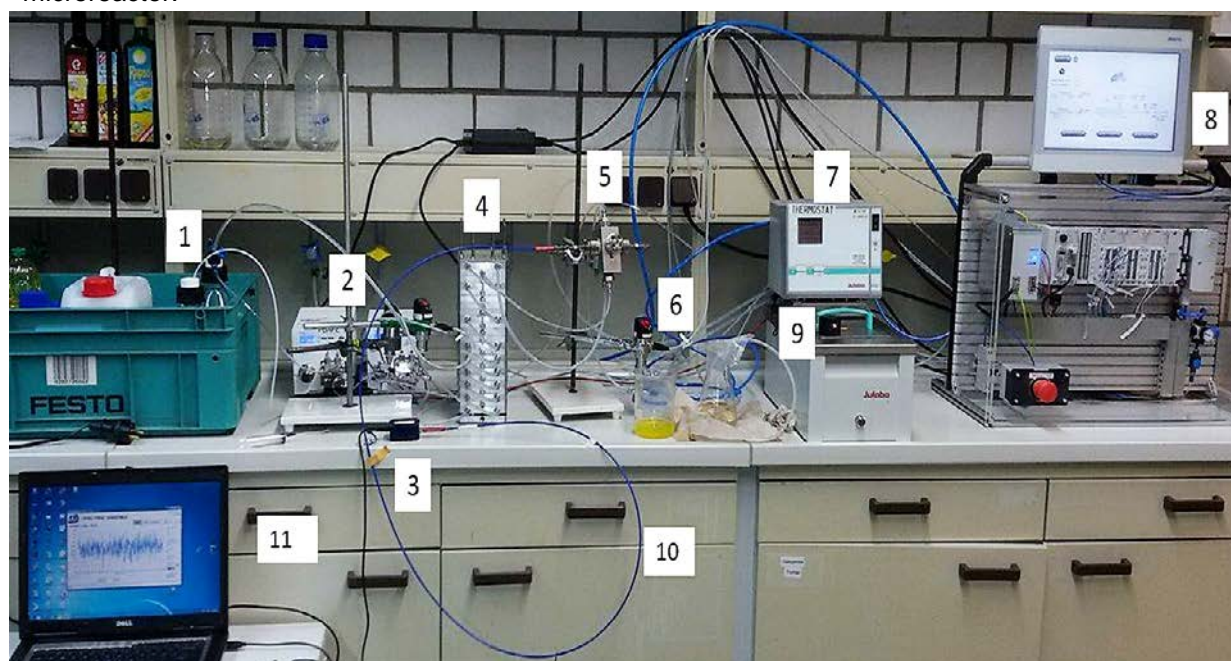


Figure 4: Laboratory test-setup for biodiesel production. 1) Pressurized glass bottles for Oil and Methanol with KOH solution, 2) HPLC pumps, 3) Spectrometer N 2.0, 4) Microreactor construction, 5) Flow cell, 6) Pressure sensor, 7) Thermostat Device, 8) PLC Panel with touch screen, 9) Light source, 10) Optical Fiber, 11) Laptop installed with software to collect spectral data.

Initially, the light source and spectrometer were installed in flow cell horizontally but due to signal saturation issue, an optical fiber (9) was installed to reduce the light intensity. The mixture of reaction products and unreacted reactants finally collected into the flask/beaker for further offline analysis or purification steps. Isopropanol is recommended for cleaning of the microreactor system, once the production cycle is complete.

4.2.2 Selection of Parameters for Pre-experiments

The various factors influencing the transesterification of oil are discussed in section 2.1.1 in detail. In current microreactor setup, temperature, flow rate and the molar ratio of Oil to Methanol were selected as controllable factors and their influence on transesterification was studied while other factors were kept constant. The aim of the project was to optimize the biodiesel production in the microreactor while measuring the spectral changes for these factors. Therefore it was decided to conduct pre-experiments to select maximum and minimum limits for above-mentioned factors to perform DoE.

In order to start pre-experiments, it was necessary to make sure that biodiesel can be produced in the microreactor. Therefore some trial experiments were conducted at a molar ratio of Oil to methanol (1:6) with same catalyst amount, as used in Batch 09 & 10 with a temperature of 60 °C and flow rate of 25 ml/min. The samples were then analyzed with Lambda spectrometer, and the biodiesel produced was found to be similar to batch 09 as shown in Figure 21.

The parameters selected for pre-experiments are shown in table 1 of Appendix. For each experimental run, 5 spectra were recorded with an interval of 10 seconds using Spectral Engine N2.0. Spectral data was then analyzed with the Unscrambler, results are shown in section 5.2.

4.3 Mixing Experiments

4.3.1 Mixing experiment of Oil and Methanol with catalyst and without catalyst at room temperature

The working package 6 of project outline was initially designed to determine the limit of quantification and limit of detection of biodiesel in methanol with three different spectrometers. But finally, it was decided to perform the mixing experiment with four components as Biodiesel, Oil, Methanol, and Glycerol and create a calibration model with TIDAS NIR Spectrometer.

For calibration model to perform well there shouldn't be any reaction take place between Oil and Methanol, otherwise, it will disturb the composition of the mixture and spectra would be misleading. To make sure that there is no reaction between Oil and Methanol in the absence of KOH catalyst at room temperature the following two experiments were conducted.

Table 11: Molar ratio, temperature, rpm, mixing time, wt% of KOH and volume of methanol and oil for the two experiments to show the effect of KOH at room temperature

Experiment No.	Oil:Methanol Molar ratio	Temperature °C	Rpm	Mixing Time min	KOH wt% Oil	Methanol ml	Oil ml
1.	1:6	20	620	25	no	20	80
2.	1:6	20	620	25	1.95	20	80

The experiment with KOH already formed a homogeneous mixture with 540 rpm where the experiment without KOH still formed two phases see in Figure 5. Furthermore, a difference in color occurs. It seems that the reaction takes place at room temperature and sufficient mixing.



Figure 5: Mixtures of Methanol and rapeseed oil without KOH (left) and with KOH (right) during mixing at 540 rpm. Left: Still, two phases are formed with methanol as the upper phase. Right: Homogeneous mixing of the two components due to the started reaction.

At 620 rpm the mixing is sufficient to form a homogeneous mixture of oil and methanol in the left experiment without KOH.



Figure 6: Mixtures of Methanol and rapeseed oil without KOH (left) and with KOH (right) during mixing at 620 rpm. Left: A homogeneous mixture is formed. Right: Difference in color occurs due to the starting reaction.

4.3.2 Collection of Spectral Data

The samples were collected at the end of mixing period. For each experiment, five samples were analyzed with Lambda spectrometer, spectral range selected from 1200 nm to 2491 nm. In experiment 1 at the end of mixing period there were two phases as methanol (above) and Rapeseed Oil (below), and for experiment 2 there were also two phases achieved as Biodiesel (above) and glycerol(below)(see Figure 7), the results are discussed in section 5.3.1.

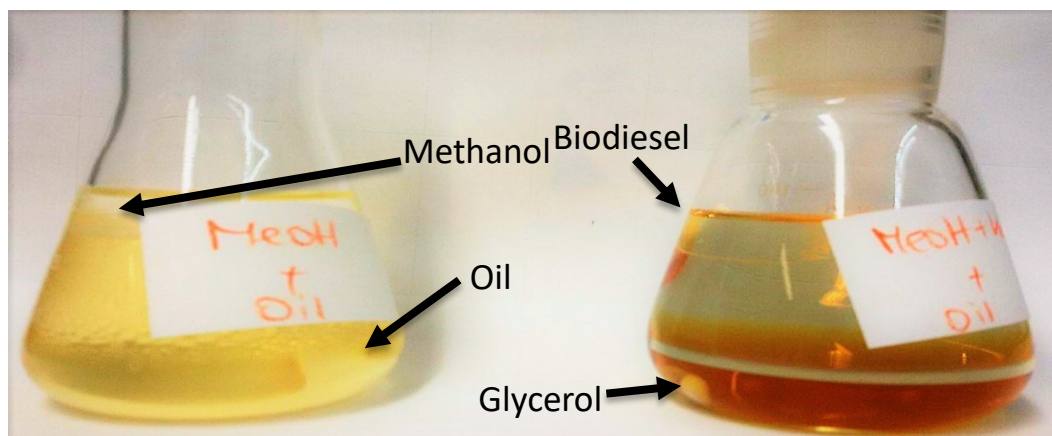


Figure 7: Mixtures of Methanol and rapeseed oil without KOH (left) and with KOH (right) after mixing. Methanol and rapeseed oil separates (left). Glycerol and biodiesel are formed (right)

4.3.3 DoE for Mixing Experiment

4.3.3.1 Factors Selection

In transesterification reaction Figure.1, each component shows characteristic absorption in NIR region. Therefore each component was selected as a factor to create a DoE. The maximum and minimum limits for factors were selected by considering the possible process environment in the Microreactor setup as shown in the following table:

Table 12: Minimum and maximum values in wt% for the DoE

Factors	Minimum Value(wt %)	Maximum Value(wt %)
Rapeseed Oil	0	100
Biodiesel	0	100
Methanol	0	100
Glycerol	0	10

Intransesterification reaction, one mole of oil reacts with 3 moles of methanol to produce 3 moles of Biodiesel and 1 mole of glycerol. The stoichiometric calculations show that if there is 100% forward reaction takes place than the glycerol produce will be the 10% of the reaction product by weight fraction and as a molar ratio of methanol to oil increases the weight fraction of glycerol in final product decreases.

4.3.3.2 Response Selection

There were no responses selected for Mixture Design because the Unscramble was used to develop the calibration model.

4.3.3.3 Design Selection for Mixing Experiment

The Design Expert software v.10.0.3 provides a variety of Mixture Designs. For current mixing experiment, D-optimal Mixture Design was selected because it works well for the multi-components system with unequal components range.

4.3.3.4 Changes in Design

The Design Expert software provides the flexibility to change the values of individual run according to experiment environment. The D-optimal design gave 23 experimental runs for four component system. The values were then manually changed such that there are more levels for each component in the whole range. Some experiments were replicated so that a good calibration model could be developed, as shown in the table 12.

4.3.3.5 Column Graph for Oil to methanol for Biodiesel

The column graph shows in Figure 8 a smooth change in biodiesel wt fraction with relative change in methanol and Rapeseed Oil wt fraction across the design space.

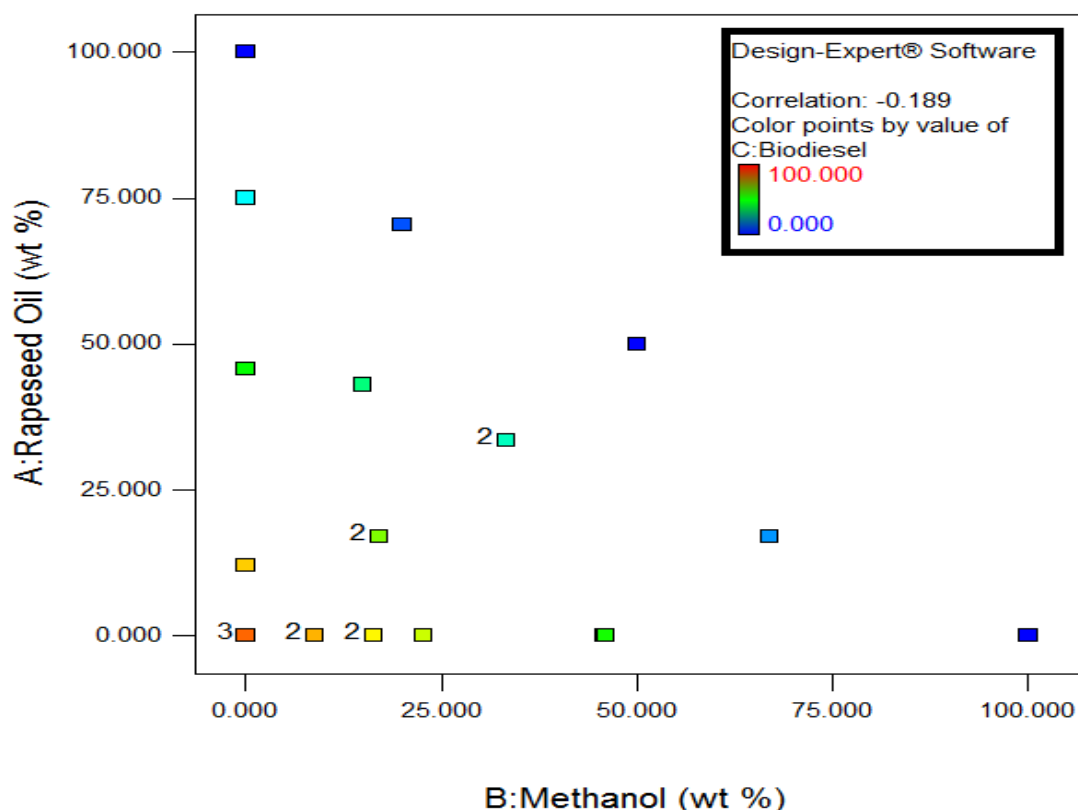


Figure 8: Column Graph for oil to methanol for biodiesel in wt% based on the D-optimal design

4.3.3.6 Final DoE

In table the final DoE with wt% of the four components for each run are shown. With the DoE the weights for each run were calculated see in the appendix table A. With this calculations the components were weighed in 250 mL flasks and a magnet stirrer was added. After fixing the flasks with laboratory clamps mixing was started. At a homogeneous state of the mixture, the measurements were started.

Table 13: Final DoE with the wt% for all components for each run

Run	Component 1 A:Rapeseed Oil wt %	Component 2 B:Methanol wt %	Component 3 C:Biodiesel wt %	Component 4 D:Glycerol wt %
1	0,00	22,78	69,92	7,30
2	33,43	33,24	31,33	2,00
3	43,00	15,00	38,00	4,00
4	0,00	45,79	50,21	4,00
5	0,00	8,90	82,50	8,60
6	0,00	0,00	90,00	10,00
7	75,00	0,00	25,00	0,00
8	45,79	0,00	50,21	4,00
9	0,00	100,00	0,00	0,00
10	50,00	50,00	0,00	0,00
11	0,00	16,40	75,70	7,90
12	100,00	0,00	0,00	0,00
13	33,43	33,24	31,33	2,00
14	16,99	17,10	62,36	3,56
15	12,15	0,00	79,95	7,90
16	0,00	8,90	82,50	8,60
17	16,94	66,95	14,72	1,39
18	70,50	20,00	8,12	1,38
19	0,00	0,00	90,00	10,00
20	0,00	46,00	52,00	2,00
21	16,99	17,10	62,36	3,56
22	0,00	0,00	100,00	0,00
23	0,00	16,40	75,70	7,90

4.4 Experimental Set-Up

For the mixing experiments, the TIDAS spectrometer and the inline NIR probe connected by optical fibers were used to measure the different mixtures. In 250 mL flasks, the components were weighed and a magnet stirrer was added. To fix both the inline NIR probe and the flask laboratory clamps were used. Due to the high intensity of the light source, an additional optical fiber was interconnected to reduce the intensity. Otherwise, the spectra will not be plotted completely.

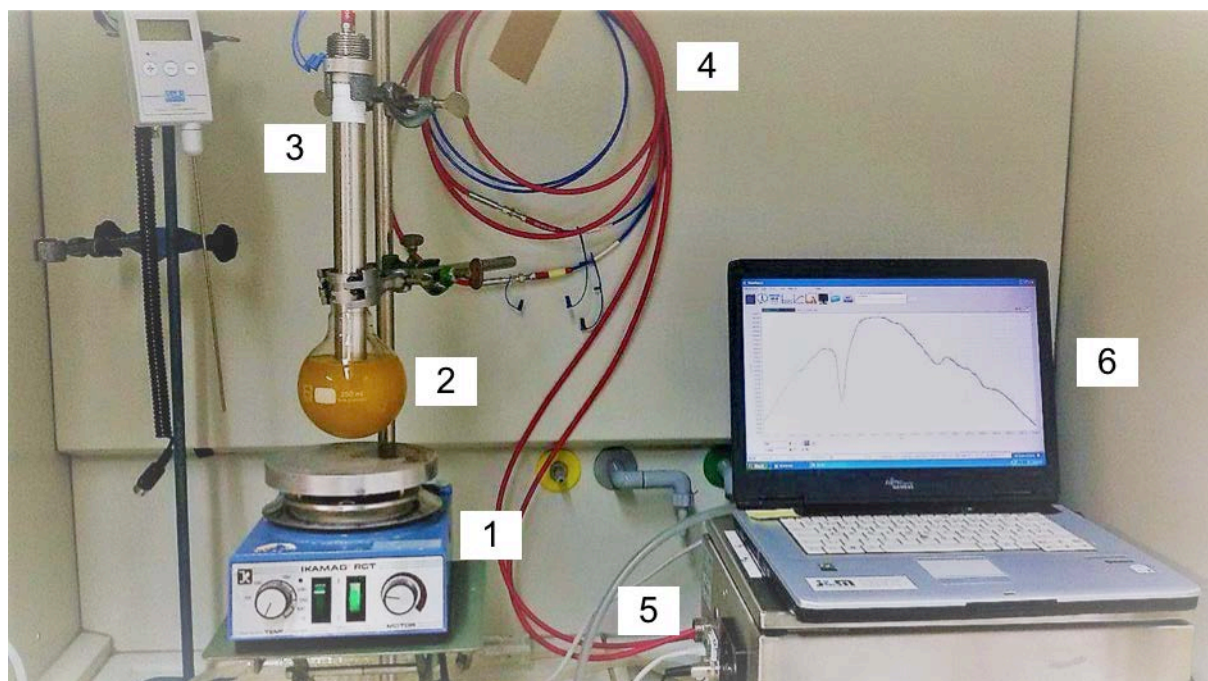


Figure 9: Laboratory setup for the mixing experiments: 1) hotplate with stirrer function 2) 250 mL flask 3) inline NIR probe 4) optical fiber 5) TIDAS spectrometer 6) PC with software

4.5 Spectrometer Parameters and References

4.5.1 Lambda 1050

The Lambda 1050 UV/Vis/NIR spectrophotometer was used to measure all samples of the batch reactions and purification steps. For this project a method with the suitable wavelength range from 1200 nm to 2600 nm was created with the software.

4.5.1.1 Air as Reference

For all sample measurements with the Lambda 1050 air was used as a reference. H₂O was not used as a reference because of broad absorption bands in NIR range. Methanol has a similar refractive index as water but methanol is present as a component for the batch reactions and the mixing experiments.

4.5.2 TIDAS

The TIDAS spectrometer is used with an NIR probe for the batch reactions and the mixing experiments. For inline measurements during the reactions or mixing a continuous and homogeneous mixing is required. For inline measurements with the TIDAS spectrometer an NIR range from 1200 nm to 2100 nm can be measured. For batch 5 to 8 integration time of 3,3 ms and averaging of 10, for batch 9 to 11 averaging of 650 and for the mixing experiments averaging of 200 was used.

4.5.2.1 Air as reference

For both experiments batch reactions and mixing experiments air is used as a reference. H₂O was not used as a reference because of broad absorption bands in NIR range. Methanol has a similar refractive index as water but methanol is present as a component for the batch reactions and the mixing experiments.

4.5.3 Spectral Engine

The spectrometer from Spectral Engine was used to record spectra of biodiesel produced in the microreactor. There were two spectrometers available as Spectral sensor N-series 2.0 and Spectral sensor N-series 2.5, but only Spectral Sensor N 2.0 was used, due to time limitation. For all experimental runs integration time 0.1 ms and averaging 3 was used. Main features of both spectral sensors are given in table2.

Table 14: Characteristic Features of Spectral Engine Mobile Spectrometers

Features	Spectral sensor N2. 0	Spectral sensor N2. 5
Wavelength	1550 nm - 1990	2000 nm - 2450
Integration Time	0.1 ms	0.1 ms
Operating Temperature Range	0 ° C TO 70 ° C	0 ° C TO 70 ° C
Detector Type	InGaAs	InGaAs
Price	€3,000	€3,000

4.5.3.1 Methanol as Reference

For all the pre-experiments, methanol was used as reference spectra because pure methanol solution was available every time and it was also possible to maintain a steady flow in the flow cell to take reference spectra without any hindrance. While the feasibility to use air as reference was not suitable, for that we need to dismantle the flow cell and clean it before we start any experiment.

In the spectral region of 1500 and 1990 nm methanol shows different absorption band as compared to biodiesel therefore if there is biodiesel produced in microreactor it will not overlap characteristic absorption band of biodiesel in this spectral range.

4.6 Saponification Number

For the experiments, with a molar ratio and the associated calculation, there are needed the molecular weights of all used substances. Because we used oil from the supermarket, we had no information about the molecular weight of this rapeseed oil.

A common method to investigate the average molecular weight of oil is the determination of the Saponification number. This number shows the amount of free acid groups in oil. There is a direct connection between the saponification number and the average molecular weight.

It was worked with DIN Norm "DIN ISO 3657" "Tierische und pflanzliche Fette und Öle- Bestimmung der Verseifungszahl".

Oil was weighted in in a round flask and 25 mL of a KOH-solution with a concentration of 0.5 g/mol was added. This mixture was boiled under reflux for an hour. To the still hot solution, there were added a few drops of phenolphthalein, which was used as a color indictor. The solution then was titrated with a 0.5 molar hydrochloric acid until the color change was reached.

This experiment was performed tree times and it was also performed for three times just with KOH against HCl itself, as a blind test, as mentioned in the DIN Norm. Therefore the same experiment was repeated but without the test quantity (oil).

In the tables below, there are listed the used amounts and the determine volumes of the experiments and also those of the blind test (Table 5).

Table 15: Amounts and Volumes of the determination of the saponification number, respectively the average molar weight of oil

No.	Weights of Oil [g]	Volume of HCl [mL]
1	2,008	20,40
2	2,063	20,35
3	2,006	20,50
Average amount	2,026	20,417

Table 16: Determined volumes of the blindtest for the determination of the saponification number, respectively the average molar weight of oil

No.	Volume of HCl [mL]
	6,7
2	6,4
3	6,8
Average amount	6,63

The calculation of the saponification number I_s was done by the following formula:

$$I_s = \frac{(V_0 - V_1) \cdot c \cdot 56,1}{m}$$

V_0 the consumed volume of hydrochlorid acid standard solution of the blind test in milliliter

V_1 the consumed volume of hydrochlorid acid standard solution of the experiment with oil in milliliter

c the exact concentration of hydrochlorid acid standard solution in mol per liter

m the amount of the test quantity in gramm

$$I_s = \frac{(20,417 - 6,63) \cdot 0,5 \text{ mol/L} \cdot 56,1 \text{ mol/L}}{2,026}$$

$$I_s = 190,88$$

$$I_s \approx 191$$

The saponification number of the rapeseed oil of the company "gut & günstig" is 191.

The calculation of the average molar weight $\bar{M}(\text{Oil})$ of oil was done by the following formula:

$$\bar{M}(\text{Oil}) = \frac{1}{I_s} \cdot 168300 \frac{\text{g}}{\text{mol}}$$

$$\bar{M}(\text{Oil}) = \frac{1}{191} \cdot 168300 \frac{\text{g}}{\text{mol}}$$

$$\bar{M}(\text{Oil}) = 881,15 \frac{\text{g}}{\text{mol}}$$

The average molar weight $\bar{M}(\text{Oil})$ of oil is 881,15 g/mol.

5 Results and Discussion

5.1 Evaluation of the Batch Experiment Data.

5.1.1 Comparison of the batch production as in the master thesis of Matheo Baumann and the POL group.

In this chapter, the batch production of biodiesel was carried out in a similar way as described in the master thesis of Matheo Bauman [78] with the aim to reproduce the desired biodiesel in batch. The new spectra of substances like biodiesel step A, step B, step C (produced by actual POL group), methanol, methanol with KOH, rapeseed oil, and different standard biodiesels are compared with the spectra of the same substances produced by Matheo.

The Principle Component Analysis (PCA) with the program Unscrambler® X serves for the interpretation of the data. As preprocessing of the data, the baseline correction of the spectra from 1200 nm to 2500 nm was done. This PCA in Figure 10 separates different components like standard biodiesel, step C, step B and methanol, methanol with KOH, step A on the PC1, which accounts for 99%. The second main component PC2 accounts for 1% of the total variance. Thereby, 100% of the data are already explained.

The substances which contain alcohol are located on the negative side of PC1. The old and new measured spectra of them shows minimal or no differences. One outlier inside the new group, containing methanol with KOH, can be determined on the PC1. This could trace back to wrong or not correct measurement procedure. The oil contained substances lie on the positive side of PC1. Again, here there are almost no differences between the old and the new spectra. Also, the biodiesel standard of last semester, which was measured this semester again, and used as a biodiesel standard for this work, manifested no differences in spectra. This shows, that biodiesel under certain storage conditions does not lose quality over the time.

The negative correlation between the oil groups and the biodiesel groups is clearly represented on the PC2. But the variance on PC2 is only 1 %. So, PC2 can be neglected in this model and is only used for a clearer presentation of the data.

This shows that there are no contaminations or chemical changes of the molecules in the oil that could cause a negative influence of the oil quality even if the literature tell that [79].

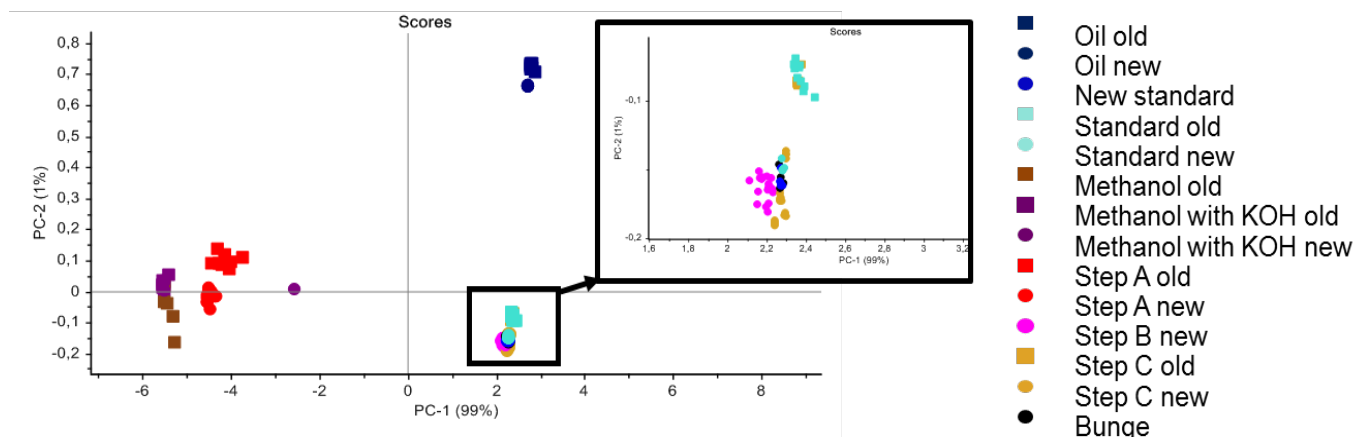


Figure 10: Score plot of the PCA after baseline correction. The old and new alcohol containing compounds can be clearly separated on PC1 from the old and new oil containing compounds. The old and new spectra of oil show great variance to old and new biodiesel spectra on PC2.

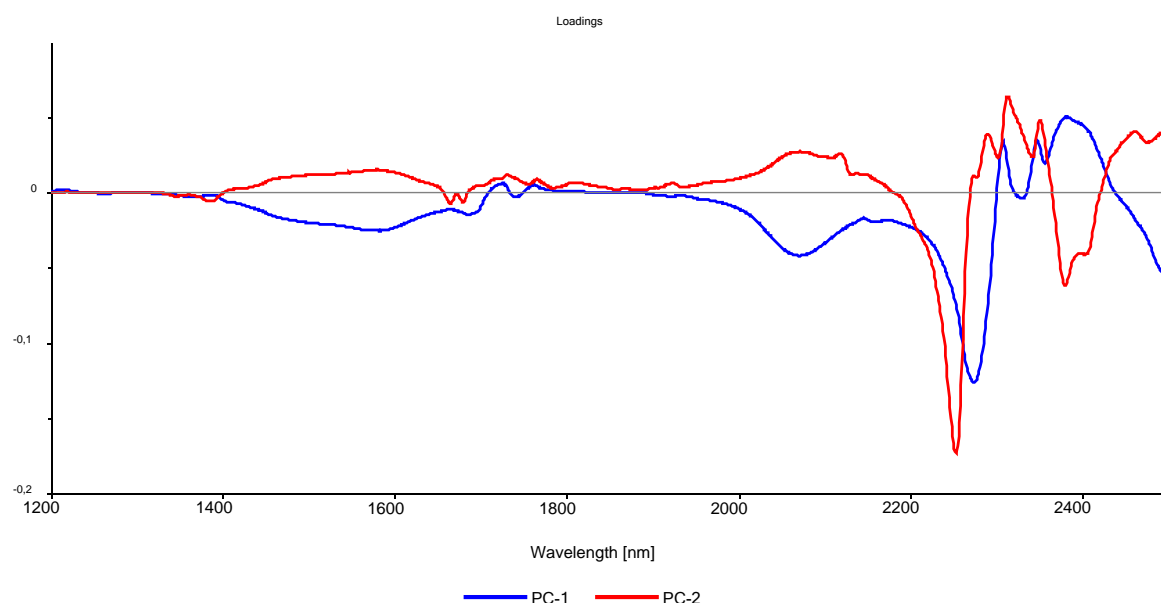


Figure 11: Loading of the PC1 (blue) and PC2 (red). PC1 and PC2 are influenced in the range of 2030 nm to 2400 nm. With PC1 the separation of the alcohol included samples from the other samples is carried out. With PC2 success the separation of oil samples and biodiesel samples

The loading plot in Figure 11 shows that the maximum variance of PC1 and PC2 is roughly located in the wavelength range between 2000 – 2500 nm. The band maxima of PC 1 are below the average of the loading plot. This means that the substances which contain alcohol have a high absorption in these regions. The band maxima of PC2 are also below-average in the loading plot. Both band regions are negatively correlated with PC2. So Bunge biodiesel and the biodiesel standards have high absorption values in these regions whereas rapeseed oil has a low absorption. This means that the loading plot also only shows the differences between the substances but no significant changes between the old and the new measured samples can be established.

5.1.2 Comparison of batch produced with and without dropping.

The comparison of batch processes with dropping, where the rapeseed oil was added dropwise into the mixture of methanol with KOH and without dropping, where the rapeseed oil was mixed together with other compounds in a flask was done, to investigate the differences between this two production methods. The line plot below shows the spectra of biodiesel (Step A, Step B, and Step C) with and without dropping. The comparison of the spectra of each step demonstrates no relevant differences between batch produced with or without dropping. This means that both production methods lead to desired product, only the production with dropping by additional preparation are more time intensive. Therefore, the without dropping method was proposed for the further experiments.

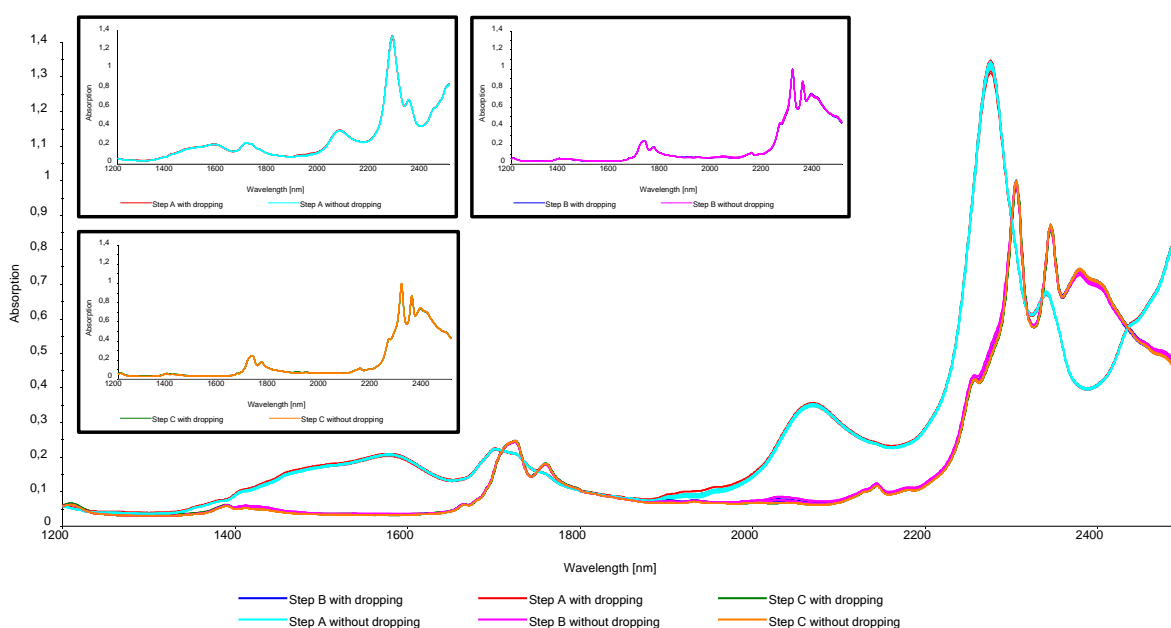


Figure 12: Spectra of four batches with Step A, Step B and Step C. Two of them was produced with dropping and two without. It can be detected no or minimal differences between spectra within each step.

5.1.3 Comparison of step C of three different batch productions with and without mole sieve

In this part of the project the produced batches with and without mole sieve especially step C, are compared, to investigate the effect of mole sieve.

The line plot in Figure 13 shows the spectra of batch step C produced with and without mole sieve. The marked wavelength ranges are overtones and combination bands of the methyl, methylene and water groups. In the wavelength region from approximately 1730 nm to 1750 nm and from 2280 nm to 2305 nm the samples with a mole sieve have a higher absorbance. But in the wavelength region from roughly 1890 nm to 1930 nm the samples without the mole sieve are more absorbed. In this range, the combination bands of water are represented. Therefore, it can be assumed, that the samples without mole sieve contain more water inside as the samples with mole sieve. Because of this, the drying process of biodiesel step C with mole sieve can be more effective for reduction of water in the samples as the drying process without a mole sieve.

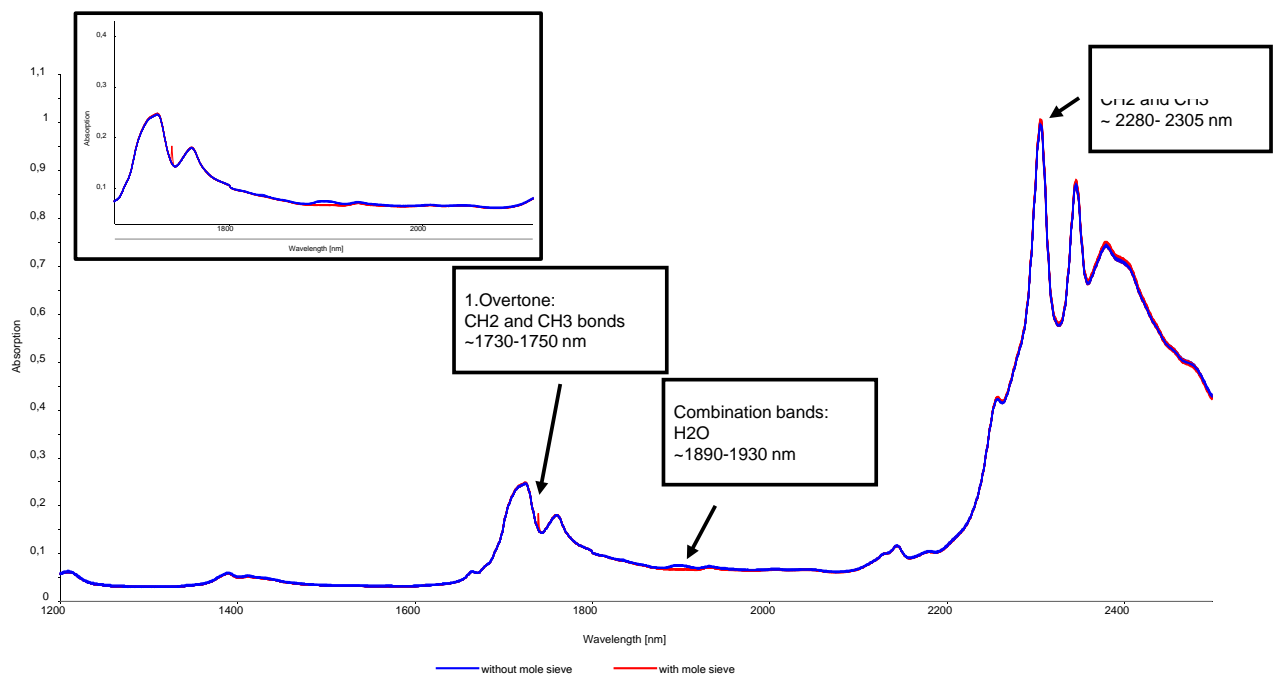


Figure 13: Spectra of batch step C. When comparing the samples of batch step C a difference in the absorption units of the spectra in the wavelength range ~1730- 1750 nm, ~ 1890-1930 nm and ~ 2280-2305 nm is visible.

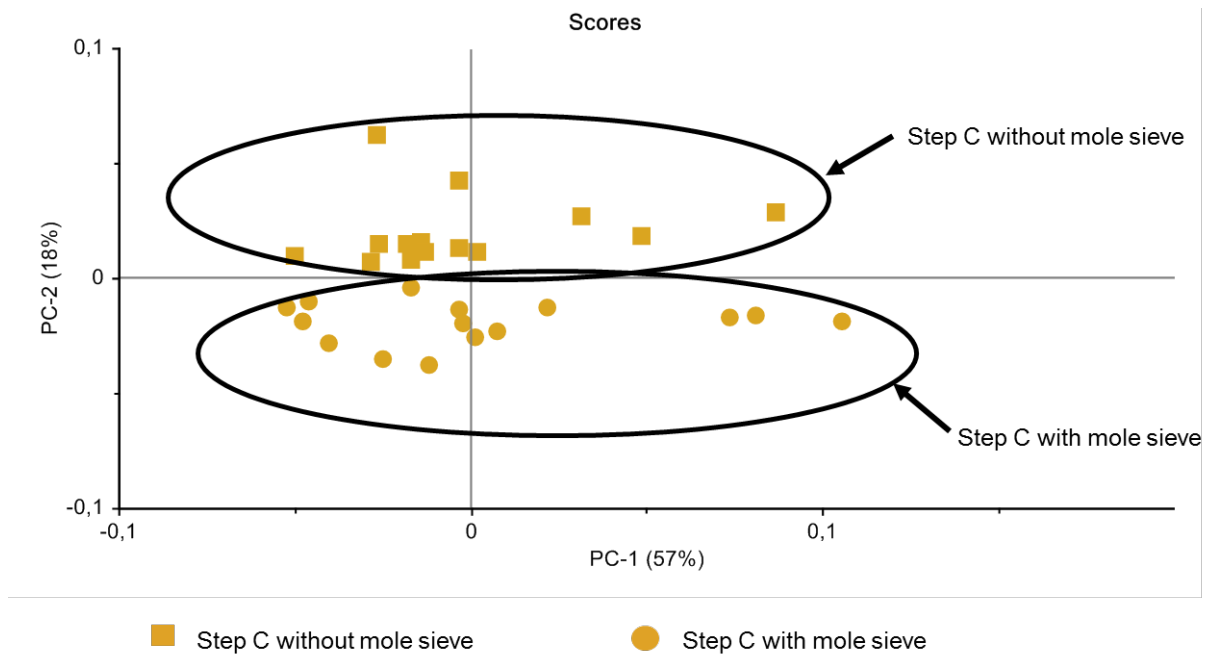


Figure 14: Score plot of the PCA. The PC1 is explained by 57% against the PC2 explained by 18%. The samples are an irregular distribution on the scores plot. But the samples of batch step C with mole sieve can be distinguished from samples without mole sieve.

In the score plot it can be seen, that the samples are randomly distributed on the PC1. Scores of step C without mole sieve are located above the average on PC2. Thereby the samples dried with a mole sieve are lying below the average on PC2. In total, nearly 75 % of the data can be described by the first two PCs. Thereby, about 57 % by PC1 and 18 % by PC2. These variances between the sample groups can be effected through the different amount of remaining water in the samples.

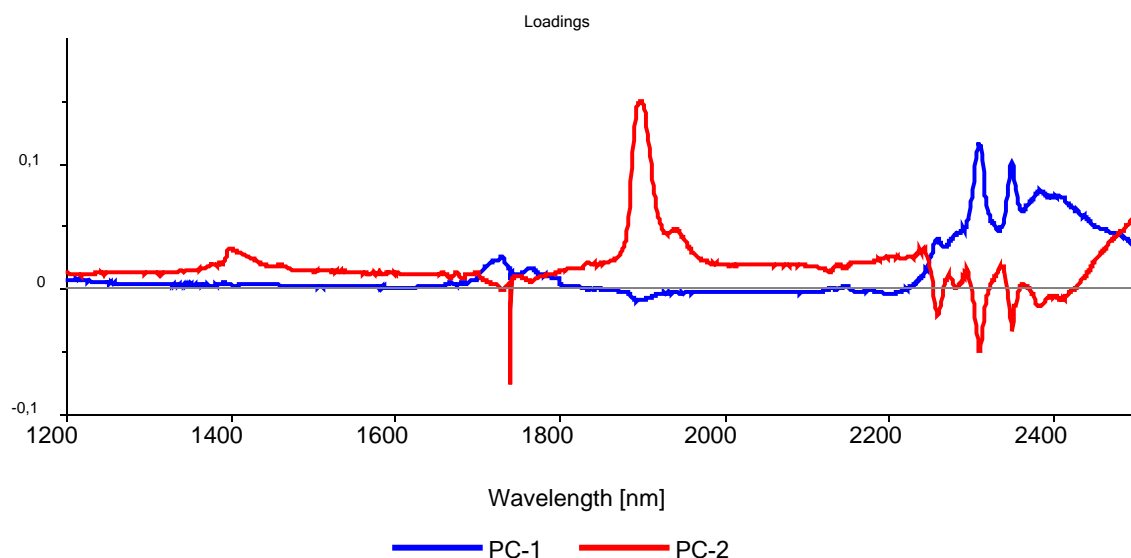


Figure 15: Loading plot of PC1 (blue) and PC2 (red). The maximum variance of PC1 is located at the wavelength range 2290- 2400 nm. The PC2 shows the variance at several regions. The first one is at the wavelength at ~1730nm, the second one in the wavelength range 1890- 1930 nm and the third one is located in the wavelength range 2250- 2400 nm.

Considering the line plot in Figure 13 and the loading plot in Figure 15 PC2 shows a variance at roughly 1730 nm and at 2250- 2400 nm. This means, that the samples with mole sieve have a higher absorbance in this region. That can be influenced by CH₂-CH₃- 1.overtone and CH₂-CH₃- combination band in this wavelength range. In addition, the spectra of the both sample groups can be distinguished through the combination bands of water (1890-130 nm) at the PC2. Here the samples without mole sieve have higher absorbance. That indicates residual water content within the samples.

5.1.4 Comparison of batch produced with volumetric and molar ratio.

The volumetric ratio of alcohol with a catalyst to rapeseed oil was used for the preparation of batch in the previous experiments. It was found, that in the production of the batch, a relatively large amount of methanol was used which is removed in the next step by vacuum rotary evaporators. To find out the correct ratio of the alcohol with a catalyst to oil, the molar ratio was calculated and two next batch with this ratio were produced.

Figure 16 demonstrates the score plot of PC1 and PC2. This model explains a total variance of 100% of the data with 94% variance on PC1 and 6% on PC2. The distribution of the samples shows a clear pattern. The samples of methanol with KOH and biodiesel step A volumetric ratio are negatively correlated to the samples of Bunge biodiesel, biodiesel step B, step C and step A molar ratio on the PC1. By using the molar ratio for batch production, the amount of the required alcohol is reduced in comparison to the volumetric ratio. This explains the difference between the samples of step A with a volumetric ratio (the amount of residual alcohol is great) and steps A with a molar ratio (the amount of residual alcohol is small). The sample groups of the other steps (step B and step C) produced with both ratios show no difference in the score plot. However, the samples from the last step C with volumetric and molar ratios are located close to the standard Bunge biodiesel, which indicates, that desired final product can be made with the molar ratio and the excess amount of the alcohol used by volumetric ratio can be saved.

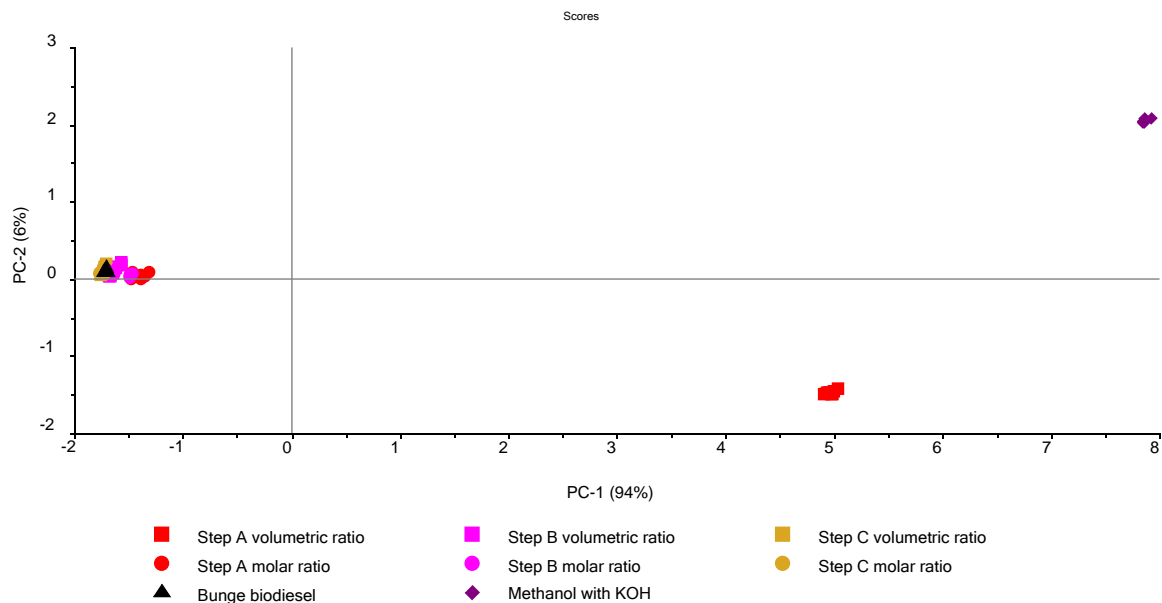


Figure 16: Score plot of the PCA of spectra. The samples of methanol with KOH and biodiesel step A volumetric ratio can be clearly separated on PC1 from the samples of Bunge biodiesel, step B, step C and step A molar ratio. The methanol with KOH and biodiesel step volumetric ratio groups shows the difference on the PC2, where the methanol with KOH is above-average on PC2 and the biodiesel step A volumetric ratio is below average on PC2.

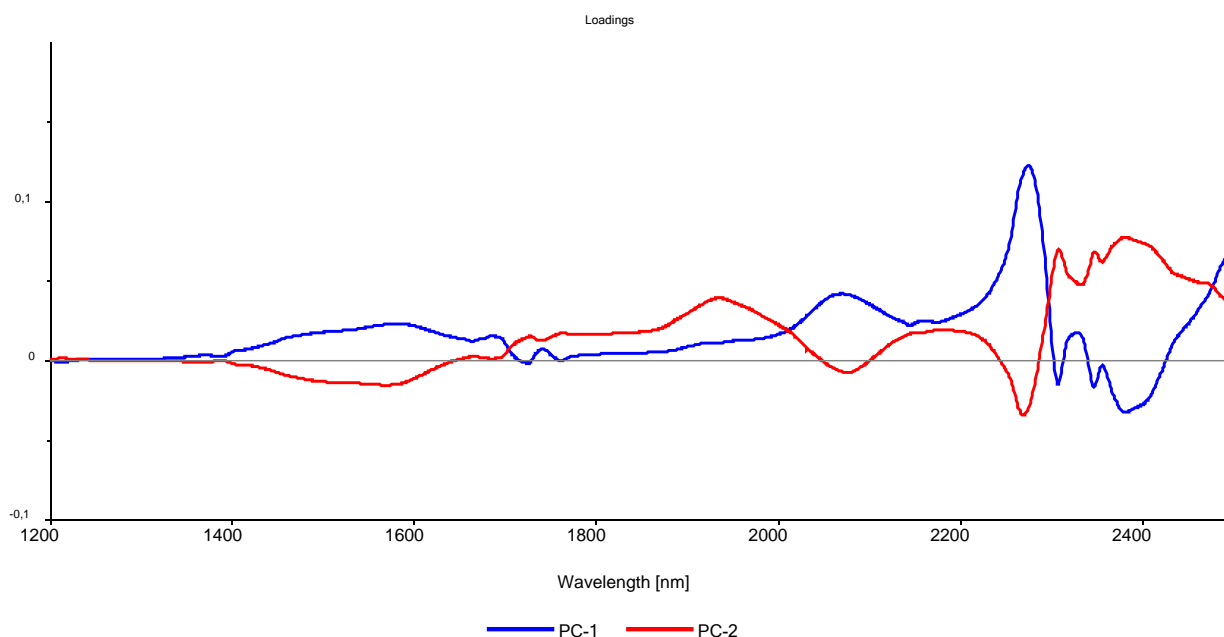


Figure 17: Loading plot from PC1 (blue) and PC2 (red). The variance on PC1 is largely determined by the CH₃ and CH₂ combination bands. On PC1 two sample groups (step A volumetric ratio and methanol with KOH), which lie above average, can be clearly distinguished from the other groups (step A molar ratio, steps B, steps C and Bunge biodiesel), which lie below average. On PC2, the step A volumetric ratio has negative absorption and the samples of methanol with KOH have positive absorption.

At the loading plot in Figure 17, it can be seen that the maximum variance of PC1 is roughly located in the wavelength range 2030 – 2400 nm. Bands at the wavelength from 2030 nm to 2280 nm are above average in the loading plot. It means that biodiesel (step A volumetric ratio) and methanol with KOH have a high absorption in this regions. Bands in the region from 2280 nm to 2400nm correlate negatively with PC1. So biodiesel (step A volumetric ratio) and methanol with KOH have a lower absorption in this regions as Bunge biodiesel and the other sample groups (step A molar ratio, steps B, and steps C). So, PC1 is most likely associated with methanol dominated by the spectra. As a result, the CH₃ combination bands in the range of 2280 nm to 2400 nm have to be assigned to the methanol. Thus, the large variance between step A volumetric ratio and step A molar ratio, steps B, steps C and Bunge biodiesel can be explained by the methanol excess in step A volumetric ratio.

PC2 shows its maximum variance roughly within the region 2280 – 2400 nm. The first band region (at about 2280 nm) is negatively correlated with PC2. The combination bands CH₃ and CH are represented in this region. So biodiesel (step A volumetric ratio) has high absorption values in this regions. However, the methanol with KOH has a high absorption at the second band region (at about 2330nm-2400nm), which is positively correlated with PC2. It means that a substance which is included in the biodiesel step A volumetric ratio ensures the differentiation between methanol with KOH and the step A volumetric ratio. That is probably glycerol.

5.1.5 Comparison of batch produced with methanol and ethanol.

To investigate whether the ethanol is also suitable for biodiesel production as methanol, the batches with both substances were produced. Due to lack of time, only one batch of ethanol was produced.

In Figure 18a) is shown the line plot with spectra of the methanol and ethanol. The spectra exhibit large differences in whole wavelength ranges. Figure 18b) (step A with methanol and ethanol) also shows differences in the spectra at the wavelength range from 1400 nm to 1670nm, where the 1.overtone of OH-alcohol is represented and at 2000 nm to 2500 nm. In these ranges, the step A with ethanol has high absorption as the samples of step A with methanol. Probably the amount of ethanol is more presented in the samples. This can be explained by the fact, that the molar ratio of alcohol with a catalyst to oil was only calculated for biodiesel production with methanol and that other might be necessary for the biodiesel production with ethanol.

In the Figure 18c) (step B with methanol and ethanol) the spectra differences lie only at the wavelength range roughly 2000 nm – 2500 nm, but not at the wavelength range from 1400 nm to 1670 nm as in the figure before. In step B, the excess alcohol is removed. This can be an explanation for no clear differences within the region 1400 – 1670 nm.

The step C with methanol cannot be compared with step C with ethanol because by preparation of step C with ethanol no relevant samples could be taken. After the same washing procedure (with acid and water) as for production of biodiesel step C with methanol, we get by biodiesel step C with ethanol white-yellowish emulsion. This had a large optical difference to samples of step C with methanol (clear yellow substance). This can be caused by different pKa values of alcohols. The pKa value of methanol

is 15.5 and of ethanol, the pKa value is higher and lies by 15.9. Thereby, the purification process of biodiesel step C with methanol need to be adapted to ethanol.

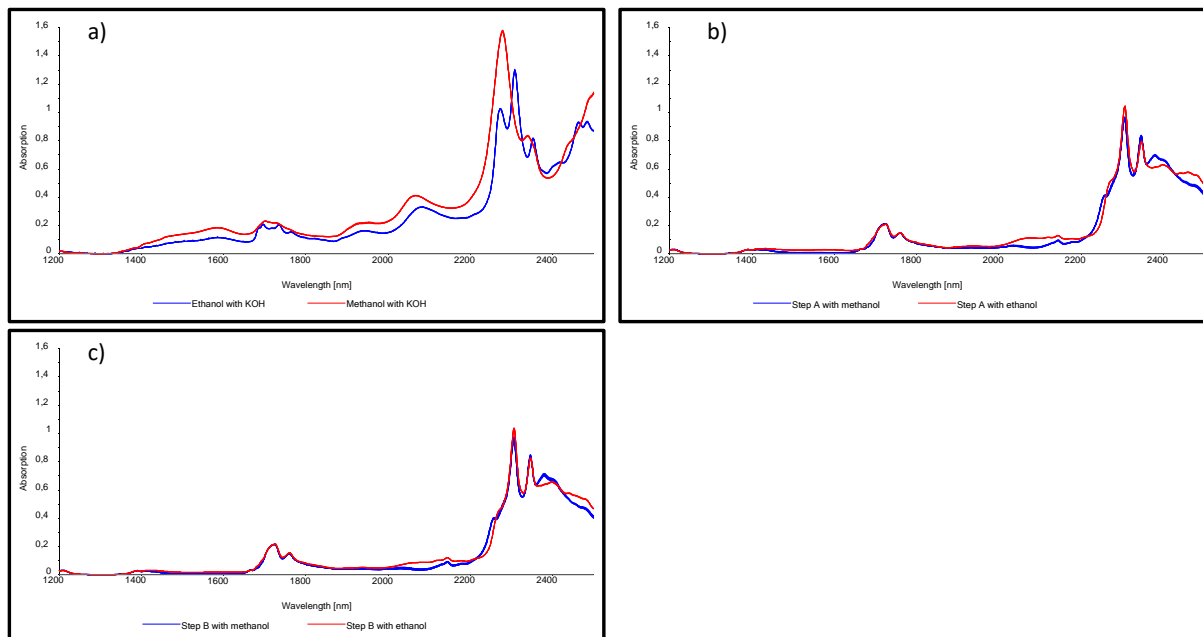


Figure 18: Line plots of baseline corrected spectra. In the Figure 18 a) the spectra of ethanol with KOH and the spectra of methanol KOH are shown. The Figure 18 b) and 18 c) demonstrate spectra of step A as well as step C produced with methanol and ethanol.

5.1.6 Evaluation of inline measurements

The purpose of the inline measurements investigation was to find out when rapeseed oil and methanol with KOH is reacting to biodiesel, how is the process of transesterification going and when the reaction is finished. This experiment was done for about one hour. Thereby every minute a measurement was done by the TIDAS NIR spectrometer from company J&M. The spectra of measurements were pre-analyzed. After 30 min no changes in the spectra was observed, so the remaining spectra were not used and deleted for further evaluation. Additionally, 5 measurements of rapeseed oil, methanol and Bunge biodiesel were done by the spectrometer under the same adjustments as for biodiesel production.

Score plots in Figure 19 show the score of PC1 to PC2. The influence of PC1 on the sample spectra's is 97%. The influence of PC2 on the sample spectra's is only 2%. In the Figure 19a) the first measurements (0-9 min) of Batch 5 and the measurements of methanol are located below average on PC1 and PC2. Most measurements from 10 min until 19 min and all measurements from 20 min to 30 min are located below average on PC1 and above average on PC2. By Batch 5 no movement of measurement can be detected after 30 min. All measurements of Batch 6 are located below average on PC1 and above average on PC2. The measurements of the last minutes shift nearby to the positive site of PC1, where the rapeseed oil and Bunge biodiesel was located. After roughly 12 min no movement of measurements was observed.

The small differences between batch 5 and batch 6, despite identical preparation, could be caused by possibly wrong starting temperature, an incorrect mixing ratio of substances or also problems with the spectrometer.

In the Figure, 19b) the measurements of batch 7 and batch 8 moved very similar from negative PC1 and PC2 site, where the methanol is located, to the positive site of PC2 as well as the negative site of PC1 (but here also small deposition in the direction to the positive site of PC1). After around 30 min no relevant movements of measurements was observed.

So the reaction of transesterification in the batch was pretty much finished after around 30 min. The continuous movement of the measurements from methanol in the direction of biodiesel could also be observed.

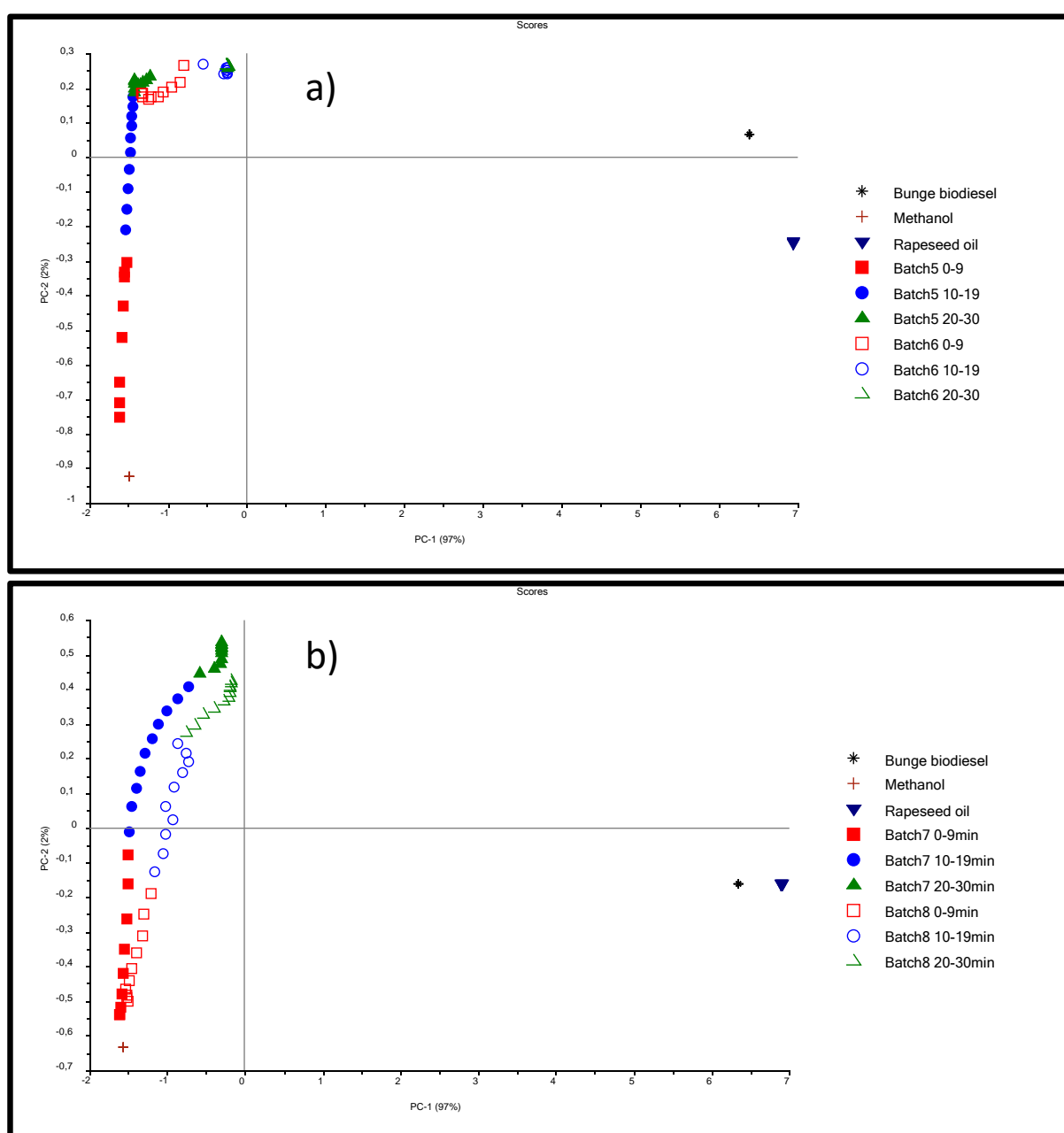


Figure 19: Scores plots of inline measured Batch 5, Batch 6, Batch 7 and Batch 8. The Figure 19 a) shows the distribution of scores from batch 5 (filled symbols) and 6 (not filled symbols) after baseline correction, smoothing

and recalculation of outliers. The Figure 19 b) demonstrates the scores of batch 7 (filled symbols) and batch 8 (not filled symbols) after baseline correction and smoothing according to Savitzky-Golay polynomial fit. In addition, in both scores plots the samples of Bunge biodiesel, rapeseed oil and methanol can be seen.

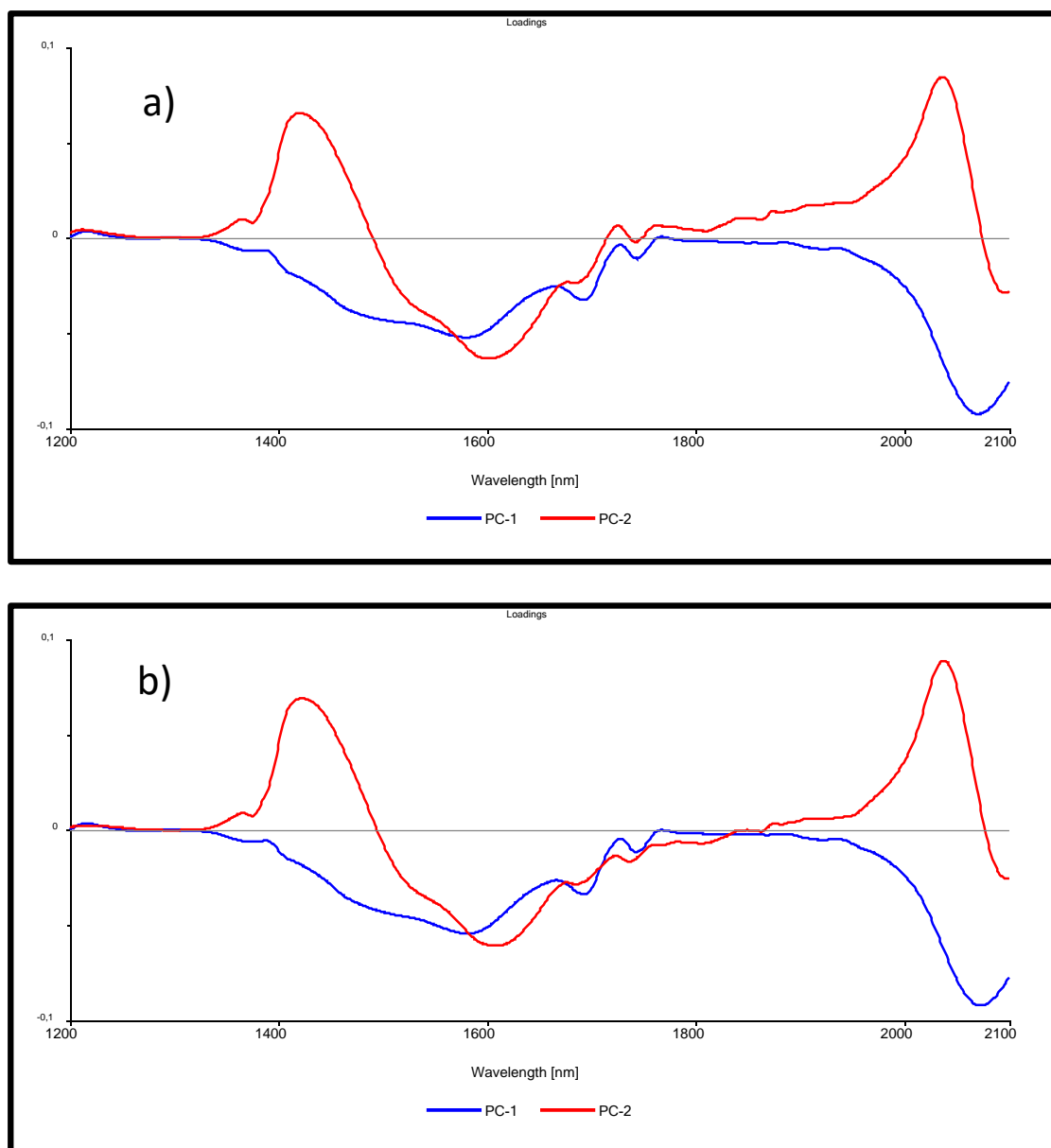


Figure 20: Loading plots of PC1 (blue) and PC2 (red). The variance on PC1 is more determined by the overtones CH₃ & CH groups and ROH group at 2000 nm to 2100 nm. The absorption maxima on PC2 are at roughly ~ 1420 nm and at ~ 2060 nm. The absorption minimum lies at ~ 1610 nm.

In the loading plots, the methanol level can be explained by PC1. Probably the first band ~ 1590 nm and the second band ~ 2080 nm on PC 1 can be related to the spectra of samples, which include alcohol. The band at ~1610 nm lie below average on PC2. So the methanol has a high absorbance in this region. Thereby, two bands at ~ 1420 nm and ~ 2060 nm are above average on PC2. The Bunge biodiesel and biodiesel (step A) samples have a high absorbance in this region. It means that a substance which is included in the biodiesel (step A) is similar to the chemical structure of Bunge biodiesel.

5.1.7 Conclusion

The results of the batch experiments show:

the reproduction of biodiesel in batch according to the approach described in the master thesis of Matheo Baumann can be carried out successfully. Produced biodiesel look very similar to the bunge biodiesel and other biodiesel standards.

The production of biodiesel using methods with and without dropping lead to desired product. The method with dropping is more complex as well as time intensive, because of additional equipment and dropping time. Therefore, the without dropping method is proposed for the further experiments.

The drying process of biodiesel step C with mole sieve is more effective than without mole sieve. With mole sieve, more water from the sample can be removed. This leads to the better quality of the desired product.

The production of biodiesel with molar ratio make more sense because the amount of needed alcohol with the catalyst can be precise calculated and wastage of alcohol can be reduced.

The biodiesel production with ethanol was not successful. The purification of step C was performed according to biodiesel production with methanol. That is probably not possible. Thereby, the purification process of biodiesel step C with methanol need to be adapted to ethanol or new purification procedure for biodiesel step C with ethanol need to be designed.

The results of evaluation and analysis of inline measurements of biodiesel step A demonstrate continuous movement of the measurements from methanol in the direction of biodiesel. This means, that biodiesel step A is successfully performed. In addition, it was found, that the reaction time of transesterification in a batch is only 30 min.

5.2 Evaluation of Microreactor Preexperiments Data

5.2.1 Comparison of Microreactor Biodiesel vs. Batch 09 Biodiesel

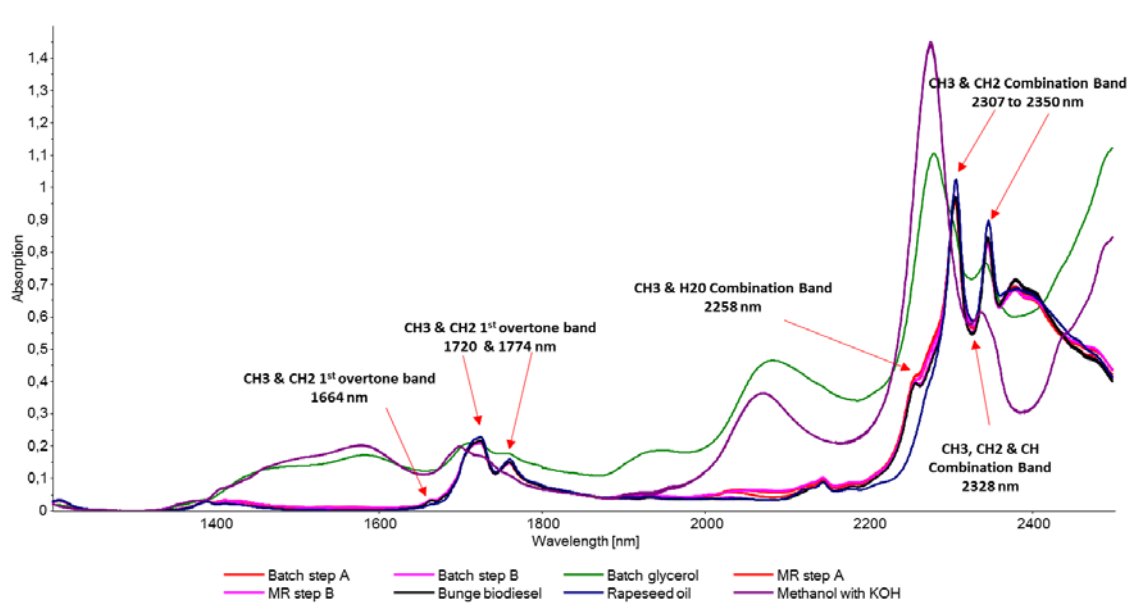


Figure 21: All spectra are baseline corrected. The biodiesel samples from microreactor before demethanolization MR step A (red) and after demethanolization MR step B (light purple) were compared with step A & step B biodiesel samples of batch 09 and Bunge Biodiesel sample. Microreactor biodiesel samples show all the characteristic CH₃, CH₂ and CH band peaks similar to Batch 09 and Bunge Biodiesel. Microreactor sample carries slightly higher absorption from 2000 to 2050 nm and also at 2258 nm which may be due to some glycerol dissolved in the sample.

5.2.2 NIR Spectra of Biodiesel, Rapeseed Oil and Methanol with KOH

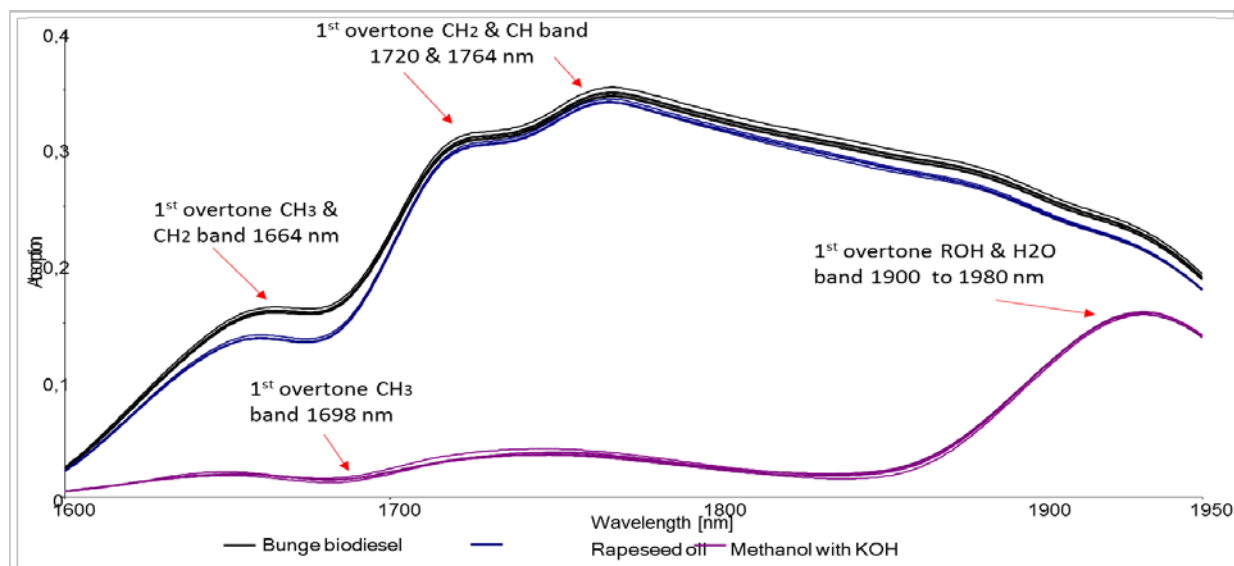


Figure 22: Baseline corrected and smoothed with Savitzky-Golay polynomial fit (2nd order, points 25) spectra of Bunge Biodiesel, Rapeseed Oil and Methanol with KOH measured with Spectral Engine N2.0. The 1st overtone bands of CH₃, CH₂ and CH are visible from 1650 nm to 1780 nm. Also the 1st overtone bands ROH & H₂O are prominent from 1900 nm to 1950 nm. Oil and Biodiesel show same characteristic peaks at 1720 and 1764 nm, but biodiesel exhibits higher absorption at 1664 nm. While methanol shows maximum absorption from 1900 nm to 1960 nm due to hydroxyl bond stretching.

In order to see the effect of each factor on biodiesel production, the spectra of the individual component (i.e Biodiesel, Rapeseed Oil and Methanol with KOH) was collected and evaluated as shown in Figure 22.

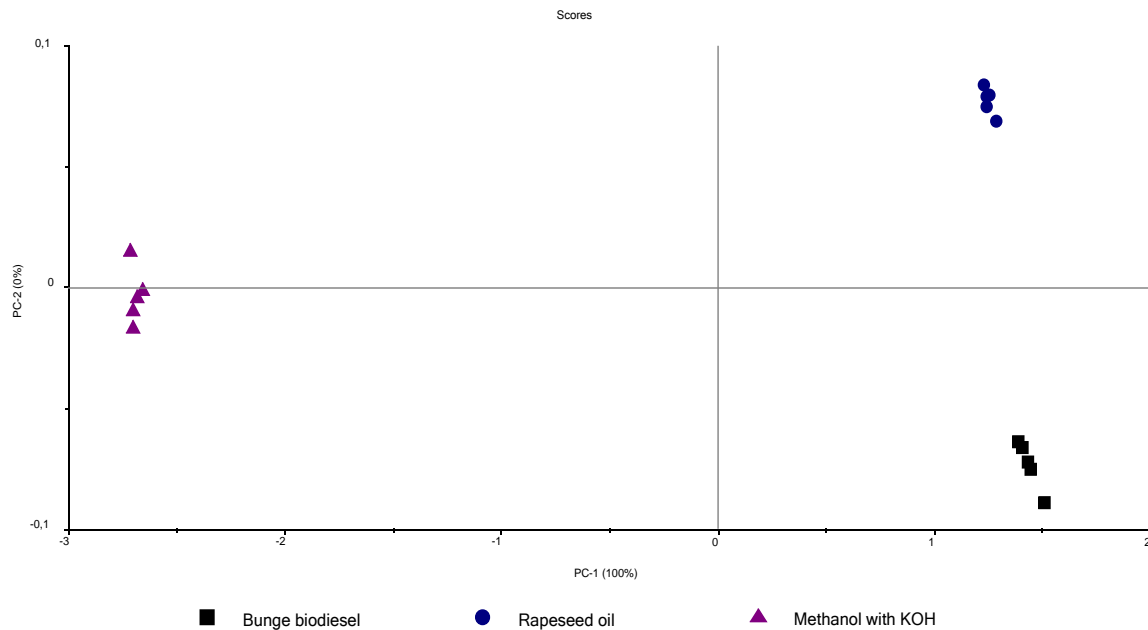


Figure 23: Shows Score plot of pure components, PC1 explains the 100% variance between samples that differentiates methanol samples from the biodiesel and rapeseed oil samples. Methanol is below average on PC1 and other two sample groups are above average on PC1. PC2 explains 0% variance in samples, here methanol is slightly below average, while biodiesel and rapeseed oil separate out into two different groups, but this separation is meaningless.

The characteristic peaks of the individual component were compared with their spectra obtained from Lambda in the same wavelength region from 1500 nm to 1980 nm. The CH₃, CH₂ and CH absorption peaks for Biodiesel and Rapeseed Oil are similar to Lambda measurement at 1664, 1720 and 1764 nm (see Figure 22). Whereas for methanol the 1st overtone CH₃ and OH absorption bands are not identical to its Lambda measurement, this may be due to the fact that methanol was used as a reference for Spectral Engine N2.0 measurements and air for Lambda measurements. For the PCA model, the wavelengths from 1600 nm to 1950 nm were selected, the spectral region below and above this range was removed due to the noise. PC1 represents the 100% variance in samples and separates the methanol from the methyl esters as shown in Figure 24:

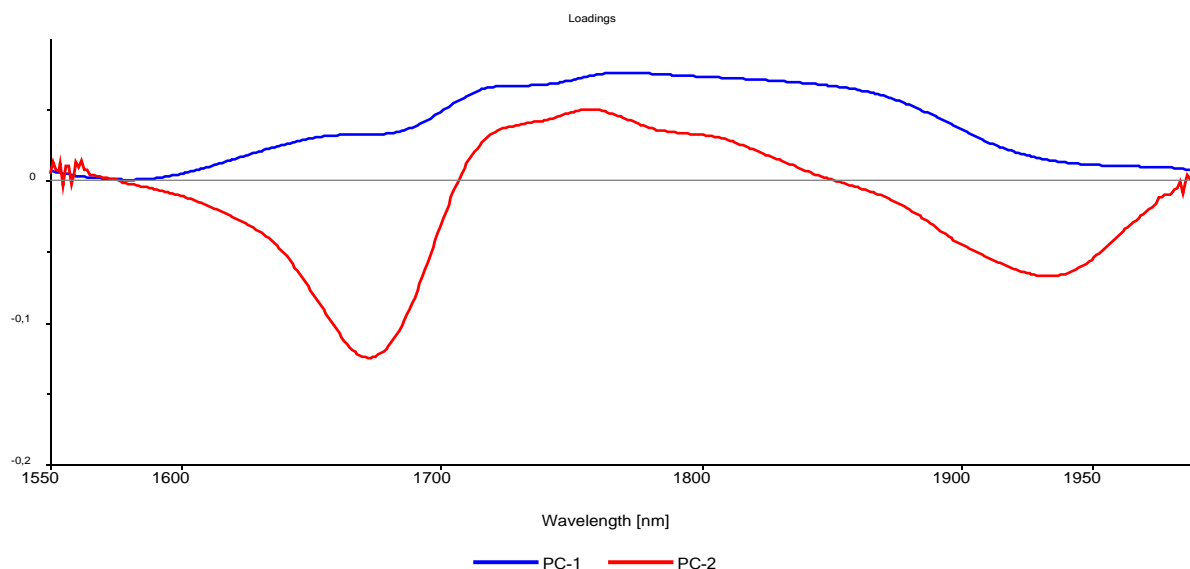


Figure 24: In Loading plot, PC1 shows positive loadings for characteristic peaks of CH₃, CH₂ and CH absorption bands at 1664 nm, 1720 nm & 1774 nm respectively, which represents that biodiesel and oil. The negative loading peaks on PC2 represents methanol with characteristic 1st overtone CH₃ absorption bands at 1680 nm and 1st overtone ROH and H₂O absorption bands from 1900nm to 1980nm.

5.2.3 Temperature

The previous experiments show that transesterification reaction also takes place at room temperature, and as the temperature increases the rate of reaction increases till boiling point of methanol. Therefore to find the optimum temperature range for biodiesel production in microreactor setup and to see the spectral changes, experiments were conducted at 40 °C, 50 °C, 60 °C and 65 °C with oil to methanol molar ratio of 1:6 and at 25 ml/min flow rate.

The line plot in Figure 25 shows the effect of temperature on spectra of biodiesel produced in the microreactor. At a temperature of 40 °C and 5 °C, it was observed that the solution was highly turbid when it reached the flow cell, and caused a high amount of scattering. As a result, the spectra was too noisy as shown in Figure 1 of Appendix., and after pretreatment, the spectra at 40 °C and 50 °C lies between Biodiesel and Oil spectra and group closer to oil in PCA model (see Figure 26). From reaction kinetics point of view, it is assumed that at these temperatures and flow rate of 25 ml/min there was not enough time for the reaction to complete in the microreactor.

At a temperature of 65 °C the solution was clear when it reached the flow cell, but due to high temperature the excess methanol starts boiling up and caused a disturbance in spectra. At 60 °C the spectra were quiet smooth and there was no boiling observed in the microreactor. Also, the spectrometer detects the characteristic band peaks for biodiesel and the methanol at this temperature therefore for other pre-experiments 60 °C was selected as best temperature to observe spectral changes.

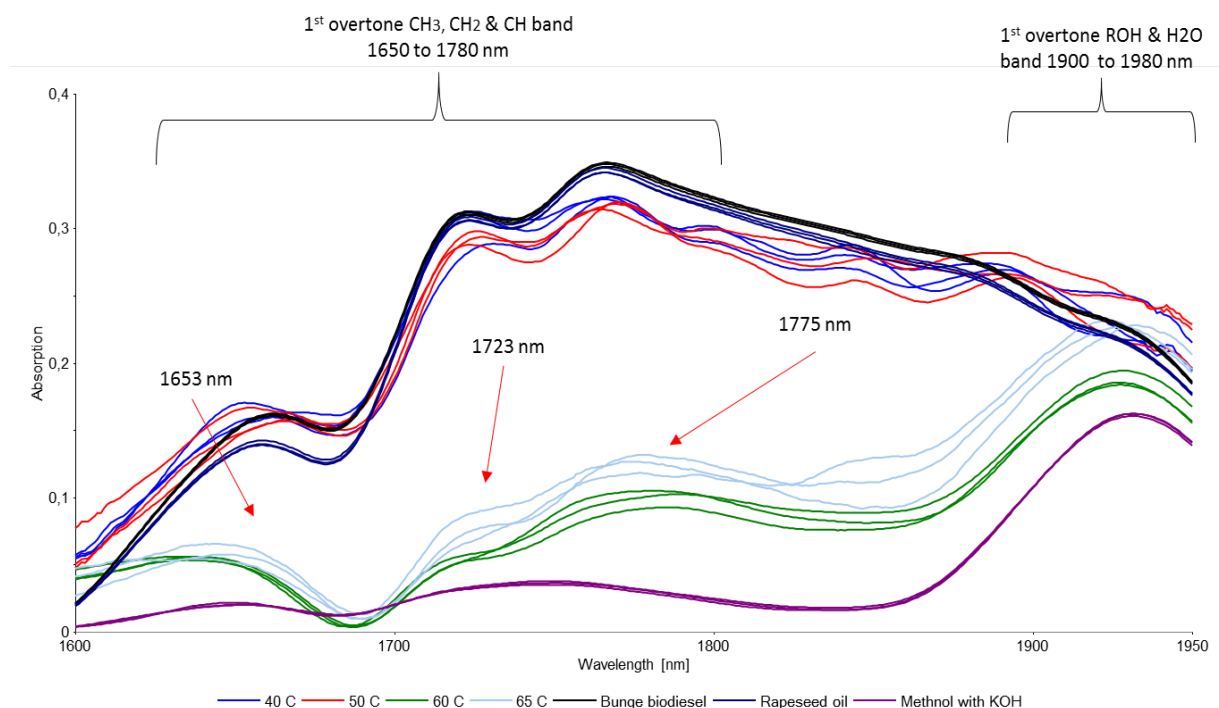


Figure 25: Spectra are baseline corrected and smoothed with Savitzky-Golay Polynomalfit(2nd order, points 25). The 1st overtone of CH₃, CH₂ and CH absorption bands are visible in the wavelength range of 1650 nm to 1780 nm for all temperatures. From 1900 to 1950 nm, hydroxyl groups shows stretching at 60 °C and 65 °C.

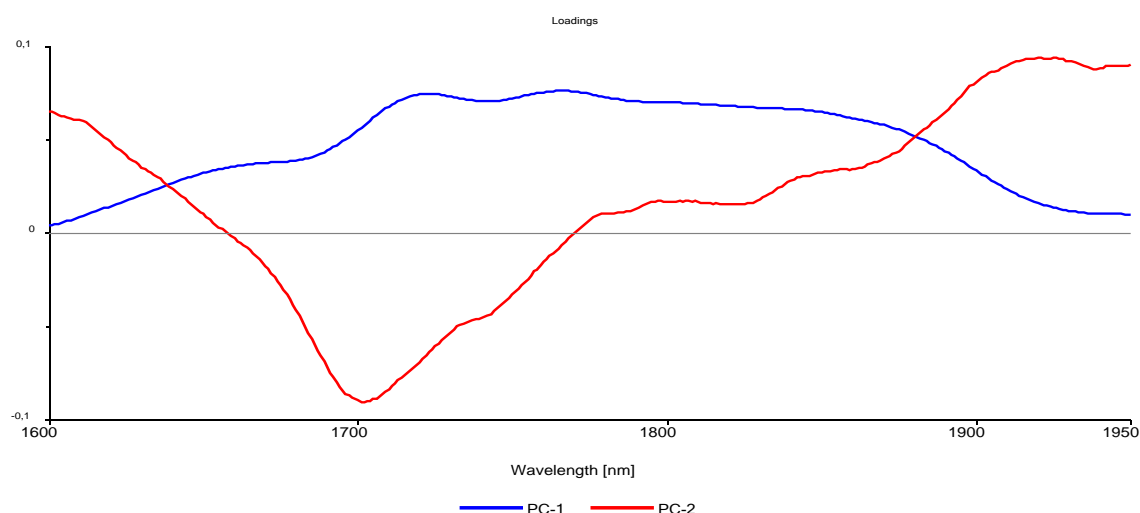


Figure 26: For PCA model wavelength from 1600 nm to 1950 nm was selected. PC1 explains 98% variance in the samples. The samples at 40 °C and 50 °C group closer to oil as discussed above. The samples of 60 °C and 65 °C group in between the biodiesel and methanol

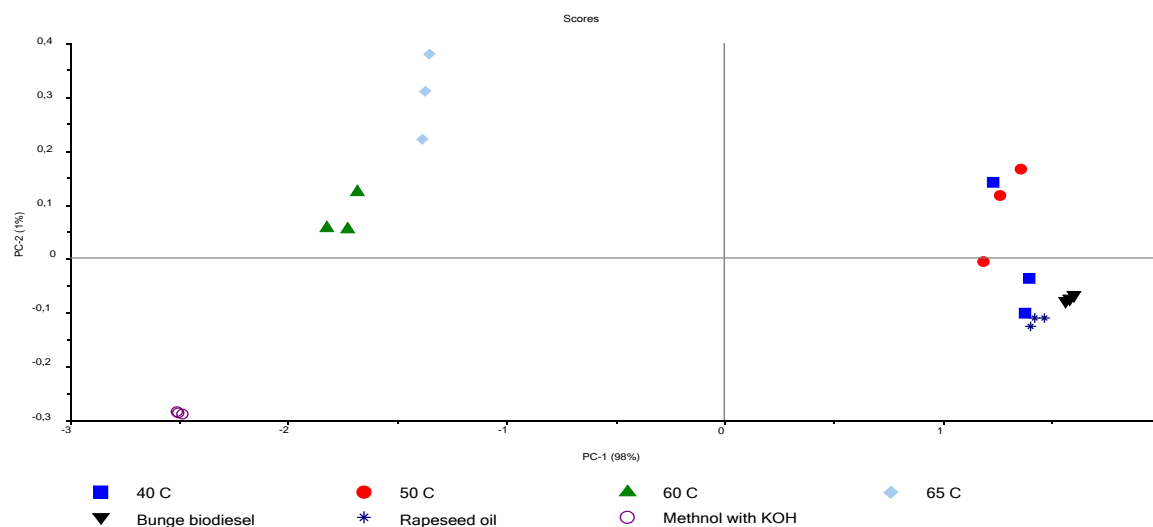


Figure 27: On PC1 the variance is mainly due to CH₃, CH₂ and CH vibrations, which represents the biodiesel and oil groups. On PC2 the two separate groups can be visualized, negative loading from 1650 to 1750 nm which are due to 1st overtone CH₃ vibrations, represents methanol group and the positive loading from 1800 to 1900 nm are due to CH₂, CH and ROH vibrations, which are most probably due to the Glycerol phase in solution.

5.2.4 Oil to Methanol Molar Ratio

The molar ratio of oil to methanol also influence the transesterification reaction as discussed in section 2.2.5. To find the optimum molar ratio ranges for biodiesel production in the microreactor, experiments were conducted with molar ratios of 1:2, 1:3, 1:4, 1:6, 1:9 and 1:12 at a temperature of 60 °C and flow rate of 25 ml/min.

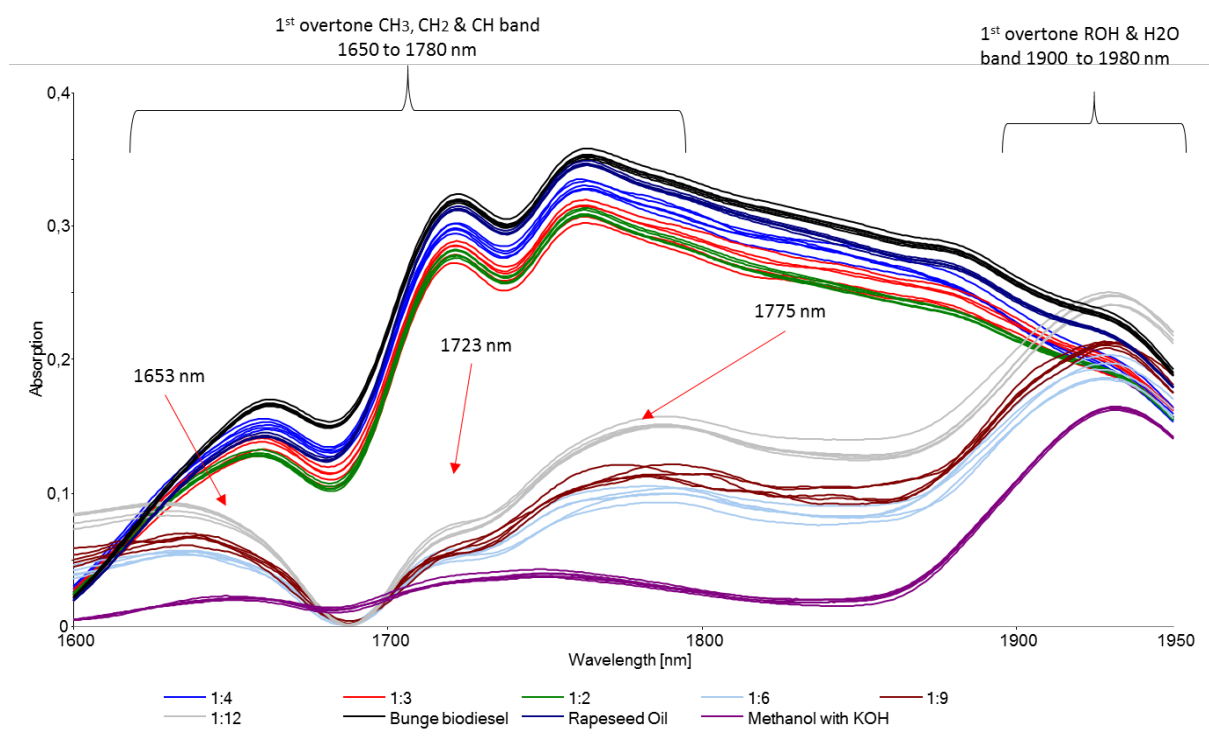


Figure 28: All spectra are baseline corrected and smoothed with Savitzky-Golay Polynomial fit (2nd order, points 15). At molar ratios below 1:6, spectra are identical and closer to oil spectra. While samples with a molar ratio of 1:6 and above show 1st overtone

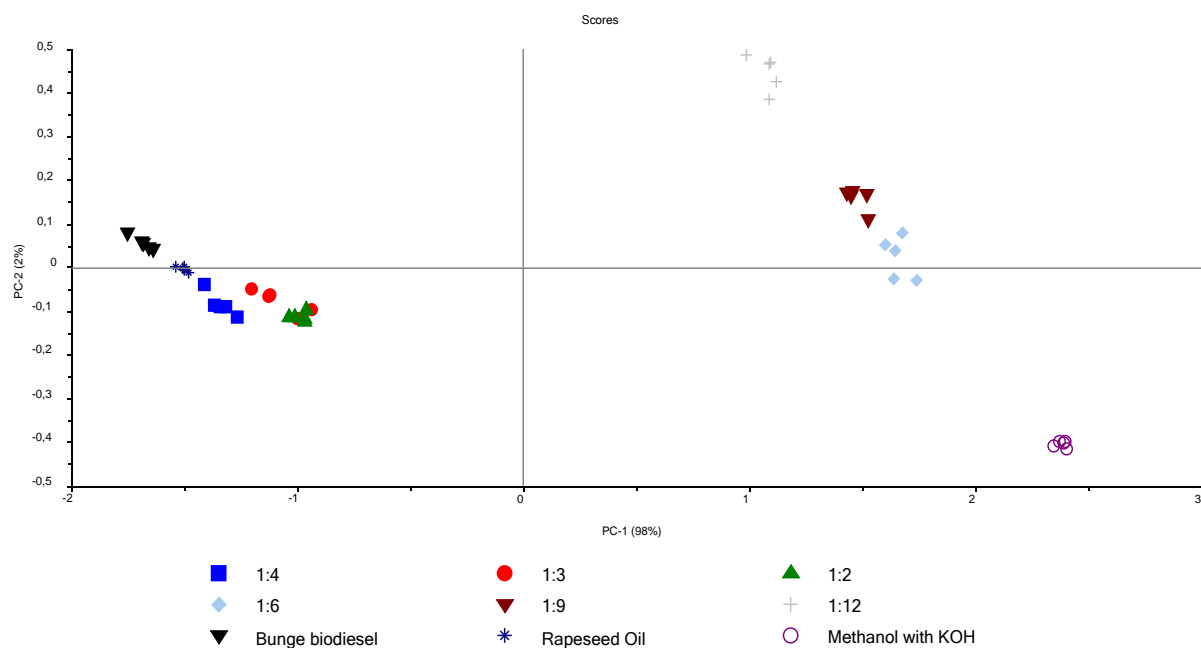


Figure 29: PC1 explains 98 % variance in samples, separates sample into two groups on behalf of 1st overtone CH₃, CH₂ and CH absorption bands in the wavelength range from 1650 nm to 1800nm. The samples with oil to methanol molar ratio below 1:6 group closer to oil, indicating that there was not much reaction took place. While on PC1 samples with oil to methanol molar ratio at 1:6 and above, group in between biodiesel and methanol samples. This is possibly because of glycerol formation and intermediate products as mono-, and di- glycerides. PC2 covers only 1% of variance which is mainly due to negative score of Methanol

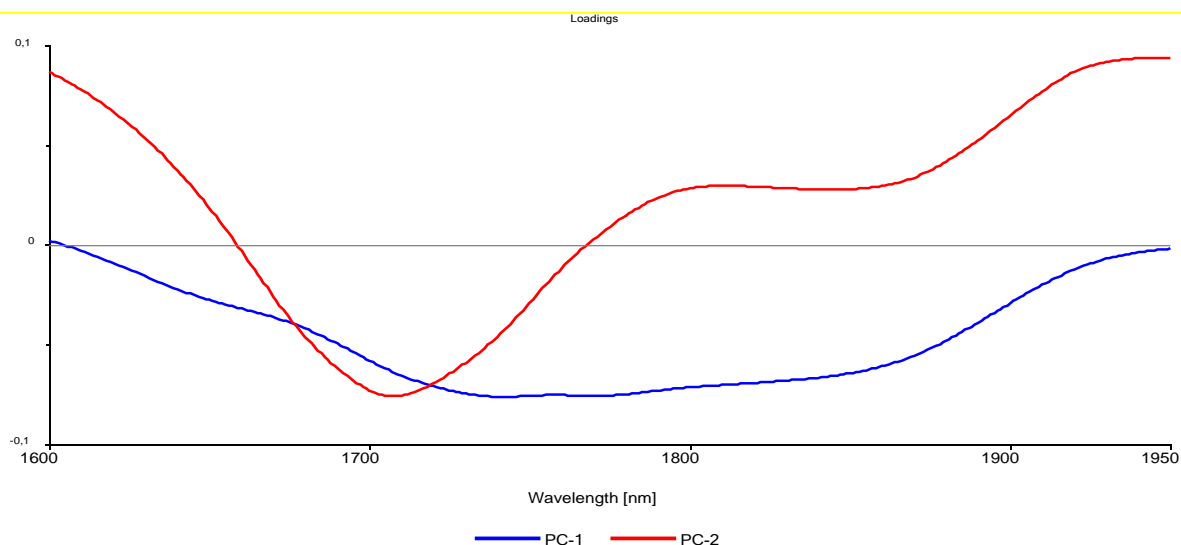


Figure 30: On PC1 the variance is mainly due to CH₃, CH₂ and CH vibrations, which represents the biodiesel and oil groups. On PC2 the two separate groups can be visualized, negative loading from 1650 to 1750 nm which are due to 1st overtone CH₃ vibrations, represents methanol group and the positive loading from 1800 to 1900 nm are due to CH₂, CH and ROH vibrations, which are most probably due to the Glycerol phase in solution.

5.2.5 Flow Rate

The microreactor setup provides a continuous mean of biodiesel production. The oil and methanol KOH solution are mixed in suitable molar ratio under suitable temperature conditions in the microreactor. The residence time of reactant in microreactor depends on a total flow rate of pumps selected. Higher the flow rate there will be less time for transesterification reaction and vice versa. Therefore to determine the optimum total flow rate range for biodiesel production in the microreactor and to see the effect on spectral changes, total flow rates selected as 10, 15, 20 and 25 ml/min with temperature 60 °C and oil to methanol molar ratio 1:9.

The Figure 31, shows the baseline corrected spectra of pre-experiment conducted at different total flow rates along with pure components. At a flow rate of 10 ml/min, there was maximum time available for transesterification and maximum biodiesel produced. It was also observed that at 10 ml/min the solution was clearer as compared to other flow rates when it was leaving the microreactor. It is expected that at this flow rate glycerol phase settled down in microreactor as a result there was no ROH absorption peak observed from 1900 to 1950 nm.

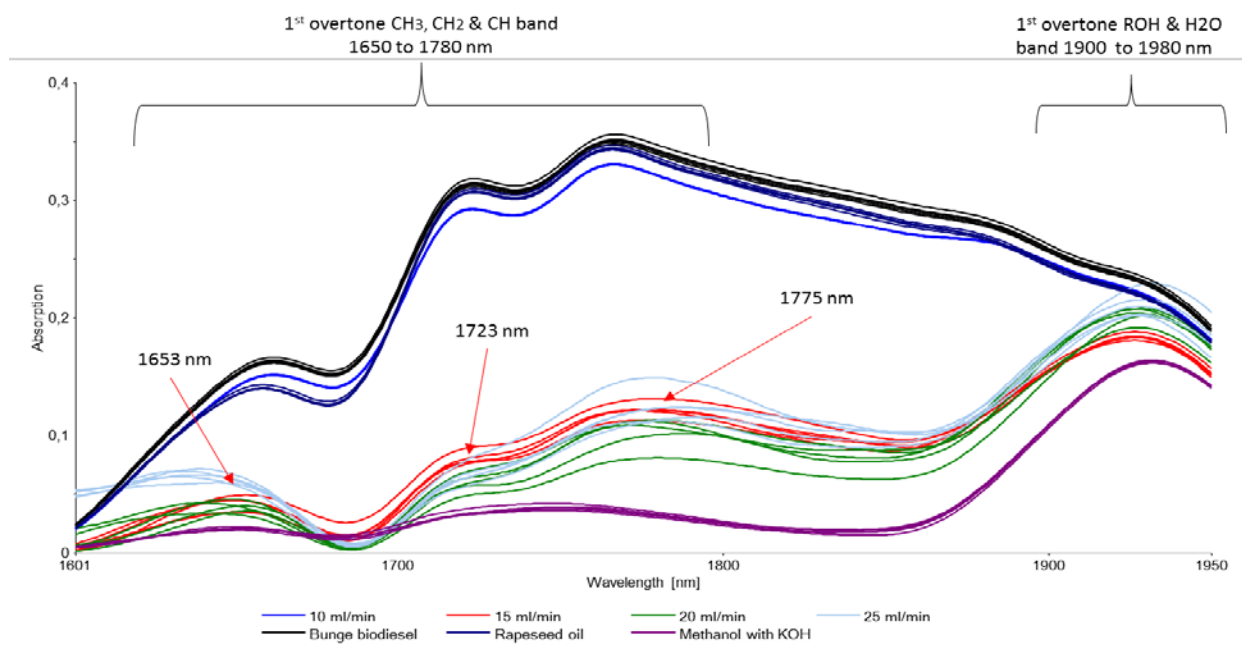


Figure 31 All spectra are baseline corrected and smoothed with Savitzky-Golay Polynomial fit (2nd order, points 25). At a flow rate of 10 ml/min, spectra are identical and closer to Biodiesel spectra. While samples at 15 ml/min, 20 ml/min and 25 ml/min show 1st overtone CH₃, CH₂ and CH bands between 1600 nm and 1800 nm, and ROH absorption bands from 1900nm to 1950 nm.

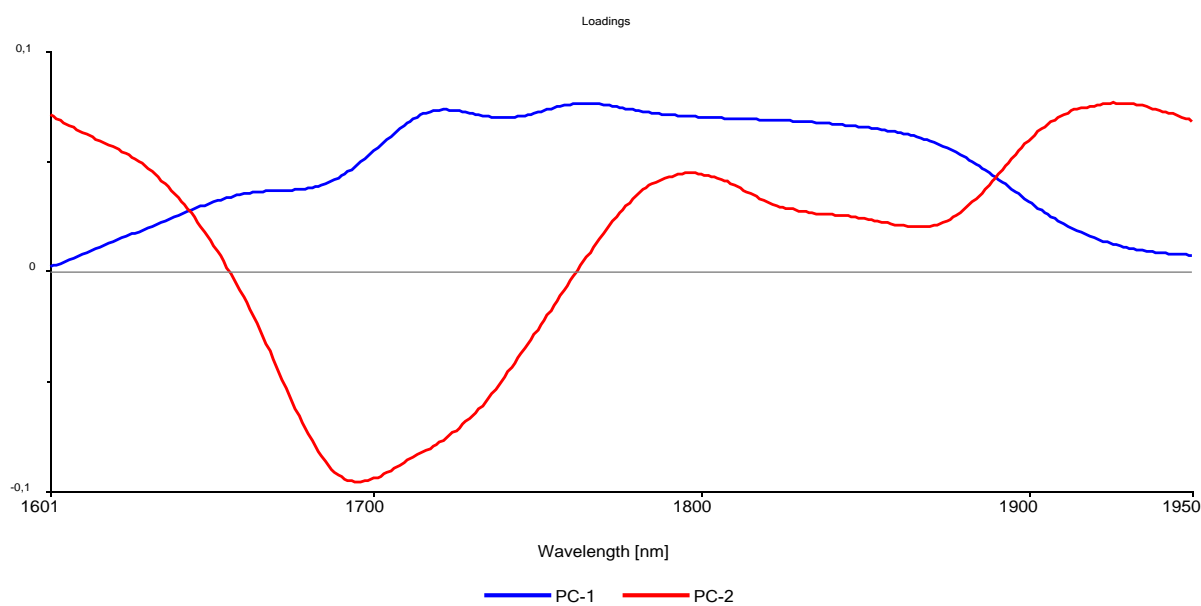


Figure 32: PC1 explains 99% variance in the samples. The samples at 10 ml/min are above average on PC 1 while the samples at other flow rates are below average on PC1. PC2 explains only 1 % variance, which is mainly due to negative scores of Methanol.

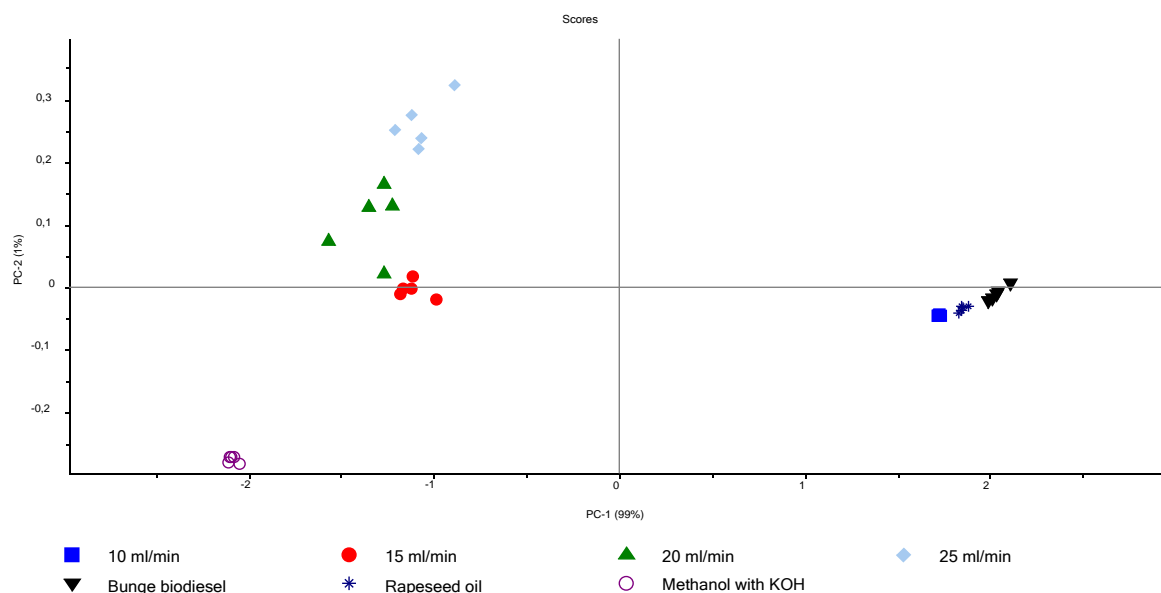


Figure 33: On PC1 the variance is mainly due to CH₃, CH₂ and CH vibrations, which represents the biodiesel and oil groups. On PC2 the two separate groups can be visualized, negative loading from 1650 to 1750 nm which are due to 1st overtone CH₃ vibrations, represents methanol group and the positive loading from 1800 to 1900 nm are due to CH₂, CH and ROH vibrations, which are most probably due to the Glycerol phase in solution.

5.2.6 Conclusion

- The Lambda measurements of the biodiesel produced in the microreactor at temperature of 60 °C, flow rate of 25 ml/min and oil to methanol molar ratio of 1:6, show that this laboratory test setup can be successfully used to produce biodiesel comparative to batch 09 biodiesel and Bunge Biodiesel (see section 5.2.1).
- The prototype spectrometer, Spectral Engine N2.0 with a wavelength range from 1500nm to 1990nm provides a suitable mean for online monitoring of biodiesel produced in microreactor when methanol is used as a reference. The characteristic 1st overtone CH₃, CH₂ and CH vibrations of biodiesel are visible between 1650 nm to 1780 nm. The spectra of pure biodiesel samples show slightly higher absorption from 1650 nm to 1698 nm that distinguish it from pure Oil sample as shown in Figure 22.
- The optimum range of factors to perform DoE from spectral analysis of pre-experiments can be summarized as:
 - The suitable temperature for transesterification of rapeseed oil with methanol KOH solution in microreactor was found to be 60 °C as suggest in reference [65],[73] and [100]. At this temperature, minimum noise in spectra observed due to the emulsion and also there was no disturbance in spectra due to bubbling.
 - Therefore for DoE 60 °C is selected as maximum temperature and for the lower limit of temperature 55 °C could be selected, but the amount of noise in spectral at this temperature need to be observed.
 - The minimum oil to methanol molar ratio was found to be 1:6 and the maximum limit can be selected as 1:12.

4. At a total flow rate of 10 ml/min, the spectra were similar to Biodiesel spectra, it is expected that at this flow rate the glycerol phase separates out into the microreactor that may lead to blocking of flow channels. Therefore the suggested range for total flow rate would be from 15 ml/min to 25 ml/min.
5. The suggested limits of factors to perform DoE are summarized in the following table:

Table 17: Limits of factors to perform the DoE for the microreactor preexperiments

Factors	Temperature °C	Oil to Methanol Molar ratio	Total Flow rate ml/min
Lower Limit	55	1:6	15
Upper Limit	60	1:12	25

5.2.7 Recommendations

The suggested parameters for biodiesel production in the microreactor need to be verified because there was no calibration model available to compare the yCield of biodiesel produced. For that purpose following measures are highly suggested:

- Determine the limit of detection and quantification of Biodiesel in methanol for Spectral engine N2.0.
- The mixing experiment should be performed in a similar way as mention in section 5.3. to develop a calibration model for Spectral Engine N2.0. In this case, methanol should be used as a reference. The disturbance in spectra due to TDIAS probe should be evaluated.
- To enhance the yield of biodiesel at higher flow rates, few more reaction plates should be added to microreactor assembly, increasing the residence time for reactants in the microreactor. Mixing Experiments

5.2.8 Mixing experiment of Oil and Methanol with catalyst and without catalyst at room temperature

The wavelength region from 2200 nm to 2300 nm was selected and baseline corrected to perform PCA. In this wavelength region biodiesel shows characteristic CH₃ combination band peak at 2258 nm which distinguish it from Oil. While Methanol shows characteristic CH₃ combination band peak at 2275 nm.

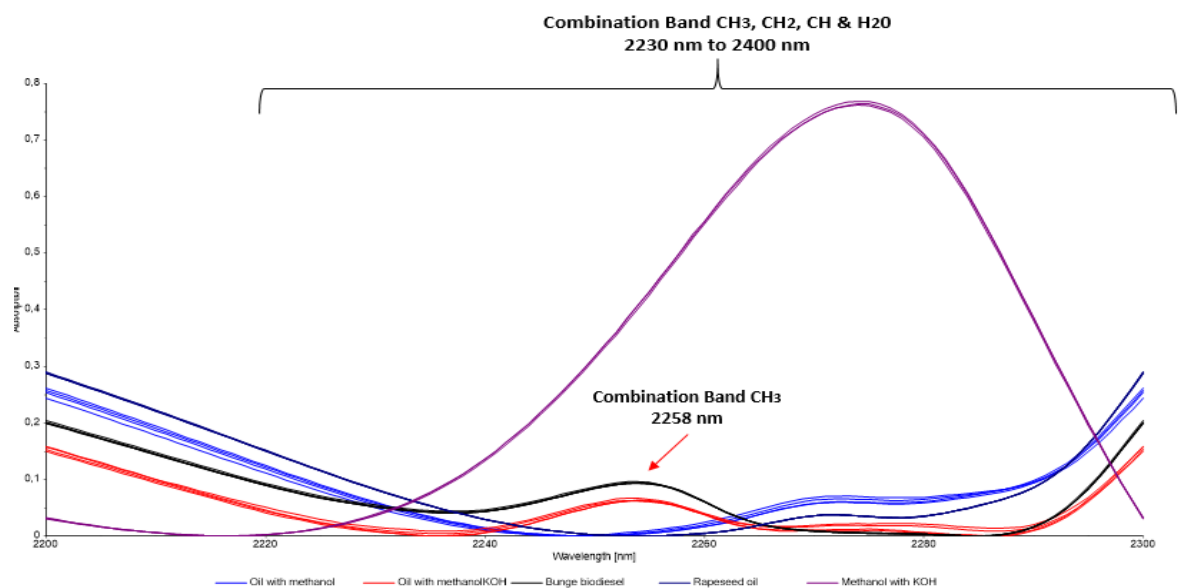


Figure 34: Baseline corrected spectra of selected wavelength region from 2200 nm to 2300nm. In this wavelength region, characteristic CH₃ combination band peak of biodiesel samples at 2258nm distinguish it from methanol and rapeseed oil samples.

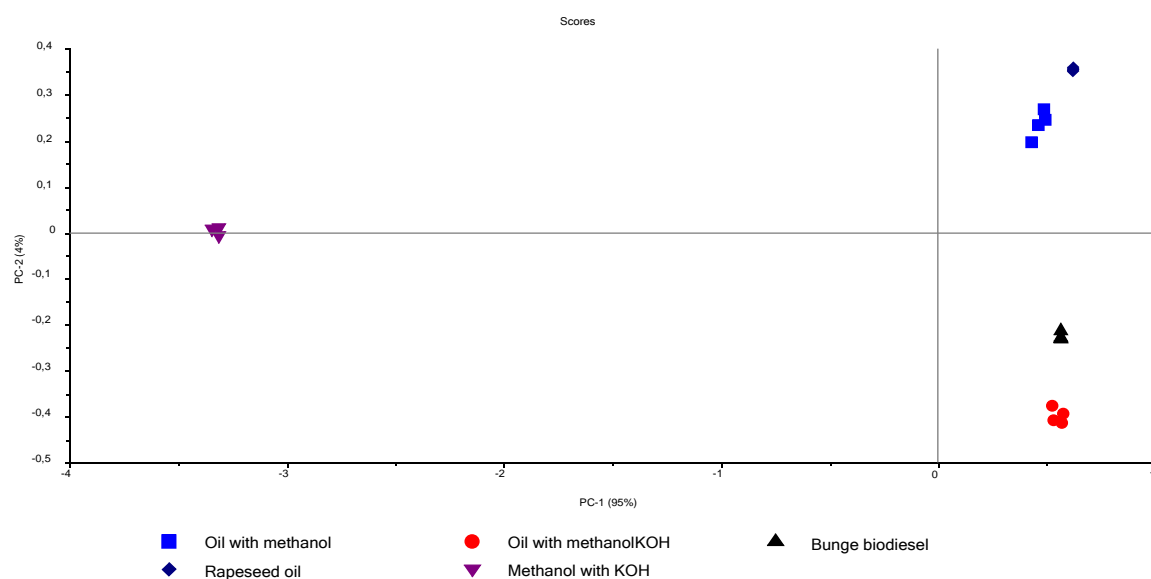


Figure 35: PC1 explains 95 % variance in the data set, the samples having Biodiesel and oil are above average on PC1 with similar scores approx. 0.5. The maximum variance on PC 1 is mainly due to methanol, having relatively high negative scores about -3

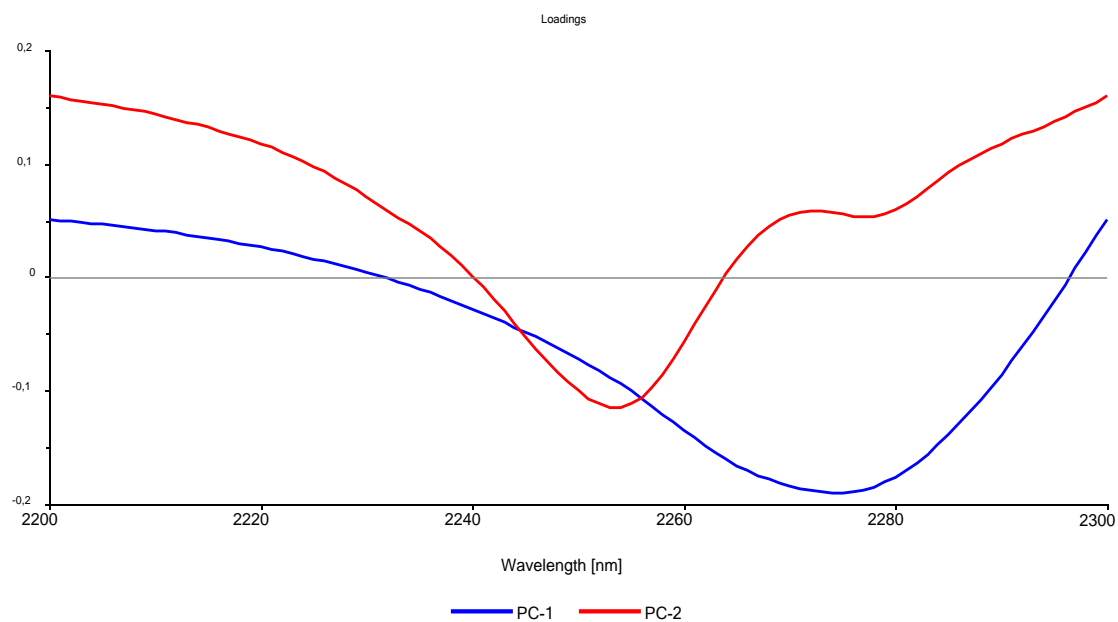


Figure 36: Baseline corrected and smoothed with Savitzky-Golay polynomial fit (2nd order, points 5) PC 1 the variance is mainly due to CH₃- and H₂O- vibrations with high negative loadings, show that the methanol is negatively correlated with it. On PC2, the two sample groups can be distinguished clearly the biodiesel phase is below average and the Oil phase above average.

6 PLS model for Mixing Experiments

The NIR inline measurements of the mixing experiments based on the D-optimal Design were then used to create a prediction model for the components of the biodiesel synthesis. With the spectra of the mixing experiments a PLS was calculated to predict the amount of the components of the biodiesel synthesis. While the products particularly biodiesel is of interest.

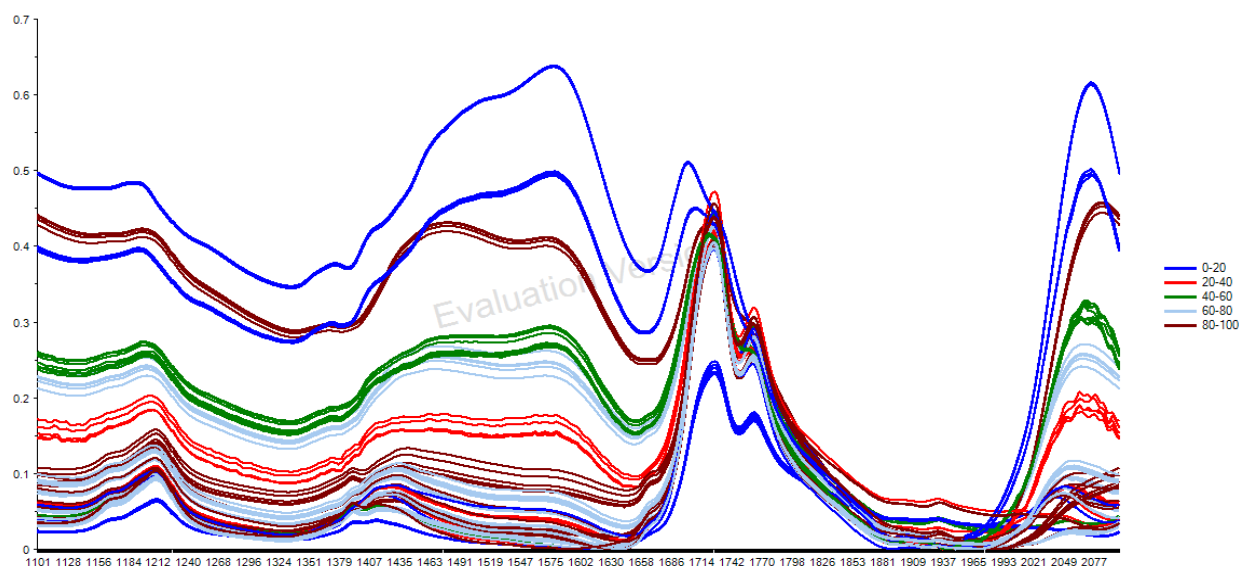


Figure 37: Baseline corrected spectra of all mixing experiments. The samples are grouped according to Biodiesel wt% in samples. The samples with 60-100 wt % of biodiesel shows characteristic CH₃ & CH₂ absorption peaks at 1664 nm. While this peaks become less prominent with lower concentration of biodiesel. Whereas in samples with biodiesel wt% from 20 – 60 %, characteristic CH₃, CH₂ and CH absorption peaks of biodiesel and Oil are visible at 1724nm and 1775 nm.

During mixing 5 spectra were measured for each run. Due to inhomogeneous mixtures depending on insufficient mixing or the components of the mixture there are some noise spectra or regions in this spectra see in Figure 1.

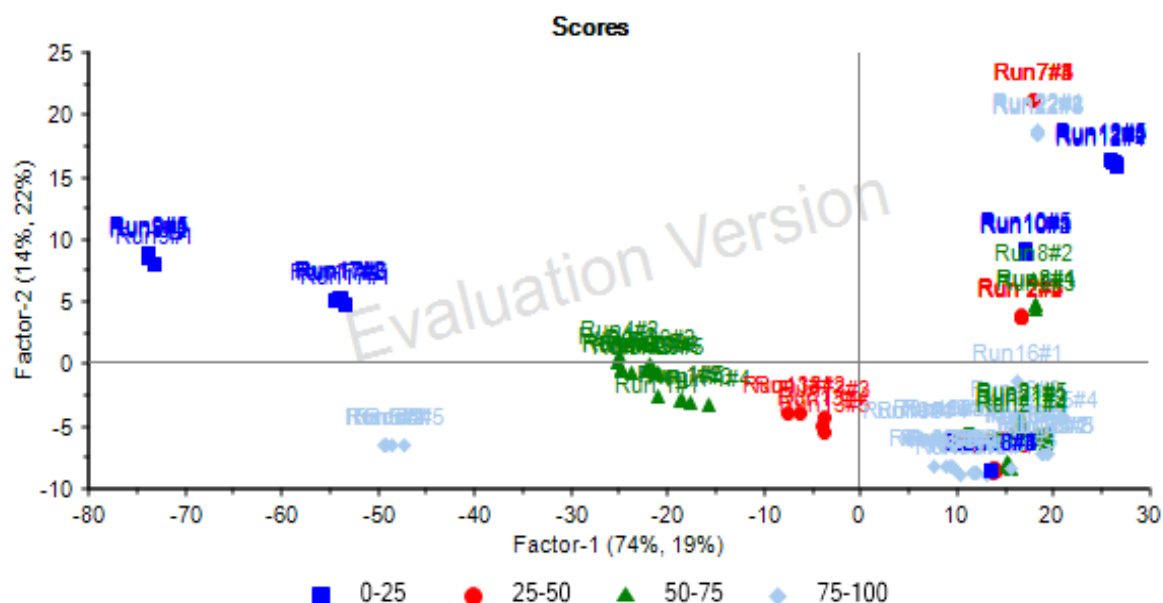


Figure 38: Shows the Score plot for wavelength ranging from 1100nm to 2100 nm. The samples are grouped according to biodiesel wt%. The factor 1 explains the 74% variance in spectra and factor 2 explains the 14 % variance in spectra.

Based on the spectra a PLS model was calculated using cross-validation method. The samples with high biodiesel and oil content group on right side of score plot, the samples with high methanol group towards the left side, whereas samples with high glycerol wt % grouped in middle of score plot as shown in Figure 38.

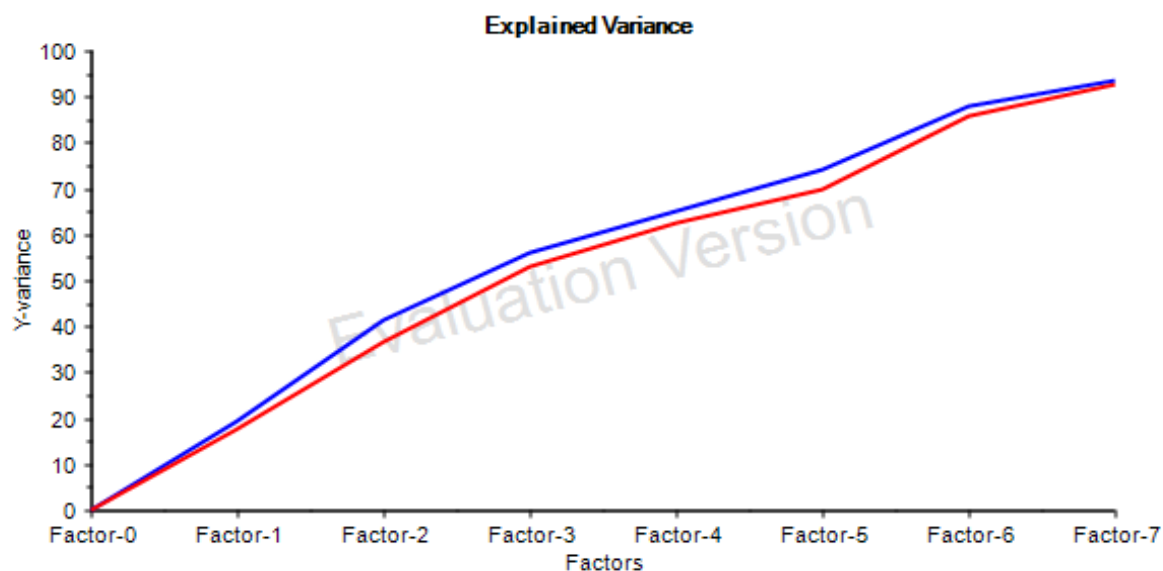


Figure 39: Shows the difference of the explained variance for the predicted (blue) and the reference (red) values. To best predict the values of components we will use 7 factors as they explain the 98% variance samples.

With this PLS we can make predictions for the percentages of each component in a mixture with the four mentioned components of the biodiesel synthesis.

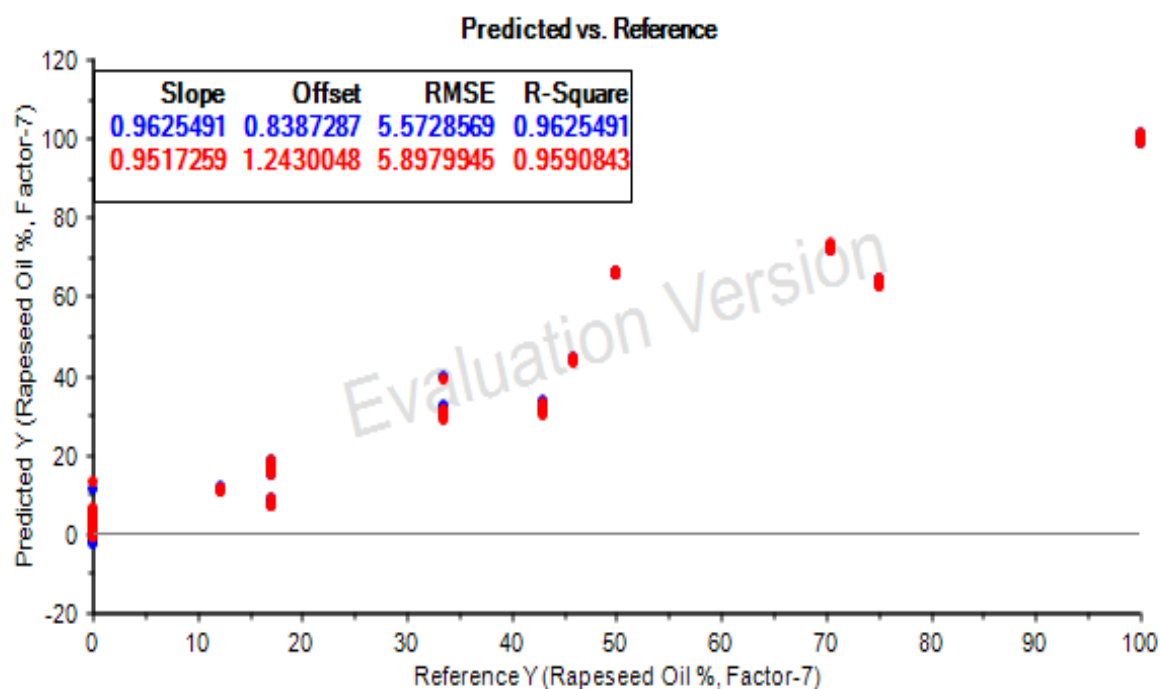


Figure 40: The model for Rapeseed Oil shows R-square value 0.95 in validation for 7 factors, and the error in cross validation is about 5.897 on scale of -20 to 120 which is about 4.21%.

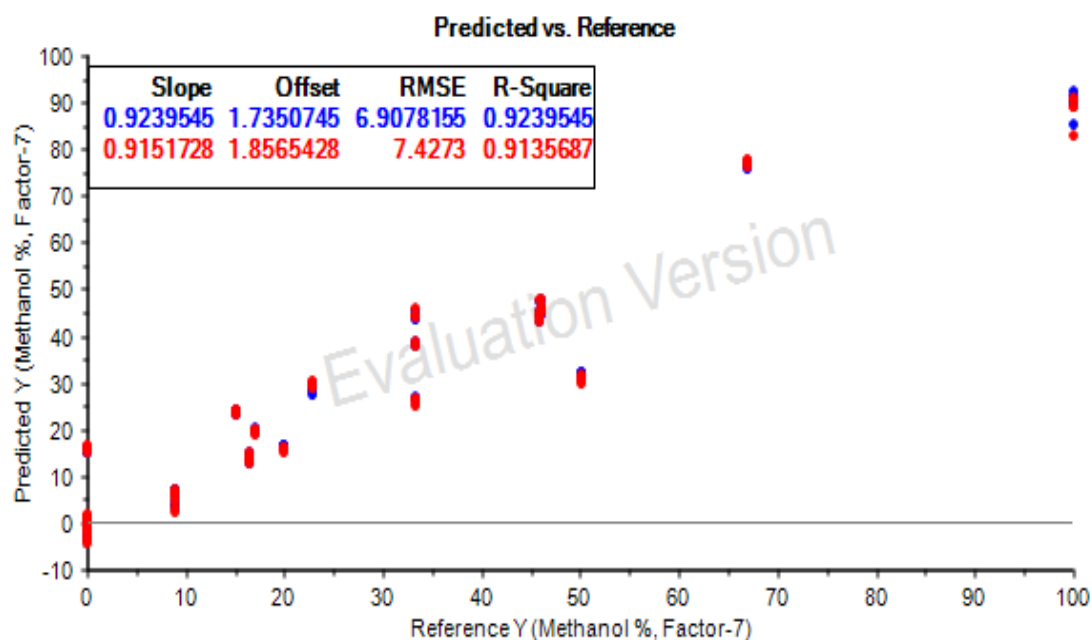


Figure 41: The model for Methanol shows R-square value 0.91 in validation for 7 factors, and the error in cross validation is about 7.42 on scale of -10 to 100 which is about 6.58%.

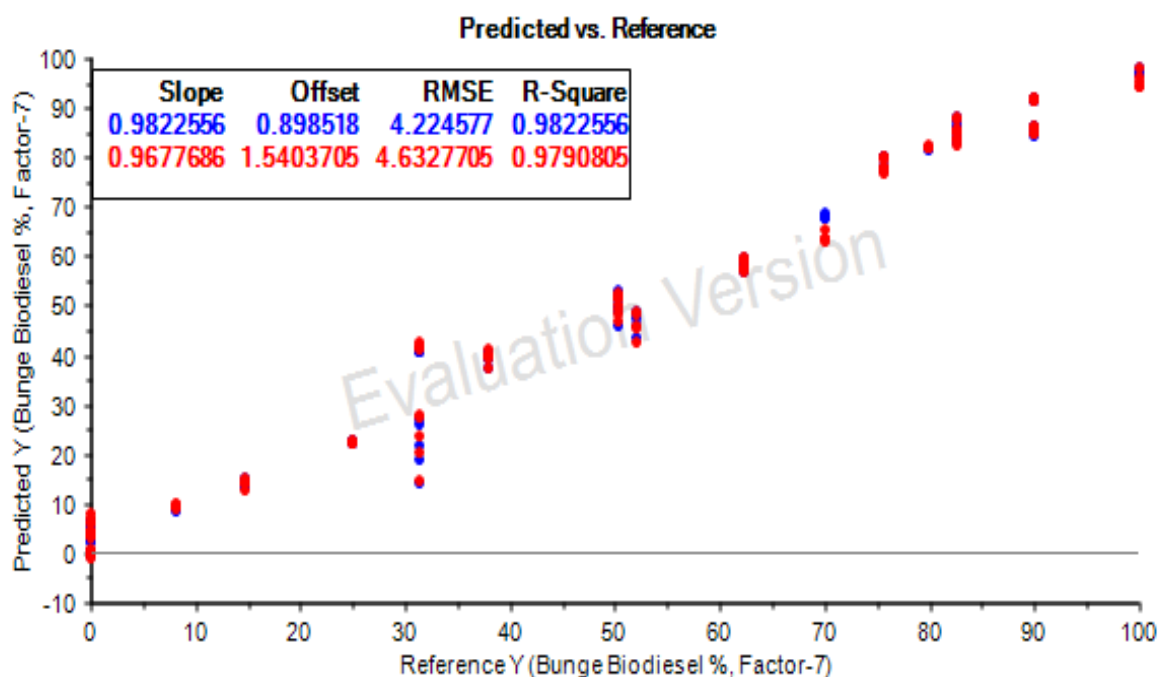


Figure 42: The model for Bunge Biodiesel shows R-square value 0.97 in validation for 7 factors, and the error in cross validation is about 4.63 on scale of -10 to 100 which is about 4.2%.

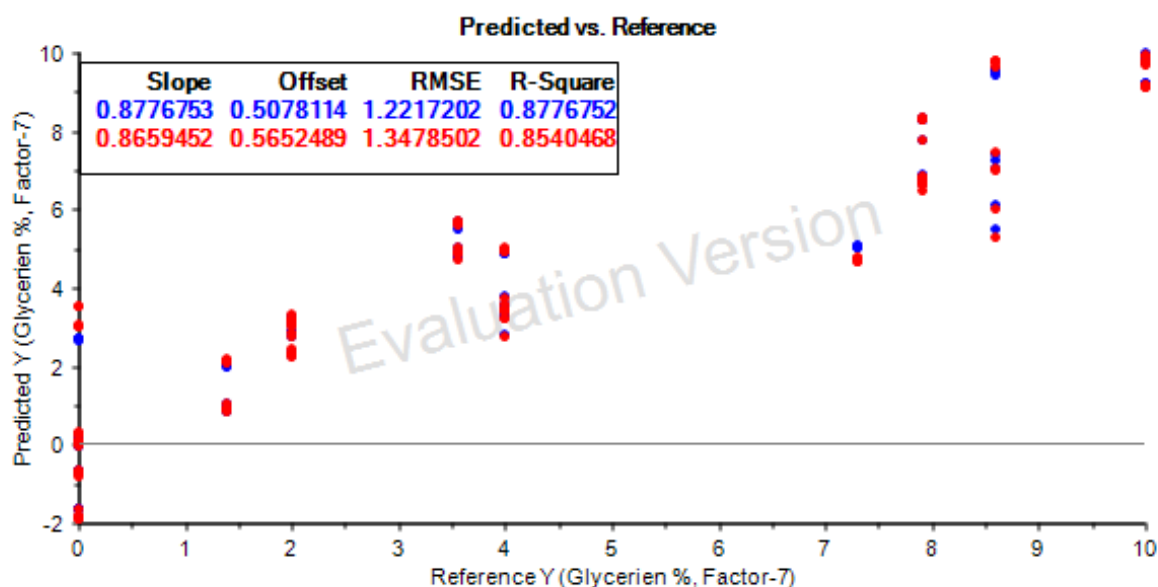


Figure 43: The model for Glycerine shows R-square value 0.85 in validation for 7 factors, and the error in cross validation is about 1.347 on scale of -2 to 10 which is about 11.2%.

6.1 Conclusion

In the mixing experiment the biodiesel was the component of interest, and thus PLS model shows minimum RMSE of 4.2 % for Biodiesel. It also predicts Rapeseed Oil and Methanol values with RMSE of 4.21% and 6.5% respectively, whereas for Glycerol it give higher RMSE of about 11.2%. One reason for higher value of RMSE for Glycerol could be that it was use in less wt % as compared to other components. Because of the insufficient spectra and prediction values it's obvious that some runs of the mixing experiments have to be repeated. Moreover it mentioned that the PLS model can only be used to optimize this mixing experiment plus it is only valid for the TIDAS spectrometer.

7 Comparison of Working Packages

WP 1: Preparatory work, research

This working package is achieved as mentioned in the project outline.

Helpful literature was found with several searching machines and a state of the art was handed in.

WP 2: Preparing project documentation and oraganisation

This working package is achieved as mentioned in the project outline.

Useful methods for project planning were used and project outline was written.

WP 3: Synthesizing Biodiesel in batches & spectroscopic measurements of each step of Biodiesel production using Lambda

This working package is achieved as mentioned in the project outline.

Biodiesel was produced in batch production on the one hand with values of previous work, which were with volumetric ratio and on the other hand with a molar ratio. All steps of the production were measured with Lambda 1050 and evaluated. All of the products had a good quality. With the result of this working package, it was possible to find a good set up for first experiments with the microreactor.

WP 4: Synthesizing biodiesel in batches (*and purification of Biodiesel*) with inline measurements

This working package is almost achieved as mentioned in the project outline.

Biodiesel was produced in batch production and measures inline with TIDAS. Therefore all experiments were done two times for comparison. Also, different set ups were chosen. Because of time reasons, the batch in which ethanol was used instead of methanol was just produced ones, after confirming not to use ethanol in the microreactor but methanol as in all experiments before.

WP 5: Data analysis

This working package is almost achieved as mentioned in the project outline.

All experiments were evaluated with methods of multivariate data analysis.

WP 6: Mixing experiment of Methanol with Biodiesel and spectral analysis with different spectrometers.

The mixing experiments took more time than expected. There were some obstacles to finding the best values of the substances, respectively a proper model of DoE. After all, a Centroid design, d-optimal,

was chosen that got adjusted for the practicability. Also the aim of evaluating “good” biodiesel was defined. Finally, the mixing experiments were performed and a PLS was calculated to predict the concentrations of biodiesel in solution.

P 7: Preexperiments for DoE parameters (for the biodiesel synthesis in microreactor.)

This working package is achieved as mentioned in the project outline.

Experiments were defined to find upper and lower limits of the individual parameter for the preparation of the DoE. All experiments were performed and evaluated.

WP 8: Creating the DoE

This working package is achieved as mentioned in the project outline.

A DoE was designed with the parameters that were found with the preexperiments.

WP 8: Doing the DoE

This working package is not achieved in this POL-project.

Because of the mixing Experiment, which took much longer than expected, there was no time for the experiments itself anymore. But the DoE is worked out for the next team.

WP 9: Biodiesel measurement after each parameter (heating, mixing, reaction,...) with the flow cell (N 2.0/N 2.5) and Lambda 1050 with different spectrometers

This working package is almost achieved as mentioned in the project outline.

There were batches produced and also measured but only with Lambda 1050 and TIDAS because the flow cells were stored at FESTO together with the microreactor.

WP 10: Project Report formation and submission

WP 11: Project Presentation

8 Prospect

Further research could be done in the yield of biodiesel in batch reactions and in the microreactor with regard to industrial processes. A new DoE and prediction model can be created to show the effects of different parameters like educts, molar ratios of the educts, the amount of KOH, temperature, reaction time or flow rate to the yield of produced biodiesel. Furthermore, the effect of water in the synthesis of biodiesel can be proved. Also, gas chromatography analysis can be performed for validation, the quantification of esters, mono-, di- and triacylglycerols and to get more insight of the reaction and the synthesis of biodiesel. Samples can be taken during and after the reaction in different time intervals. The samples can then be analyzed by a gas chromatograph and the data can be compared to references. Thus, for example, the amount of mono- and diglycerides can be measured during and after the reaction. These measurements can be used to show the progress of the reaction if the reaction is complete and to find the optimum parameters for the synthesis of biodiesel. Also, the analysis of biodiesel, glycerol, mono- di, and triglycerides in vegetable oil as well as methyl and ethyl esters is of interest for further projects. The mentioned DoEs and models are only valid for the spectrometer that was used for this procedures. Therefore the models have to be created, performed and calculated for each spectrometer of interest. Moreover, the determination of proof limit and determination limit for the spectrometers Lambda 1050, Spectral Engines N 2.0 and N 2.5 and J&M Tidas is another task for further research. With regards to the laboratory setup an inline optical fiber attenuator for all UV/Vis/NIR applications is helpful to reduce the intensity of the light source. If the intensity is too high spectra will not be plotted completely. One approach to solve this problem is to add one or more optical fibers in the light path to reduce the intensity.

Appendix

Table A 1: Pre-Experiments for biodiesel production in Microreactor

Factors	Experiment ID	Molar Ratio	Molar ratio input value	Total Flow Rate	Residence Time	Temperature
		Oil:Methanol	(Methanol for 1 ml of Oil)		Approx.	°C
				ml/min	(min)	
Temperature	Experiment 1	1:6	0.251	25.00	8.00	40
	Experiment 2	1:6	0.251	25.00	8.00	50
	Experiment 3	1:6	0.251	25.00	8.00	65
	Experiment 4	1:4	0.167	25.00	8.00	60
Molar Ratio	Experiment 5	1:3	0.126	25.00	8.00	60
	Experiment 6	1:2	0.084	25.00	8.00	60
	Experiment 7	1:6	0.251	25.00	8.00	60
Molar Ratio	Experiment 8	1:9	0.337	25.00	8.00	60
	Experiment 9	1:12	0.5	25.00	8.00	60
	Experiment 10	1:9	0.337	10.00	20.00	60
	Experiment 11	1:9	0.337	15.00	13.33	60
	Experiment 12	1:9	0.337	20.00	10.00	60

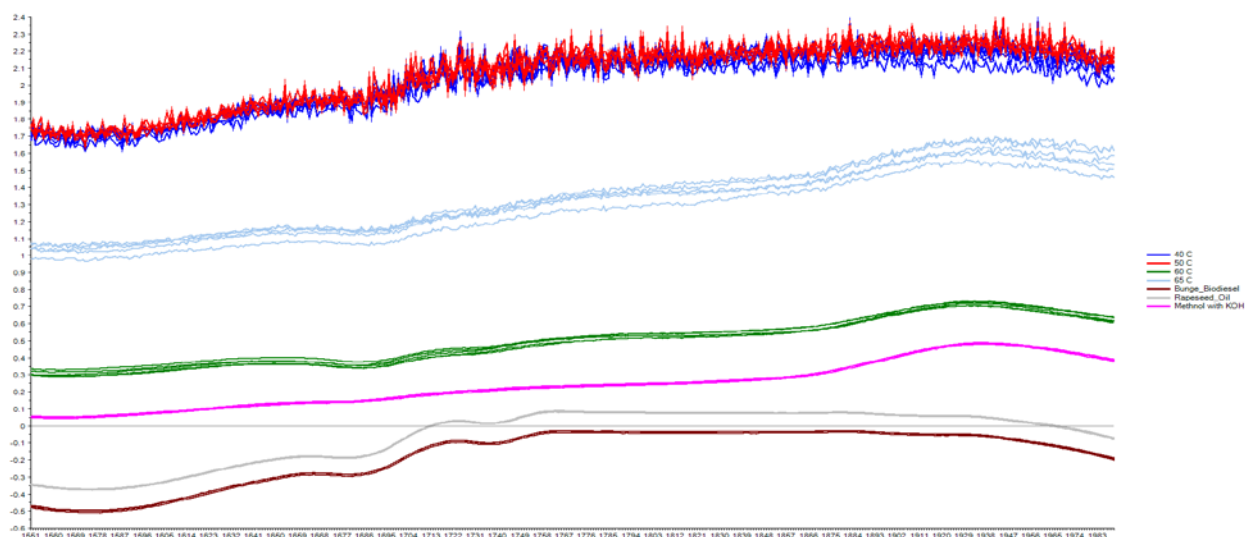


Figure A 1: The line spectra collected at different temperatures along with pure components. No pre-treatment was applied to spectral data. At temperature of 40 and 50 the spectra was noisy due to emulsion formation.

Table A 2: The DoE for the mixing experiments with calculated weights of the components for each run.

Std	Run	Component 1 A:Oil [g]	Component 2 B:Methanol [g]	Component 3 C:Biodiesel [g]	Component 4 D:Glycerol [g]	total amount
18	1	0,0	11,4	35,0	3,7	50,0
16	2	16,7	16,6	15,7	1,0	50,0
21	3	21,5	7,5	19,0	2,0	50,0
4	4	0,0	22,9	25,1	2,0	50,0
17	5	0,0	4,5	41,3	4,3	50,0
11	6	0,0	0,0	45,0	5,0	50,0
23	7	37,5	0,0	12,5	0,0	50,0
15	8	22,9	0,0	25,1	2,0	50,0
1	9	0,0	50,0	0,0	0,0	50,0
2	10	25,0	25,0	0,0	0,0	50,0
14	11	0,0	8,2	37,9	4,0	50,0
3	12	50,0	0,0	0,0	0,0	50,0
7	13	16,7	16,6	15,7	1,0	50,0
8	14	8,5	8,5	31,2	1,8	50,0
10	15	6,1	0,0	40,0	4,0	50,0
13	16	0,0	4,5	41,3	4,3	50,0
9	17	8,5	33,5	7,4	0,7	50,0
22	18	35,3	10,0	4,1	0,7	50,0
6	19	0,0	0,0	45,0	5,0	50,0
12	20	0,0	23,0	26,0	1,0	50,0
20	21	8,5	8,5	31,2	1,8	50,0
5	22	0,0	0,0	50,0	0,0	50,0
19	23	0,0	8,2	37,9	4,0	50,0
total amount		257,1	258,9	586,0	48,0	

Table A 3: The DoE for the mixing experiments with calculated volumes of the components for each run considering the densities of the components.

Std	Run	Component 1 A:Oil [mL]	Component 2 B:Methanol [mL]	Component 3 C:Biodiesel [mL]	Component 4 D:Glycerol [mL]	total volume
18	1	0,00	12,38	39,96	2,90	55,23
16	2	21,13	18,06	17,90	0,79	57,89
21	3	27,18	8,15	21,71	1,59	58,63
4	4	0,00	24,88	28,69	1,59	55,16
17	5	0,00	4,84	47,14	3,41	55,39
11	6	0,00	0,00	51,43	3,97	55,40
23	7	47,41	0,00	14,29	0,00	61,69
15	8	28,94	0,00	28,69	1,59	59,22
1	9	0,00	54,35	0,00	0,00	54,35
2	10	31,61	27,17	0,00	0,00	58,78
14	11	0,00	8,91	43,26	3,13	55,31
3	12	63,21	0,00	0,00	0,00	63,21
7	13	21,13	18,06	17,90	0,79	57,89
8	14	10,74	9,29	35,63	1,41	57,07
10	15	7,68	0,00	45,68	3,13	56,50
13	16	0,00	4,84	47,14	3,41	55,39
9	17	10,71	36,39	8,41	0,55	56,06
22	18	44,56	10,87	4,64	0,55	60,62
6	19	0,00	0,00	51,43	3,97	55,40
12	20	0,00	25,00	29,71	0,79	55,51
20	21	10,74	9,29	35,63	1,41	57,07
5	22	0,00	0,00	57,14	0,00	57,14
19	23	0,00	8,91	43,26	3,13	55,31
total amount		325,04	281,40	669,67	38,13	



Figure A 2: Left: Step B of batch 11 without water Right: 20 mL step B of batch 11 with 20 mL demineralised water. Before mixing two phases were formed.



Figure A 3: Left: Step B of batch 11 without water Right: 20 mL step B of batch 11 with 20 mL demineralised water. One phase is formed.

References

1. Abbaszaadeh, A., et al., *Current biodiesel production technologies: A comparative review*. Energy Conversion and Management, 2012. **63**: p. 138-148.
2. Gerpen, J.V., *Biodiesel processing and production*. Fuel Processing Technology, 2005. **86**(10): p. 1097-1107.
3. Fangrui Ma, M.A.H., *Biodiesel production: A review*. Bioresource Technology, 1999. **70**: p. 1-15.
4. Roseli Ap. Ferrari, A.L.M.T.P.a.K.J.P., *Biodiesel Production and Quality*. Biofuel's Engineering Process Technology, 2011.
5. Ulf Schuchardt, R.S., and Rogério Matheus Vargas, *Transesterification of Vegetable Oils: a Review*. J. Braz. Chem. Soc., 1998. **9**(1): p. 199-210.
6. Lotero E, G.J., Bruce DA, Suwannakarn K, Liu Y, Lopez DE. , *The catalysis of biodiesel synthesis*. Catalysis. 2006. **19**: p. 41-83.
7. Sharma, Y.C., B. Singh, and S.N. Upadhyay, *Advancements in development and characterization of biodiesel: A review*. Fuel, 2008. **87**(12): p. 2355-2373.
8. Enweremadu, C.C. and M.M. Mbarawa, *Technical aspects of production and analysis of biodiesel from used cooking oil—A review*. Renewable and Sustainable Energy Reviews, 2009. **13**(9): p. 2205-2224.
9. Nye, M.J., Southwell, P.H., In, *Esters from rapeseed oil as diesel fuel*. Proc. Vegetable Oil as Diesel Fuel Seminar III. Peoria: Northern agricultural energy center., 1983. **78**: p. 83.
10. Leung DY, G.Y., *Transesterification of neat and used frying oil: Optimization for biodiesel production*. Fuel Process Technology, 2006. **87**: p. 883-90.
11. Meher LC, K.M., Dalai AK, Naik SN, *Transesterification of karanja (Pongamia pinnata) oil by solid basic catalysts*. Eur J Lipid Sci Technology, 2006. **108**: p. 389-397.
12. Freedman, B., E.H. Pryde, and T.L. Mounts, *Variables affecting the yields of fatty esters from transesterified vegetable oils*. Journal of the American Oil Chemists Society, 1984. **61**(10): p. 1638-1643.
13. Bradshaw, G.B. and W.C. Meuly, *Preparation of detergents*. US patent, 1944. **2**(360): p. 844.
14. Komers, K., et al., *Kinetics and mechanism of the KOH — catalyzed methanolysis of rapeseed oil for biodiesel production*. European Journal of Lipid Science and Technology, 2002. **104**(11): p. 728-737.
15. Othman R, M.A., Ismail M, Salimon J. J Membr Sci ;348:287-97., *Application of polymeric solvent resistant nanofiltration membranes for biodiesel production*. 2010.
16. Vicente G, M.M., Aracil J. , *Integrated biodiesel production: a comparison of different homogeneous catalysts systems*. Bioresour Technol, 2004. **92**: p. 297–305.
17. Mbaraka IK, S.B., *Conversion of oils and fats using advanced mesoporous heterogeneous catalysts*. J Am Oil Chem Soc, 2006;. **83**: p. 79-91.
18. Pinnarat T, S.P., *Assessment of noncatalytic biodiesel synthesis using supercritical reaction conditions*. Ind Eng Chem Res, 2008. **47**(6801-8).
19. NC., T.-S., *Development and purification of biodiesel*. Sep Purif Technol, 2007. **20**(377-81).
20. Qiu ZY, Z.L., Weatherley L. Chem. Eng. Process. 2010, 49, 323 – 330.
21. Anita Šalić, B.Z., *MICROREACTORS - PORTABLE FACTORIES FOR BIODIESEL FUEL PRODUCTION*. 2011. **50**(2): p. 85-110,.
22. Rahimi, M., et al., *Optimization of biodiesel production from soybean oil in a microreactor*. Energy Conversion and Management, 2014. **79**: p. 599-605.
23. Gordon, R., I. Gorodnitsky, and V. Grichko, *Process for producing biodiesel through lower molecular weight alcohol-targeted cavitation*. 2013, Google Patents.
24. Yang, S.C., et al., *Homogeneous catalysts for biodiesel production*. 2014, Google Patents.

25. Asthana, N.S., et al., *Process for producing mixed esters of fatty acids as biofuels*. 2009, Google Patents.
26. Sun J, J.J., Ji L, Zhang LX, Xu NP., *Microfluidic mixing: a review*. Ind. Eng. Chem. Res., 2008. **47**: p. 1398 - 1403.
27. G. Guan, K.K., K. Moriyama, N. Sakurai, *Continuous production of biodiesel using a microtube reactor*. Chem. Eng. Trans., 2008. **14**: p. 237-244.
28. Santacesaria, E., et al., *Biodiesel process intensification in a very simple microchannel device*. Chemical Engineering and Processing, 2012. **52**: p. 47-54.
29. Canter, N., *Making biodiesel in a microreactor*. Tribology & Lubrication Technology, 2006. **62**(8): p. 15.
30. Wen, Z., Yu, X., Tu, S.T., Yan, J., Dahlquist, E. r. , S. . , *Intensification of biodiesel synthesis using zigzag microchannel reactor*. Bioresource Technology., 2009. **100**: p. 3054-3060.
31. Jovanovic GN, P.B., Parker J, Dhubabian AA. United States Patent Application. 2009, US2009/0165366A1.
32. Elizabeth C, R.D., Douglas D, Daniel G, Richard G, Brian M, Martin P, James P. Prepr. Pap. Am. Chem. Soc., Div. Fuel Chem. 2008, 53, 571-572.
33. W. Shaaban, A.H.E.-S., M.F. Elkady, M. Ohshima, *Investigation of Factors Affect Biodiesel Production in Microreactor with T-Mixer*. International Proceedings of Chemical, Biological and Environmental Engineering, 2015. **88**(3).
34. G., K., *The Biodiesel Handbook*. 2005: Taylor & Francis Ltd.
35. Xie, T.M., L.X. Zhang, and N.P. Xu, *Biodiesel synthesis in microreactors*. Green Processing and Synthesis, 2012. **1**(1): p. 61-70.
36. Knothe, G., *ANALYTICAL METHODS USED IN THE PRODUCTION AND FUEL QUALITY ASSESSMENT OF BIODIESEL*, in *American Society of Agricultural Engineers*. 2001. p. 193–200.
37. Zhang, P. and B. Wen, *I&EC 97-Microreactor technology for biodiesel production*. Abstracts of Papers of the American Chemical Society, 2008. **235**.
38. Günzler, H. and H.-U. Gremlich, *IR-Spektroskopie : eine Einführung*, in *Wiley Online Library*. 2003, Wiley-VCH: Weinheim. p. XIII, 352.
39. S. T. H. Sherazi, S.A.M., AND M. I. Bhanger, *Rapid Determination of Free Fatty Acids in Poultry Feed Lipid*. 2007. p. 4928–4932.
40. T. Yuan, E.A.-K., D. Pinchuk, F. R. van de Voort, *FTIR On-line Monitoring of Biodiesel*. 2014, IBIMA. p. 1-13.
41. R. F.Salesa, R.V., S. Mareira de Limac,M. F. Pimentela, L. Stragevitcha, A. Ferrer, *Multivariate statistical process control charts for batch monitoring of transesterification reactions for biodiesel production based on near-infrared spectroscopy*, in *Computers and Chemical Engineering*. 2016, Elsevier.
42. Knothe, G., *Rapid monitoring of transesterification and assessing biodiesel fuel quality by NIR spectroscopy using a fiber-optic probe.*, in *J. Am. Oil Chem. Soc.* 1999. p. 795-800.
43. N.M. Naresh, a.Y.G.A., *Fourier Transform Infrared Spectroscopy (FTIR) Method To Monitor Soy Biodiesel and Soybean Oil in Transesterification Reactions, Petrodiesel–Biodiesel Blends, and Blend Adulteration with Soy Oil*. 2009. p. 3773-3782.
44. P. Felizardo, P.B., M. S. Uva, J. C. Menezesb and M. Joana Neiva Correia.2007, Bd. 15, 2, S. 97–105., *Monitoring biodiesel fuel quality by near infrared spectroscopy. Journal of Near Infrared Spectroscopy*.
45. M. Coronado, W.Y., D. Wang, F. E. Dowell, *Predicting the concentration and specific gravity of biodiesel-diesel blends using near- infrared spectroscopy*. 2009, Dowell. p. 217-221.
46. Jegannathan KR, A.S., Poncelet D, Chan ES, Ravindra P. Production of biodiesel using immobilized lipase — a critical review. Crit Rev Biotechnol 2008;28:253–64.

47. Freedman, B., E.H. Pryde, and W.F. Kwolek, *Thin layer chromatography/flame ionization analysis of transesterified vegetable oils*. Journal of the American Oil Chemists Society, 1984. **61**(7): p. 1215-1220.
48. Cvengroš, J. and Z. Cvengrošová, *Quality control of rapeseed oil methyl esters by determination of acyl conversion*. Journal of the American Oil Chemists' Society, 1994. **71**(12): p. 1349-1352.
49. Knothe, G., *Analyzing Biodiesel: Standards and Other Methods*, in JAOCS. 2006. p. 823–833.
50. Freedman, B., W.F. Kwolek, and E.H. Pryde, *Quantitation in the analysis of transesterified soybean oil by capillary gas chromatography 1*. Journal of the American Oil Chemists' Society, 1986. **63**(10): p. 1370-1375.
51. MARIANI C., B.P., VENTURINI S., FEDELI E., *Vegetable oil derivatives as diesel fuel substitutes. Analytical aspects. I: Determination of methyl esters, mono-, di- and triglycerides*. Vol. 68. 1991, Milano, ITALIE: Arti Grafiche Stephano Pinelli.
52. Plank, C. and E. Lorbeer, *Quality control of vegetable oil methyl esters used as diesel fuel substitutes: Quantitative determination of mono-, di-, and triglycerides by capillary GC*. Journal of High Resolution Chromatography, 1992. **15**(9): p. 609-612.
53. Arquiza AC. Bayungan MC, T.R., *Production of Biodiesel and Olechemicals from used frying oil*. University of Philippines, Los Banos, 2000.
54. Guo, Y., Leung, Y.C. and C.P. Koo, *A Clean Biodiesel Fuel Produced from Recycled Oils and Grease Trap Oils*. Department of Mechanical Engineering, The University of Hong Kong, 2002.
55. Phan, A.N. and T.M. Phan, *Biodiesel production from waste cooking oils*. Fuel, 2008. **87**(17): p. 3490-3496.
56. Predojević, Z.J., *The production of biodiesel from waste frying oils: A comparison of different purification steps*. Fuel, 2008. **87**(17–18): p. 3522-3528.
57. Cvengrošová, Z., J. Cvengroš, and M. Hronec, *Rapeseed Oil Ethyl Esters as Alternative Fuels and Their Quality Control*. Petroleum Coal, 1997. **39**: p. 36-40.
58. Carvalho, M.S., et al., *Chromatographic analyses of fatty acid methyl esters by HPLC-UV and GC-FID*. Journal of the Brazilian Chemical Society, 2012. **23**(4): p. 763-769.
59. Tiyaopongpattana, W., P. Wilairat, and P.J. Marriott, *Characterization of biodiesel and biodiesel blends using comprehensive two-dimensional gas chromatography*. Journal of separation science, 2008. **31**(14): p. 2640-2649.
60. Saifuddin, N. and K. Chua, *Production of ethyl ester (biodiesel) from used frying oil: optimization of transesterification process using microwave irradiation*. Malaysian Journal of Chemistry, 2004. **6**(1): p. 77-82.
61. Wang, Y., et al., *Preparation of biodiesel from waste cooking oil via two-step catalyzed process*. Energy conversion and management, 2007. **48**(1): p. 184-188.
62. Wang, Y., et al., *Comparison of two different processes to synthesize biodiesel by waste cooking oil*. Journal of Molecular Catalysis A: Chemical, 2006. **252**(1–2): p. 107-112.
63. Meng, X., G. Chen, and Y. Wang, *Biodiesel production from waste cooking oil via alkali catalyst and its engine test*. Fuel Processing Technology, 2008. **89**(9): p. 851-857.
64. Azócar, L., et al. *Biodiesel production from Rapeseed oil with waste frying oils*. in ISWA World Congress, Amsterdam. 2007.
65. Felizardo, P., et al., *Production of biodiesel from waste frying oils*. Waste Manag, 2006. **26**(5): p. 487-94.
66. Chhetri, A., K. Watts, and M. Islam, *Waste Cooking Oil as an Alternate Feedstock for Biodiesel Production*. Energies, 2008. **1**(1): p. 3.
67. Trathnigg, B. and M. Mittelbach, *Analysis of Triglyceride Methanolysis Mixtures Using Isocratic HPLC With Density Detection*. Journal of Liquid Chromatography, 1990. **13**(1): p. 95-105.

68. Lertsathapornasuk, V., et al., *Microwave assisted in continuous biodiesel production from waste frying palm oil and its performance in a 100 kW diesel generator*. Fuel Processing Technology, 2008. **89**(12): p. 1330-1336.
69. Lertsathapornasuk, V., et al. *Continuous transesthylation of vegetable oils by microwave irradiation*. in *Proceedings of the 1st conference on energy network*. 2005.
70. Lozano, P., et al., *Measurement of free glycerol in biofuels*. Fresenius' journal of analytical chemistry, 1996. **354**(3): p. 319-322.
71. Foglia, T.A. and K.C. Jones, *Quantitation of Neutral Lipid Mixtures Using High Performance Liquid Chromatography with Light Scattering Detection†*. Journal of liquid chromatography & related technologies, 1997. **20**(12): p. 1829-1838.
72. Holčapek, M., et al., *Analytical monitoring of the production of biodiesel by high-performance liquid chromatography with various detection methods*. Journal of chromatography A, 1999. **858**(1): p. 13-31.
73. Jacobson, K., et al., *Solid acid catalyzed biodiesel production from waste cooking oil*. Applied Catalysis B: Environmental, 2008. **85**(1-2): p. 86-91.
74. Darnoko, D., M. Cheryan, and E. Perkins, *Analysis of vegetable oil transesterification products by gel permeation chromatography*. 2000.
75. Chand, P., et al., *Thermogravimetric quantification of biodiesel produced via alkali catalyzed transesterification of soybean oil*. Energy & Fuels, 2009. **23**(2): p. 989-992.
76. Goodrum, J., *Volatility and boiling points of biodiesel from vegetable oils and tallow*. Biomass and Bioenergy, 2002. **22**(3): p. 205-211.
77. Çaylı, G. and S. Küsefoğlu, *Increased yields in biodiesel production from used cooking oils by a two step process: Comparison with one step process by using TGA*. Fuel processing technology, 2008. **89**(2): p. 118-122.
78. Baumann, M., *Implementierung von Inline-NIR-Spektroskopie, Datenauswertung und Reaktionskinetik zur Regelung einer Synthese von Biodiesel in einem Mikroreaktor*, in *Reutlingen Research Institute*. 2016, Reutlingen University.
79. Zhang, W.-B., *Review on analysis of biodiesel with infrared spectroscopy*. Renewable and Sustainable Energy Reviews, 2012. **16**(8): p. 6048-6058.